esa BR-05
October 1981

Challenges & Prospectives of Microgravity research in space

Basic Phenomena and Mechanisms
Case Studies
Technological Aspects

by Y. Malméjac
A. Bewersdorff
I. Da Riva &
L.G. Napolitano

european space agency / agence spatiale européenne
8-10, rue Mario-Nikis, 75738 PARIS CEDEX 15, France

CHALLENGE AND PROSPECTIVES OF MICROGRAVITY RESEARCH IN SPACE (ESA BR-05 ISSN 0250 – 1589)

Edited and published by: ESA Scientific & Technical Publications Branch

Printed by: ESTEC Reproduction Services (812040)

Price: 80 FF for ESA Member States, Austria, Canada and Norway. A 20% surcharge will be levied on orders from 'other States'.

Distribution Office: ESA Scientific and Technical Publications Branch, ESTEC, Postbus 299, 2200 AG – Noordwijk, The Netherlands

About two years ago, the Materials Sciences Working Group (MSWG) of the European Space Agency published a report, MAT(79) 6, entitled 'Long-term planning in materials sciences under microgravity'. This document, while not being a formal scientific proposal for an ESA Materials Science Programme, could be considered as an initial step towards it. In fact, it became one of the cornerstones of the recently adopted ESA Microgravity Programme, in that it showed how such a programme should follow on from the customary practices and divisions of classical materials science activities.

At the same time, many problems encountered in the development of the experiments for the First Spacelab Payload and in some of the proposals received by the ESA/MSWG demonstrated the urgent need for another type of scientific document, one that would enable each potential investigator to enhance the scientific relevance of his experiment and increase his chances of success by improving the precision and efficiency of his preparatory work. The present brochure is intended to be such a document. Nevertheless, the authors are aware that it may well have many shortcomings and that it will need periodic revision and updating. Any criticism or suggestions for improvement from our readers and future co-workers in the field of microgravity will therefore be very welcome.

Materials Science in space is a new scientific venture, one that ignores the limits of classical scientific disciplines. As such, it requires the involvement and active participation of interested bona-fide scientists of all kinds. This brochure is intended to promote a dialogue – the ball is now in your court and ESA awaits its return.

Yves Malmèjac
Chairman of the ESA/MSWG

Contents

Foreword

This brochure addresses those who have recently discovered the new possibilities for the materials sciences offered by the reduced gravity environment in space, but who may not yet be entirely familiar with the accompanying constraints and limitations of 'microgravity' research. Its prime aim is to nucleate interest, to encourage new users and to provide guidance, not by artificially overselling the microgravitational environment, but by providing the most up-to-date and scientifically sound information on the physical mechanisms that operate in space, and by explaining the many challenges that this new environment poses to the imagination and ingenuity of even the most inquisitive investigator.

In contrast to the usual presentation and sequencing of other similar reports, this document attempts to move away in its description of the scientific potential of the microgravity environment from the up to now prevailing applied research presentation towards a more logical 'phenomena-oriented treatment'. This assists the elucidation for the new user of those new difficulties that arise from the lowering of gravity forces and the consequent increased relevance of phenomena that are negligible on earth.

Our intention is to promote rigorous analysis by future experimenters and to induce them to approach this new field of investigation with an open mind, alerted to the dangers of too heavily preconceived opinions. If this new environment were not to hold some surprise, it would not merit the initiation of widespread programmes of space investigation.

The authors do not pretend that they can cover exhaustively the full range of future materials-sciences activities in space in this short treatise: the content of the brochure is limited to those physical mechanisms that are most likely to be involved in the first-generation experiments. Having explained what a microgravity environment is, what it implies and what its essential features are, and what one has to pay for its scientific exploitation, the brochure summarises what has already been learnt about the conduct of experiments on existing microgravity platforms, and about the uncertainty of seeking too rigorously predetermined results. Its other objective is to help any potential user to develop an intuitive feeling for the elementary mechanisms in microgravity: scientists have regarded the force of gravity as an ever-present modulator of the results of their investigations, for so long that it is now difficult to conceive of new experimental methods in reduced gravity.

It must be emphasized that materials-sciences operations in space will not benefit from a constant microgravity level, but will have to accommodate a wide spectrum of residual if small accelerations, in terms of both amplitudes and directions and/or frequencies. We must therefore ask ourselves:

- Is the state of art adequate for assessing all the exploitable effects of gravity levels on materials- and fluid-sciences phenomena?

- If not, what areas need further development?

Although we might not yet be in a position to formulate exhaustive replies to such questions, they are worth posing if only to make us more aware of some possible pitfalls in the present early period.

Good science has never been easy even with the gravity level on earth; it will certainly not be any easier under the fluctuating conditions of reduced gravity we will have to deal with in space-borne investigations. Nevertheless, the *challenge* is worth taking up and we hope that this brochure will help to better promote a successful programme.

1 Introduction

1.1 Microgravitational environment

A microgravitational environment can be attained in any non-inertial frame in which the d'Alembert forces nearly balance the Earth's (or a planet's) gravitational acceleration. What remains may be conveniently referred to as the 'residual' or 'effective' gravitational acceleration. Its magnitude and direction are function of the instantaneous position of the elementary mass in the non-inertial frame and, in general, also of time.

A microgravitational environment can be achieved, for different time durations, on any of the following platforms:
- satellites,
- orbiting space stations,
- rockets,
- aircraft,
- drop tower,

and may be simulated, in certain cases and to a certain extent, in ground-based laboratories (see §2.6).

The attainable g-levels are influenced by absolute rotation and angular accelerations of the platform, forces acting on it and non-uniformities of the external force fields. Optimum conditions are achieved when (i) the rotation of the platform is zero, (ii) the apparatus is as close as possible to the platform's center of mass, and (iii) reaction and surface forces vanish.

'Nominal' gravitational levels and durations achievable with the above-mentioned platforms are shown in Figure 1.1. The orders of magnitude of the contributions of the main factors that either systematically or occasionally grade down the gravitational level are shown in Figure 1.2. Intensity, direction and duration of occasional disturbances define the 'quality' of the platform's nominal gravitational level.

With space-borne platforms, all contributions other than those due to crew activities or moving mechanisms within the spacecraft depend upon the orbit characteristics and attitude of the spacecraft.

Two concepts have been developed:

1. Inertially-fixed attitude used by the Skylab;
2. Gravity-gradient stabilised attitude (spacecraft orientation fixed with respect to the local vertical direction) currently planned for Spacelab-3.

They are schematically shown in Figure 1.3 for the case of a circular orbit.

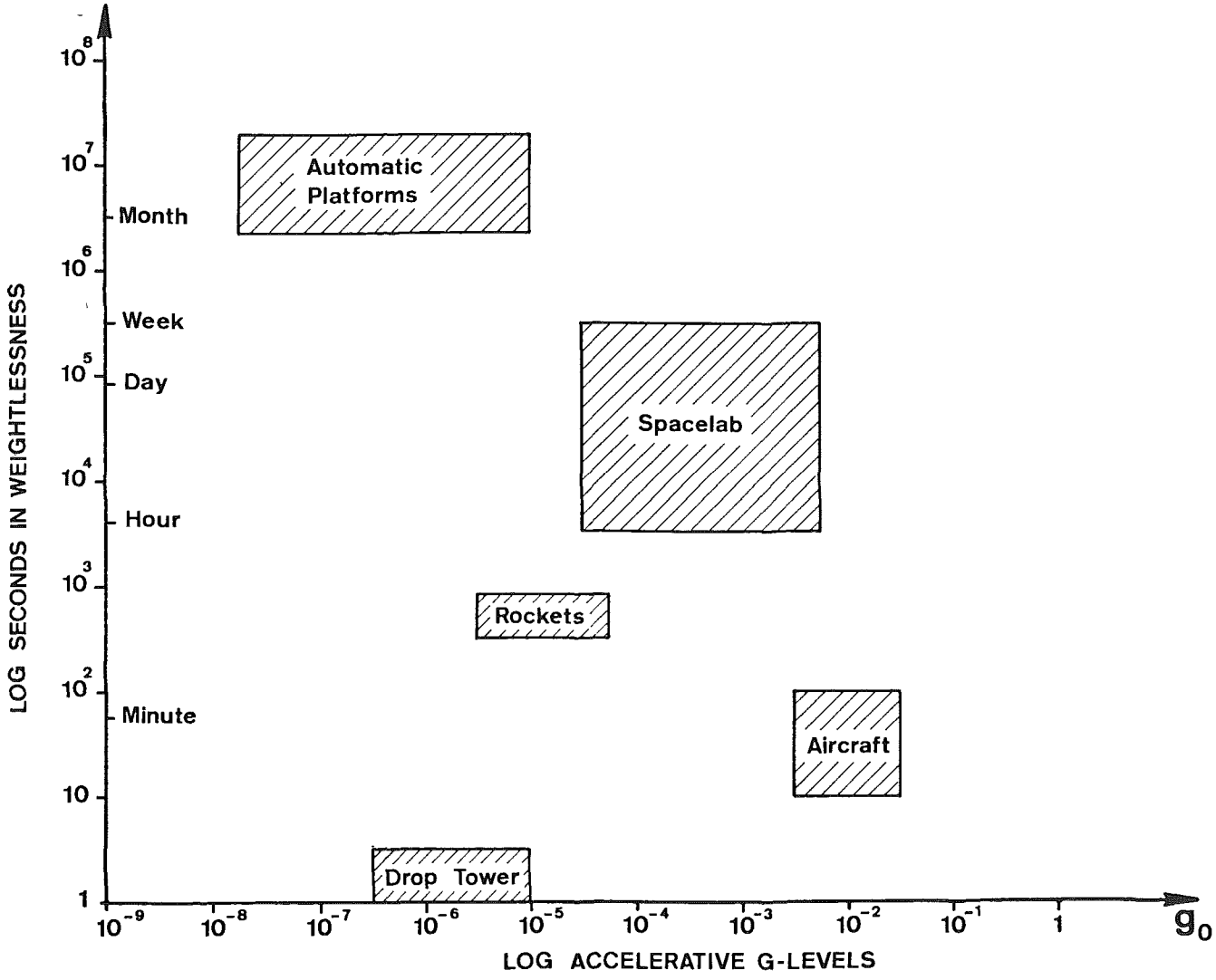

Figure 1.1. Nominal gravitational levels as a function of durations achievable with the main available microgravity platforms.

In an *inertially-fixed attitude spacecraft:*

- the residual gravity varies periodically in magnitude and direction during an orbital period (the relative positions in the earth's gravity field of the spacecraft's center of mass C and of the point P where the experiment apparatus lies vary, as shown in Figure 1.3, during an orbital period);
- the atmospheric drag likewise varies periodically in intensity (due essentially, aside from atmospheric density changes, to periodical changes of the spacecraft cross-sectional area normal to the direction of motion) and direction during an orbital period.

Conversely, in a *gravity-gradient stabilised spacecraft*, the residual gravity is constant in direction and magnitude, the atmospheric drag has constant direction and its possible magnitude changes are only due to density variations of the atmosphere. Timewise these contributions can be defined as quasi-steady.

Thruster firings needed to maintain orbit attitude introduce intermittent contribution to the effective gravitation. The number of firings depends rather strongly on the deadband setting and on the level of crew activity. Simulations of Spacelab mission flights (Fig. 1.2) predict, depending on the crew activity level, 25 to 80 thruster firings per orbit for a 1° deadband and 90 to 350 firings for a 0.1° deadband [Ref. 1.1].

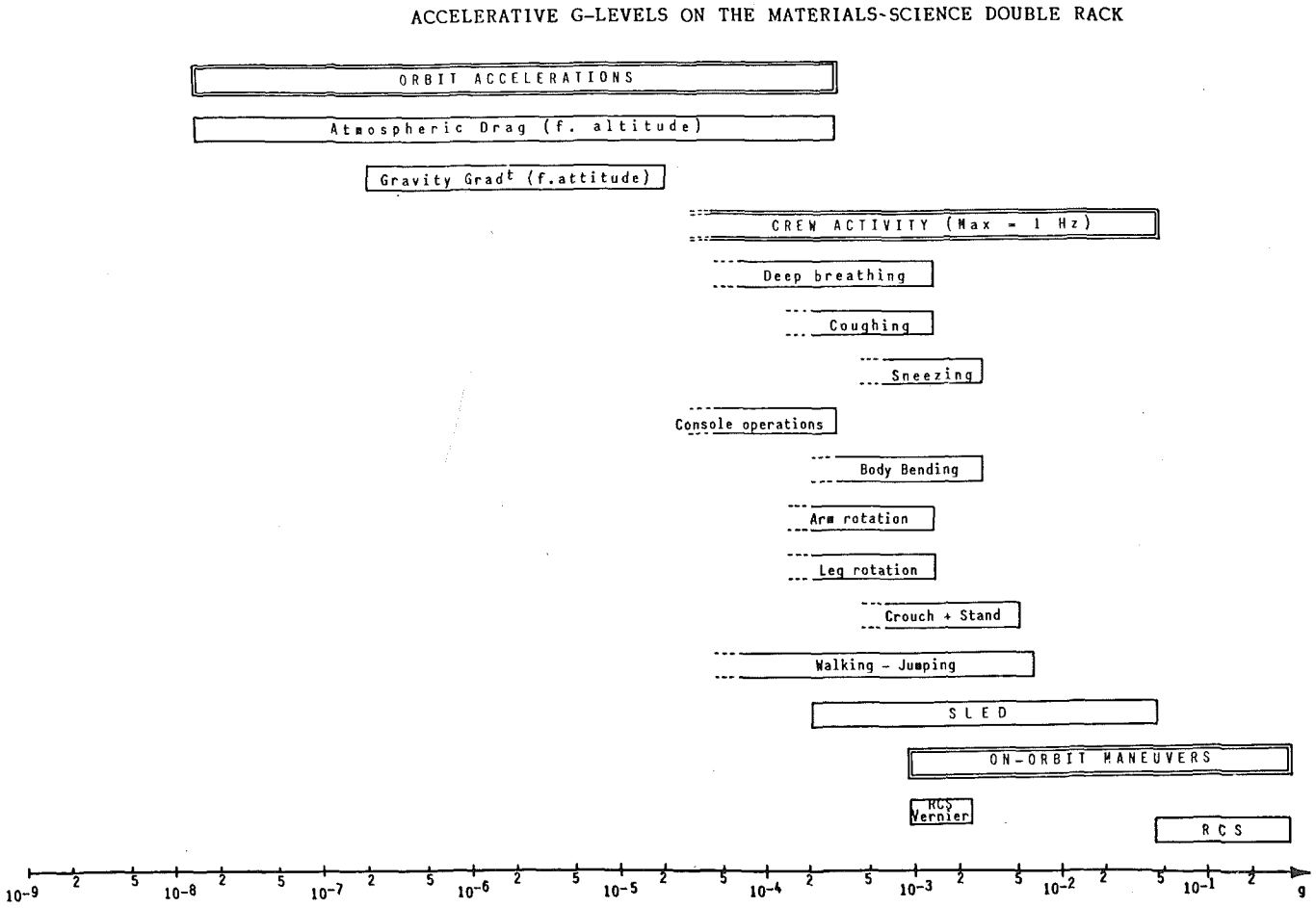

Figure 1.2. Orders of magnitude of the main factors being able to grade down the gravitational level of the STS-Spacelab system. Orbit accelerations are quasi-steady but their intensity and direction may vary during an orbital period. Crew activity gives rise to a random frequency band varying from 0.1 to 3 Hz. In-orbit manoeuvers are responsible for step function accelerations of various levels and directions.

Timewise these disturbances result in the imposition of net accelerations (torque averaging to zero over a sufficiently long period of time and force not necessarily averaging to zero, as a consequence of the thrusters locations and orientations). These forces may induce substantial transient motions in fluid bounded by container walls and in the position of free-floating bodies.

It is noteworthy to observe that any $10^{-3}\,g$ residual acceleration can induce a displacement of about 1 cm during the first second and that crew motion may induce stronger disturbances than thruster firings (Fig. 1.2).

The required g level and its acceptable 'quality' depend on the type of experiment and, for a number of them, the appropriate measures are not yet established on firm scientific grounds.

1.2 Main consequences

A microgravitational environment changes substantially the relative importance between the gravitational force and the other forces acting on an elementary mass but does not necessarily change the relative importance among forces other than gravitational. It opens up interesting basic and applied research areas, some of which already show potentialities for promising new processes.

Only a thorough detailed understanding of microgravity environment phenomenologies, which may be rather complex and substantially different from those occurring on earth, can lead to the knowledge necessary to take the fullest advantage of the positive features and to foresee and cope with the drawbacks. It is in this perspective that the main consequences of a microgravitational

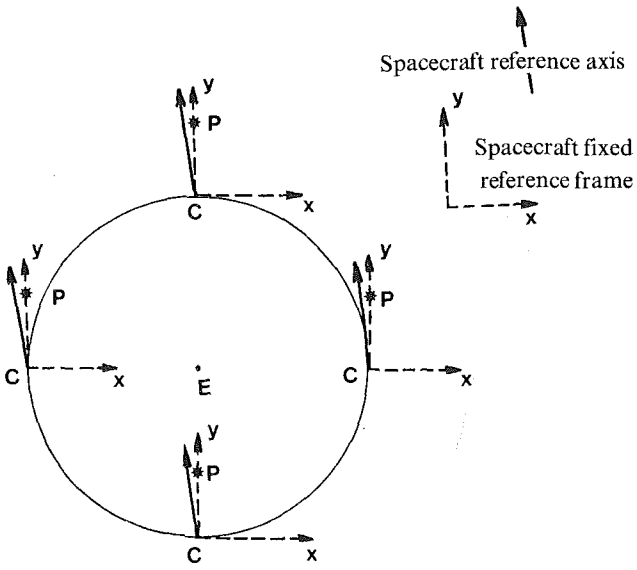

C: Spacecraft center of mass
P: Position of experimental apparatus
E: Earth's center

a) Inertially fixed attitude

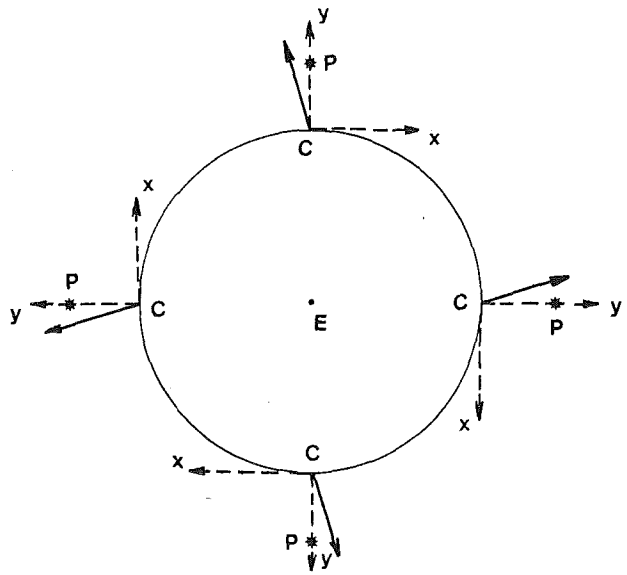

b) Gravity gradient stabilised attitude

Figure 1.3. Residual gravity contribution due to two possible attitudes of the spacecraft.

environment will be briefly discussed in a sequence that does not imply any order of importance since this clearly depends on the nature and goals of the investigation envisaged.

(a) Surface and contact line phenomena can acquire greater importance. Substantially higher floating zones, wider menisci, larger free, hanging or leaning drops or bubbles (and so on) can be achieved (§ 2.3). Also, interface instabilities (chapter 3) can be studied more readily and suitable models can be tested and validated. In general interfacial phenomena can be more efficiently investigated (§2.2 and 2.4).

(b) Natural convection in fluids can be greatly reduced in many configurations that imply gradients of temperature or concentration. This can lead to the formation or unusual extension of concentration boundary layers on both sides of an interface (§3.3). On the other hand flows driven by interfacial tension may become more prominent and new flow patterns be established that are to date not sufficiently investigated neither theoretically nor, a fortiori, experimentally (§2.4.4).

Situations in which surface effects are relevant are very often met also on earth. However, the combination of increased extension of interfaces and the potentially enhanced role of other forces opens up entirely new fields and revitalises some of the old ones. A case in point is the renewed interest in the thermodynamics and dynamics of surface and line phases (§2.2.3) including those that are far from equilibrium conditions.

(c) Microgravitational environment offers a chance for gaining deeper knowledge on a number of phenomena due to forces whose effects, on earth, are negligible (and therefore cannot be studied experimentally in the needed depth) compared to those due to gravity. Thus, for instance, material properties and cohesion and adhesion forces can be better and more efficiently studied. Particle transport phenomena due to forces other than gravitational, whose theoretical importance and practical relevance is discussed in §2.5, can likewise more conveniently be investigated.

(d) The possibility of achieving more homogeneous single-phase systems in a microgravitational environment offers unprecedented chances for

experiments of very fundamental nature in systems undergoing transitions between qualitatively different states which may be so sensitive to gravity to the point where their true behaviour cannot be studied at earth gravity level (§3.1.1 and 3.1.2).

The degree of freedom afforded in attaining arbitrary particle distributions in multiphase systems explains the interest that scientists working on composite materials are increasingly taking in microgravity experiments. On the other hand, the near annihilation of the main driving force acting on suspended particles renders their distribution very 'stiff'. It would thus take considerable time to render uniform a distribution 'prepared' in an earth environment (§2.5).

(e) Possibilities for containerless positioning are enhanced since it can be achieved with compensating forces of relatively low intensity. This reduces disturbances by side-effects such as inhomogeneous heating, vibration, generation of convection, deformation and splitting of the sample. The elimination of contact helps to avoid undesirable effects that container's walls may have, such as chemical contamination or heterogeneous nucleation. It is thus of particular interest for studies on melts of materials with high melting points for which non-contaminating containers may not exist.

However, even under reduced gravity containerless processing of liquid or solid presents its shortcomings. Advantages and drawbacks of the more promising containerless positionings are summarised in §6.3.

The microgravity environment brings chances to any materials scientist curious enough to get access to new or up to now hidden second-order phenomena. But each chance introduces its own counterpart, and thus there is a need for such scientific pioneers *to forget the conventional limits of their former field of excellence.* The advantages of space-borne experiments cannot be gained without taking into account the corresponding constraints and possible traps, and even the simplest experience will require an extensive pre-flight and post-flight methodical effort, running over the intellectual eases of a priori opinions. In this whole spectrum of necessarily new attitudes or approaches lies in essence the challenge and the appeal of Microgravity Materials Science.

2 Phenomena and/ or Physical Mechanisms

2.1. Forces acting under microgravity

In a microgravity environment, the types of forces acting on a particle are not different from those existing in any other environment. Nevertheless, it is worthwhile to consider them briefly for two reasons. Firstly, to recognise the achievable levels and their qualities, one needs to analyse in some detail the different contributions to the residual gravitational vector and the factors that influence them. Secondly, it is convenient to have a list of all possible forces acting on a particle because, as already mentioned in § 1.2, some of them may acquire considerable relevance in a microgravity environment as their effects are no longer masked by a 'strong' gravity field.

The contributions to the residual gravity are shown schematically in Figure 2.1 and listed, together with their main influencing factors, in Table 2.1. Similarly, the forces acting on a particle in a microgravity environment are listed, together with their influencing factors, in Table 2.2.

2.2 Surface tension and related topics

In the presence of reduced gravity, interfaces may increase in extent and the forces acting on them acquire greater relevance. A clear understanding of surface phenomena and, in particular, of surface tension, is consequently needed.

2.2.1 *The interphase layer*
Two immiscible bulk (or volume) phases are separated by an interphase layer, whose thickness is usually a few molecular diameters, through which the properties vary 'smoothly' from one phase to the other. Modelling the interphase layer at either the molecular (microscopic) or phenomenological (macroscopic) level is still, to a large extent, an open problem. Even less well established is the bridging between the microscopic and macroscopic descriptions of its properties.

The interphase layer is an open system that may exchange mass, momentum and energy with the adjoining volume phases. At the macroscopic level it may be modelled as a surface whose properties depend on the relevance, nature and characteristics of its interaction with the bulk phases.

When this interaction is negligible, the surface can be assumed to be a purely geometrical massless surface devoid of any thermodynamic property. This is most often the case for gas/solid interfaces. When volume

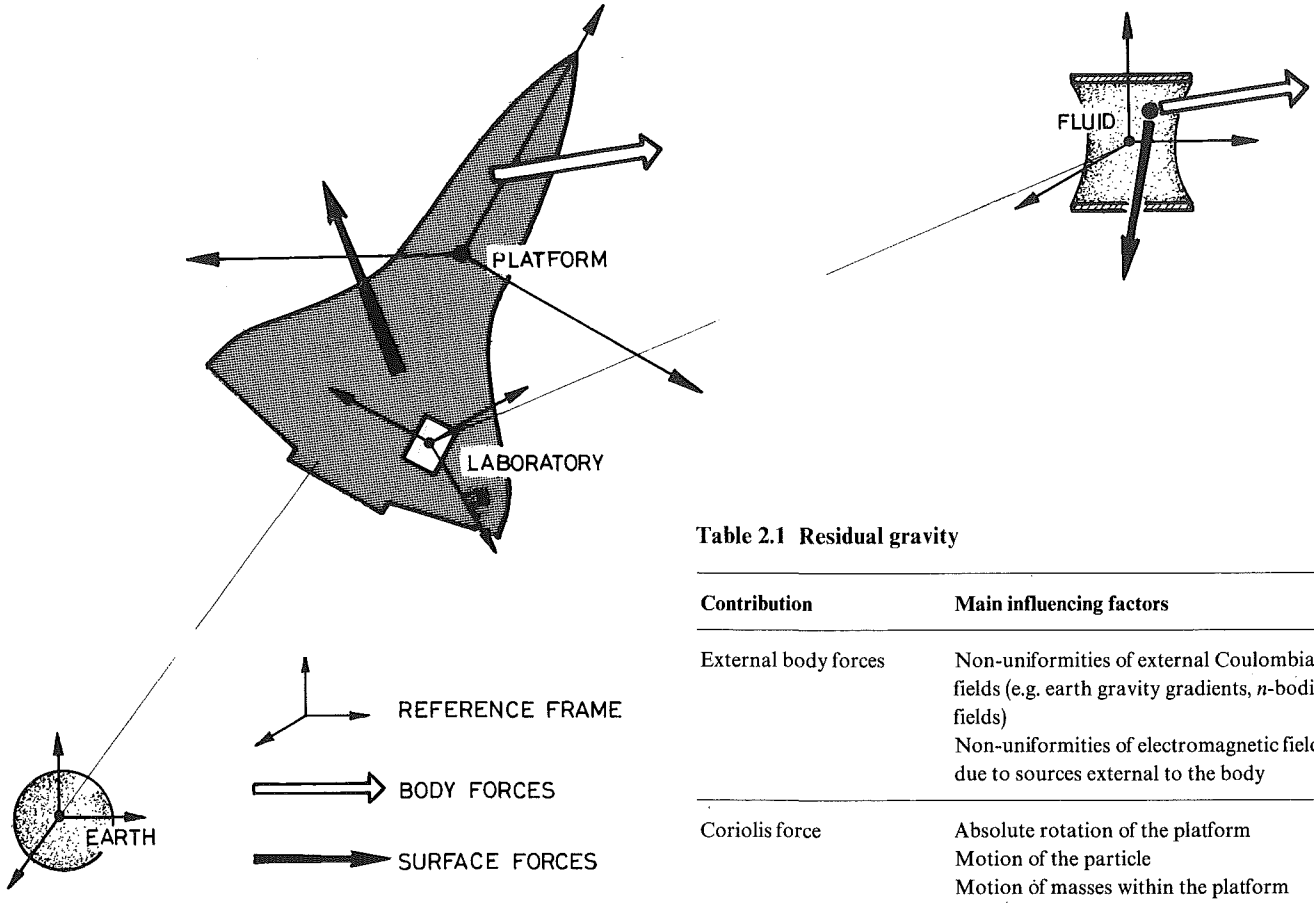

Figure 2.1. Body and surface forces acting on a space platform and on a fluid particle.

phases are quiescent, uniform, homogeneous and in thermodynamic equilibrium with the layer, the classical Gibb's dividing surface model (and generalisations thereof) apply [2.1], implying free energy but no mass (Fig. 2.1 bis).

In more complex situations a more general model must be adopted. The current approach relies on the applicability of 'local formulations [2.2] and (formally) develops thermodynamic and dynamic theories (e.g. balance equations) of the surface phase which duly account for irreversible exchanges between surface and volume phases, surface irreversibility (to within a linear approximation) and arbitrary surface motion [2.3].

A number of phenomena still need to be incorporated in these models, such as, for instance, phase transitions within the layers, formation of interfaces and their 'aging', magnetic phenomena, micropolar liquids, and so on. But, most of all, there is an urgent need for more

Table 2.1 Residual gravity

Contribution	Main influencing factors
External body forces	Non-uniformities of external Coulombian fields (e.g. earth gravity gradients, *n*-bodies fields) Non-uniformities of electromagnetic fields due to sources external to the body
Coriolis force	Absolute rotation of the platform Motion of the particle Motion of masses within the platform Vibrations of laboratory frame
Centrifugal force	Absolute rotation of the platform Distance of particle from platform's center of mass
Other d'Alembert forces	Rotation of laboratory frame relative to the platform frame Motion of masses within the body Vibrations Jitters Moments of external fields of forces Moments of forces acting on external surface of the body Time rates of change of the platform's configuration
Forces acting on external surface of platform	Aerodynamic forces Radiation pressure Solar winds More generally: forces due to electromagnetic stresses
Reaction forces on platform	Motor bursts Thrusts Venting

Table 2.2 Other forces acting on fluid particle

Type	Main influencing factors
d'Alembert	Motion of masses within the body Vibrations *g*-jitters Rotation of fluid frame relative to laboratory frame Particle's velocity relative to fluid frame Rotation of fluid frame relative to platform frame Time rates of change of rotation of laboratory frame relative to platform frame
Coulombian	Attraction between masses within the body Cohesion and adhesion forces
Electromagnetic	Forces on charged particles Forces due to: Electric polarisation Magnetic polarisation Electrostriction Magnetostriction More generally: forces due to spatial non-uniformities of electric and magnetic polarisations Lorentz forces
Surface forces	Thermodynamical pressure Elastic stresses Viscous stresses (laminar fields) Reynolds stresses (Turbulent fields) Non-symmetric tangential stresses (micropolar fluids) Electromagnetic stresses Interaction with other fluids (multi-phase system) Stresses from adjoining volume phases Thermodynamic interfacial tension Gradients of interfacial tension Additional surface stresses: Non-equilibrium surface tensions Elastic stresses Viscous stresses Electromagnetic stresses
Reaction forces	Evaporation, condensation, and other phase-changes Degassing or other convective mass transfer across the fluid particle surface

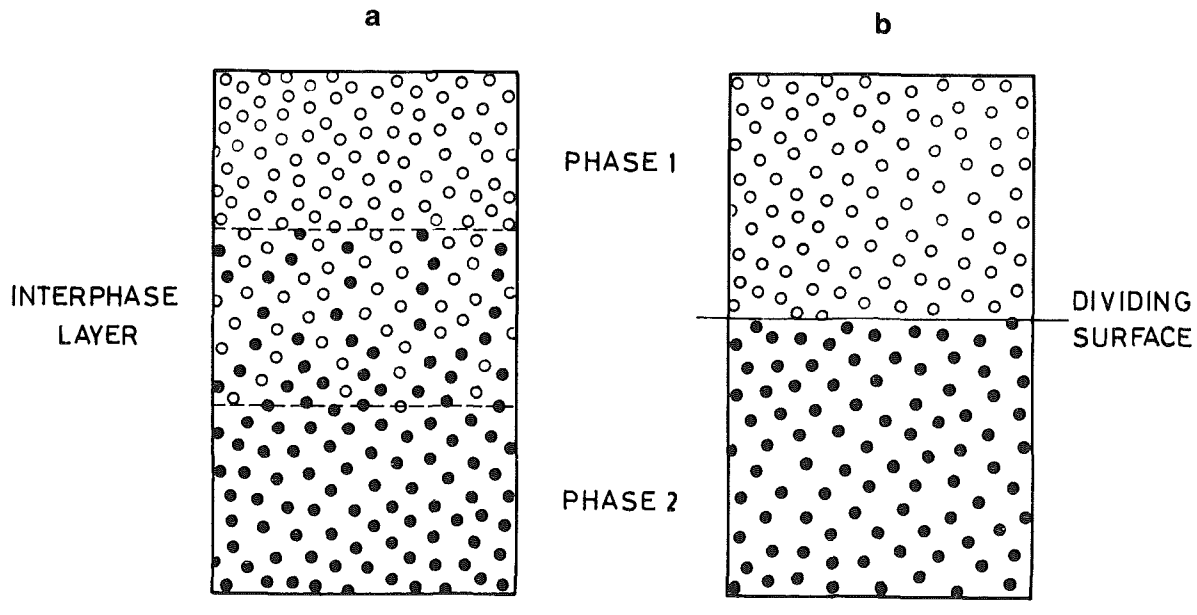

Figure 2.1bis The interphase layer separating two bulk plases (a) and the ideal dividing surface in the Gibb's model (b).

accurate experiments both for validating the theoretical models and assessing their limits of validity and for determining the equilibrium and non-equilibrium thermodynamic properties (e.g. equations of state, surface viscosity coefficient, other surface transport properties and so on) of the interfaces.

2.2.2 *Interfacial tension*
On any line element of a non purely geometrical interface there acts a normal stress per unit length (which is the counterpart of the normal stress acting on any surface element in a volume phase) usually referred to as surface tension (for liquid/vapour systems) or interfacial tension (for the other systems).

Surface tension is a component of the surface stress tensor. It is usually assumed that in static conditions this tensor reduces to an isotropic tensor, i.e. the normal stress at one point on the surface is independent of the orientation of the line element with respect to the gravity vector, and there is no reaction to deformations of the 'shape' of surface elements. The limits of applicability of this assumption are not well investigated. In principle (cf. micropolar fluids) the 'reversible' part of the stress tensor may even be non symmetric.

When local (and, a fortiori, global) formulations of thermodynamics are applicable, one can define a *thermodynamic* surface tension which is a surface property depending on the thermodynamic parameters characterising the state of the surface. It plays, for surface phases, the same role as that played by thermodynamic pressure in volume phases and can thus be defined as the partial derivative of any appropriate surface thermodynamic potential (e.g. surface internal energy) with respect to the area.

Surface tension has the dimensions of energy per unit area: hence the thermodynamic surface tension coincides with the surface energy in grand potential [2.3], whose physical meaning depends on the number of thermodynamic degrees of freedom of the interface. Thus, for instance, when the interface has only one intensive degree of freedom (single component interface layer in equilibrium with the adjoining bulk phases) the thermodynamic surface tension is the Helmholtz free energy of the surface and is a function only of its absolute temperature.

The distinction between the two notions of surface tension (as a surface normal stress or as a well-defined property of the local thermodynamic state of the interface) should always be kept in mind. Much as in volume phases, the thermodynamic pressure, even when it can be defined, may be only one part of the 'measured' surface normal stresses. Additional contributions may be present which, being due to irreversible phenomena, depend not only on the values of the intensive state parameters of the surface, but also on their gradients and on the difference between them and the analogous parameters of the adjoining bulk phases [2.3].

This subject is almost entirely unexplored and continuing experimental investigations on earth have not exhausted the field. Many questions are still open (equations of state, phase equilibria, thermodynamic stability) and quantitative findings are limited and often affected by uncertainty. The fact that the interface is not autonomous but, on the contrary, that it may be rather strongly coupled with the adjoining bulk phases does certainly not make things easier.

In the present state of knowledge, one can make the following statements concerning thermodynamic surface tension: it is *usually* positive; it is *usually* a decreasing function of the absolute temperature; and it *may be* strongly affected by the presence of contaminants, even in very small concentrations.

Orders of magnitude of σ and σ_T for liquid/gas systems are given in Table 2.3 for liquid metals, organic liquids, molten salts, silicon oils and other miscellaneous liquids [2.4]. Values of σ_T are less accurate, in general, than those of σ.

In a microgravity environment a more detailed knowledge of interface phenomena, and in particular, of the temperature and composition variation of σ (σ_T, σ_C) is required.

As outlined in § 1.2, the decreased gravity level raises the importance of the other forces. This is also true for the forces acting on the interface.

Those due to the surface tension belong to two main types:
(a) The first type acts at right angles to the interface and depends on the latter's mean curvature. Under hydrostatic conditions, as discussed in more detail in § 2.3.2, it balances the Archimedean forces on the fluid volumes partially bounded by the interface. Its increased relevance in the microgravity environment thus allows the 'containment' of greater volumes.

(b) The second type acts tangentially to the interface and is due to surface tension gradients (associated with

Table 2.3

	Dynamic viscosity μ g/cm. s	Kinematic viscosity ν cm^2/s	Thermal diffusivity α cm^2/s	Heat capacity c_p	Thermal expansion β_T K^{-1}	Surface tension σ_0 dyne/cm	Th. coeff. of surface tension σ_T dyne/cm	Prandtl number Pr	Bond length L_b cm
Liquid metals	$10^{-3}-10^{-2}$	$10^{-3}-10^{-1}$	$10^{-2}-10^{0}$	$10^{-2}-10^{-1}$	$10^{-5}-10^{-4}$	$10-10^{3}$	$10^{-2}-10^{-1}$	$10^{-3}-10^{-1}$	0.2–0.5
Organic liquids	$10^{-3}-10^{-2}$	$10^{-3}-10^{-2}$	$10^{-4}-10^{-3}$	10^{-1}	10^{-3}	10	$10^{-2}-10^{-1}$	1–10	0.1–0.3
Molten salts	10^{-2}	$10^{-3}-10^{-2}$	10^{-3}	10^{-1}	10^{-4}	10^{2}	10^{-2}	10	0.2–0.3
Silicone oils	$10^{-3}-10^{0}$	$10^{-2}-10^{1}$	10^{-4}	10^{-1}	10^{-3}	10	10^{-2}	$10-10^{4}$	0.1
Water	10^{-2}	10^{-2}	10^{-3}	10^{0}	10^{-4}	10^{1}	10^{-1}	10	0.2
Molten glass	10^{2}	10^{2}	10^{-2}	10^{-1}	10^{-4}	10^{4}	10^{-2}	$10^{3}-10^{4}$	0.5
Air $p=1$ atm; $T=300$ k	1.85×10^{-4}	1.6×10^{-1}	2.24×10^{-1}	2.4×10^{-1}	3.3×10^{-3}				

Liquid metals: Sb, Ce, Cs, Cu, Ga, Ge, Au, Li, Mg, Hg, Se, Si, Ag, Na, NaK
Organic liquids: Acetone, Benzene, Butyl alcohol, Ethyl alcohol, Ethyl iodide, Hexane, Hexadecane, Nitrobenzene, Nonane, Octane
Molten salts: Sodium chloride, Sodium hydroxide, Sodium nitrate, Potassium chloride, Potassium nitrate, Potassium chromate, Lithium chloride, Lithium nitrate, Silver nitrate, Zinc chloride
Silicone oils: 1 CS, 5 CS, 10 CS, 100 CS, 1000 CS Silicone oils

All values are issued from [2.4]

the gradients of surface state parameters such as temperature, composition and so on) and may be referred to as 'Marangoni force'. Its presence induces motion in the adjoining bulk phase (so-called surface-driven or Marangoni flows). The phenomenology of this motion may be complex for a number of reasons, the most important being:

- velocity, temperature and composition fields are coupled;
- force balances in volume and surface phases involve Marangoni, buoyancy, viscous, inertia and pressure forces whose relative importance may be substantially different under different conditions;
- bulk phases are often bounded both by interfaces and solid surfaces and the flow features in neighbouring regions may differ substantially from those near the interface and/or in core regions, and so on.

2.2.3 *Contact angles and contact lines*

When three different volume phases meet, their interphase layers overlap in a confluence region the modelling of which presents the same problems and features as that of the interphase layers (§ 2.2.1). The simplest model consists of a contact line defined by the intersection of the confluent interfaces.

Figure 2.2 shows the case in which a solid, a liquid, and a gas volume phase meet. Figure 2.3 shows the case in which two liquids and one gas phase meet.

As for interphase layers, more sophisticated phenomenological models of a confluence region, where the three interphase layers overlap, have been proposed [2.5]. Many questions as to the applicability of the different models and their ability to describe the dynamics of contact lines are still entirely open and will not be addressed in detail here.

In Figure 2.2. θ is the contact angle, which is measured from the liquid side of the contact line. Wetting or non-wetting conditions correspond to $\theta<\pi/2$ or $\theta>\pi/2$, respectively. Wettability and contact angles as defined here are static properties of a given liquid/solid couple or even of a liquid/liquid/solid triplet.

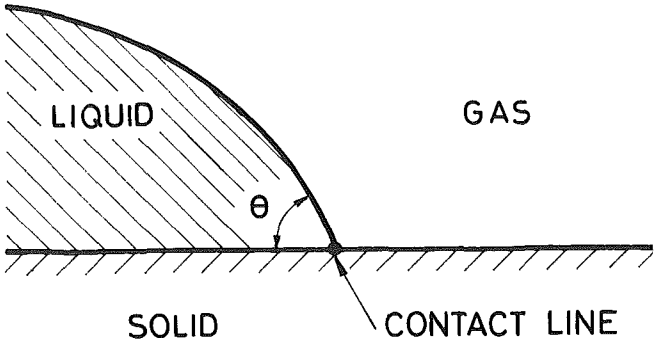

Figure 2.2 The contact line and the contact angle which appear when a solid, a liquid and a gas meet.

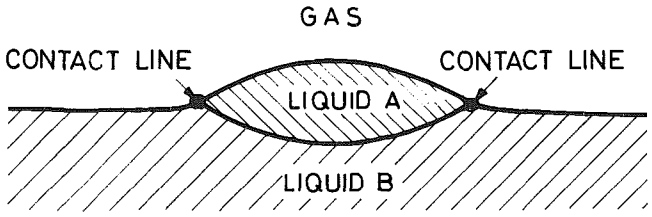

Figure 2.3 The contact line which appears when two liquids meet with a gas.

Whether or when or to what extent these properties are maintained under dynamic conditions are open questions. In addition, spaceborne microgravity experiments have produced evidence of changes in wettability (§ 4.2.1).

So far the contact line has been assumed to be at rest. Normally the contact line advances (the heavier liquid spreads on the surface) or recedes, and the contact angle depends on contact line velocity, U. The extrapolated value of θ as $U \to 0$ is called the advancing (when $U = 0^+$) or receding ($U = 0^-$) contact angle. Both values are normally different, and this peculiarity is often referred to as contact-angle hysteresis.

Contact-angle hysteresis is usually attributed to roughness (Fig. 2.4) and/or to heterogeneity of the surface (Fig. 2.5). Since any surface is rough and heterogeneous on a molecular scale, but there is no contact-angle hysteresis on certain well-prepared solid surfaces, a critical size of rugosities and heterogeneities must exist below which no contact-angle hysteresis appears. This critical size depends [2.6] on the type of

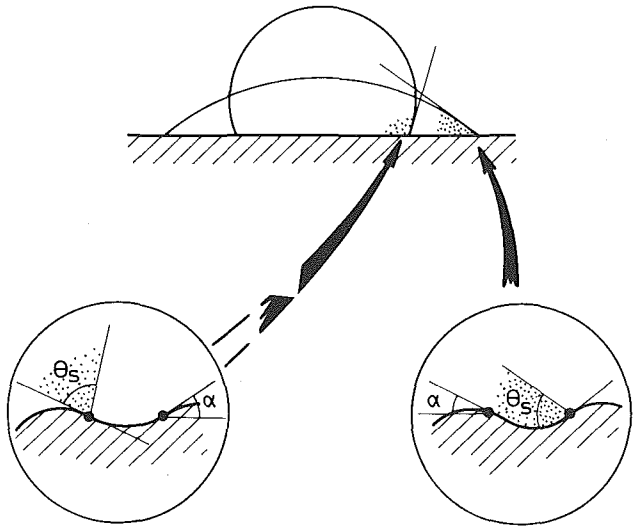

Figure 2.4 The non-uniqueness of contact angle explained on the basis of surface roughness. Although the surface looks flat and smooth on a length scale of the order of the drop radius, it exhibits small scale ondulations. Even if the actual contact angle is unique, the observed contact angle will be bounded from above and from below by $\theta_s \pm \alpha$. From [2.5].

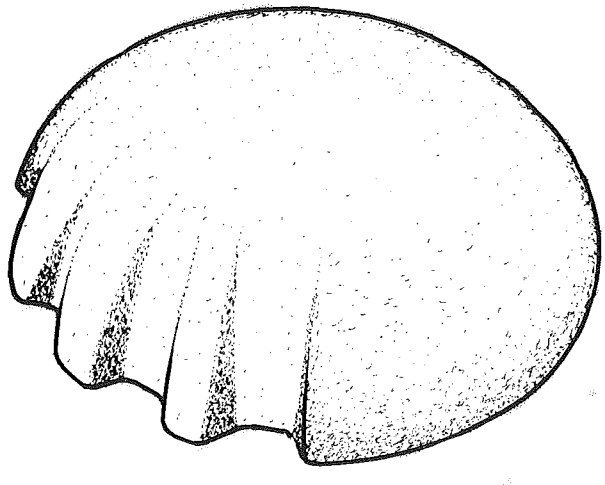

Figure 2.5 Schematic of a liquid drop leaning on a heterogeneous solid surface. Contact angle hysteresis arises when the line of contact cuts across varying percentages of the two types of surfaces [2.6].

the system and shape of the rugosities. Whether or not the gravity level has any effect on the critical size is a matter of controversy, but there is some confidence that microgravity experiments would throw some light on these problems.

Complete wetting (zero contact angle) must occur near (thermodynamic) critical points [2.7]. When two fluid phases are near a critical point in the presence of any third phase, a wetting film of one of the critical phases will separate the other two phases. Interface phase transition from complete wetting of the third phase to incomplete wetting can be induced by changing the temperature or by adding a new component to the fluid phases, in order to drive the two phases away from their critical point.

2.2.4 *Spreading of a liquid on a solid surface*
Considerable controversy exists on the details of the fluid bulk motion near a moving contact line. Notice that spreading must be compatible with no-slip at the wall. According to experiments [2.8], the moving interface rolls on or unrolls off the solid.

The macroscopic analysis of the fluid motion near a moving contact line shows that the stress in the boundary becomes infinitely large. This cannot be traced back to any kinematic incompatibility between spreading and no-slip [2.8]; rather, it is related with the use of the Navier-Stokes equations and the no-slip boundary condition.

Since the molecular analysis of the fluid region close to the contact line is exceedingly difficult, Huh & Scriven [2.9] suggested that the overall effect of this region on the flow pattern could be assessed by postulating that the fluids slip along the solid boundary. This trick has been used in rarefied gas flow, but there the procedure can be justified, and a slip coefficient estimated, whereas no rational justification appears possible here.

A different approach, based on a rough solid boundary, whose roughness height is smaller than the size of the fluid container, but larger than the molecular scale, has been considered by Hocking [2.10]. It is shown that, in an inner region near the contact line, the effect of the irregularities can be accounted for by imposing a slip boundary condition, while the outer region is calculated by assuming no-slip. The force singularity at the contact line is thus removed [2.11].

Several slip boundary conditions could, in principle, be imposed. Dussan [2.12] has shown, however, that the outer flow where almost all fluid mechanical measurements are made, is quite insensitive to the form of these boundary conditions. This is a rather discouraging conclusion, since it indicates that the mechanism of motion of the contact line cannot be elucidated by macroscopic measurements.

2.3 Hydrostatics

Hydrostatics deals with fluid masses at rest in a given reference frame (inertial or non-inertial).
Key problems addressed are:
- Conditions under which motion is absent.
- Shapes of deformable surfaces bounding the fluid.
- Stability of hydrostatic equilibrium configurations.

2.3.1 *Hydrostatic conditions*
In non-elastic quiescent fluids, the only surface forces acting on an elementary volume are those due to pressure gradients, ∇p. They balance the body force (per unit volume) $\rho\mathbf{f}$ where ρ is the density and the force per unit mass $\mathbf{f}$ includes, in addition to the gravitational force, g, the relevant d'Alembert forces in the frame in which the fluid is at rest.

When $\mathbf{f}$ is conservative, hydrostatic equilibrium is attained only if the density gradient, $\nabla\rho$ is parallel to $\mathbf{f}$. The equilibrium is usually stable when $\nabla\rho$ has the same sense as $\mathbf{f}$ and then its magnitude is irrelevant; it is unstable in the other case and then its magnitude is relevant (Fig. 2.6).

Density gradients can be due to gradients of temperature, composition, or both. Instability of stratified media is usually referred to as convective instability and will be briefly considered in § 3.2.2.

When the frame's angular acceleration is other than zero, $\mathbf{f}$ includes a non-conservative part. The necessary conditions for hydrostatic equilibrium are then less simple, as they involve both the direction (which is no longer parallel to $\mathbf{f}$) and the intensity of the density gradient (mathematically these conditions read

$$\nabla\rho \wedge \mathbf{f} + \rho\nabla \wedge \mathbf{f} = 0).$$

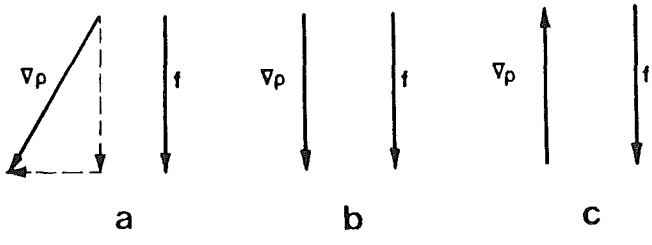

Figure 2.6 Equilibrium conditions for conservative body forces. In (a) there is a motion driven by the lateral component of $\nabla\rho$. (b) and (c) correspond to hydrostatic equilibrium configurations, but while in (b) the equilibrium is usually stable, it is unstable in (c).

Thus, for instance, neither a density gradient non-parallel to a non-conservative body force, nor a uniform density are compatible with absence of motion. Particular care should then be exercised when planning hydrostatic experiments: the platform should not have any angular acceleration (an angular acceleration of the platform of about 6 revolutions/min^2 yields an acceleration of $10^{-3}\,g$ at a point 1 m from its centre of mass).

Additional necessary conditions for hydrostatics hold when interfaces are present. They require that the surface tension be uniform, since any gradient of surface tension leads to Marangoni forces (§ 2.4.1) that induce motion on the interface and, consequently, in the bulk phases.

Examples of equilibrium hydrostatic configurations are discussed in § 2.3.2. Their stability is dealt with in § 2.3.3 and 3.2.1, with specific reference to liquid bridges.

2.3.2 *Equilibrium shapes. Bond characteristic length*

In hydrostatic equilibrium, the surface tension, σ, is uniform and the only forces acting on an element of interface separating two bulk phases are those due to σ and to the pressures of the bulk phases (Fig. 2.7). The equilibrium between surface tension and pressure forces is expressed by the Laplace equation

$$\sigma\left(\frac{1}{R_1}+\frac{1}{R_2}\right)=\delta p \qquad (2.1)$$

where R_1 and R_2 are the two principal radii of curvature at the point Q and δp is the bulk phase's pressure jump across the interface. δp is often known as capillary pressure.

Both radii of curvature are perpendicular to the interface and lie in mutually orthogonal planes. The quantity in parenthesis is twice the mean curvature, K, of the interface at Q.

In many instances the signs of R_1 and R_2 are different, as in a saddle (Fig. 2.8). Then the pressure is larger on the side of the interface on which lies the centre of curvature of the smallest radius of curvature. When, in addition, $|R_1| = |R_2|$, the mean curvature is zero and the bulk phase pressures on each side of the interface are equal (Fig. 2.9).

When hydrostatic pressure is relevant, the pressure jump δp varies in the direction of g as, if σ is constant, does the mean curvature K. For constant densities and magnitude of g, this variation is linear and proportional

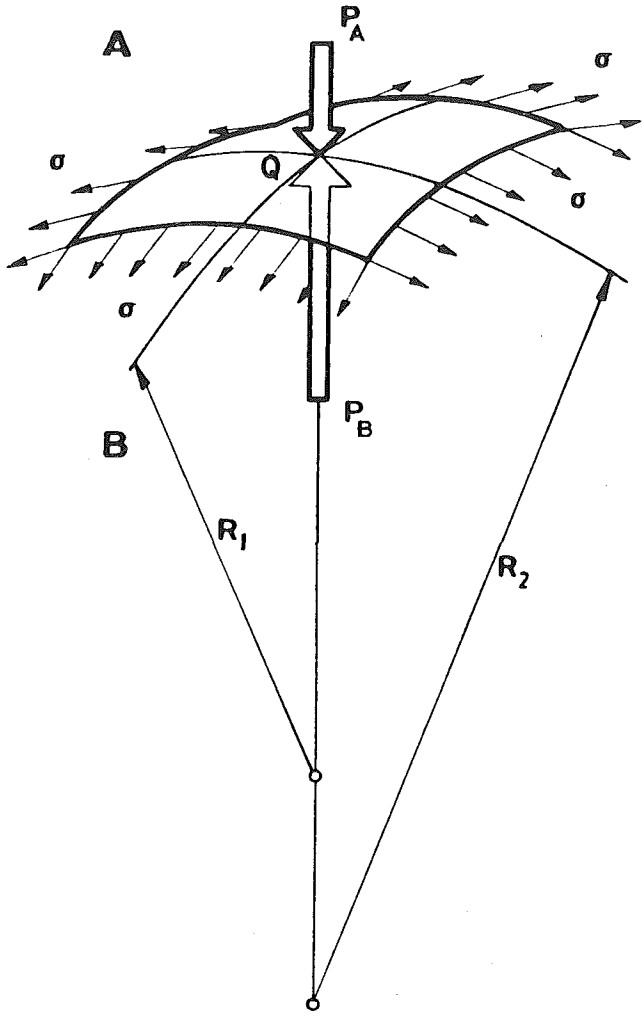

Figure 2.7 Hydrostatic equilibrium on an element of interface.

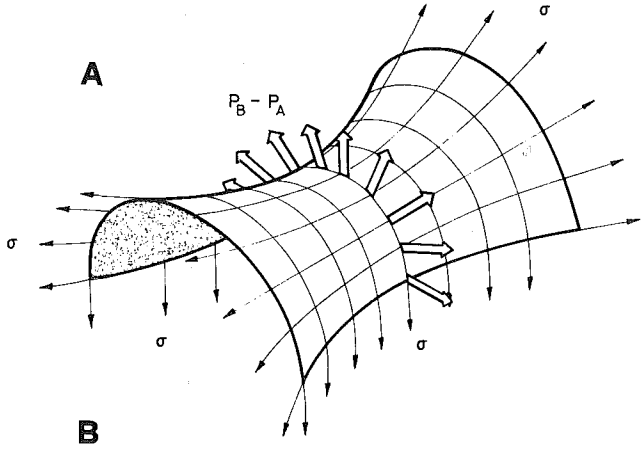

Figure 2.8 A saddle-like element of interface exhibiting two principal radii of curvature with different signs.

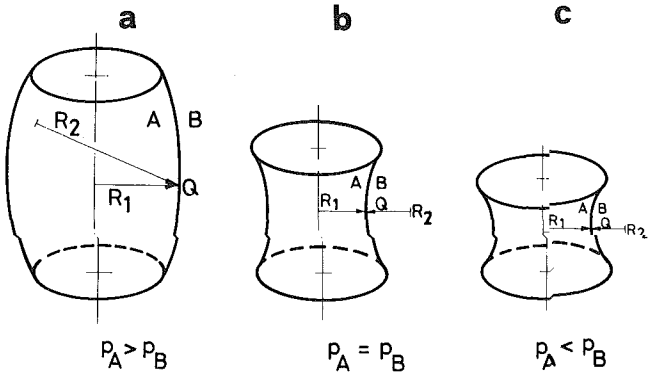

Figure 2.9 The capillary pressure δp depends on the surface tension, σ, and on the mean curvature, K, of the interface. The figure shows the two principal radii of curvature at point Q of the interface in several representative cases. In hydrostatic equilibrium, and assuming that gravity effects are absent, $p_A - p_B$ and, hence the mean curvature of the interface, are uniform in each case.

to g and to the density difference, $\delta\rho$, between the two bulk phases

$$\delta p = \delta p_0 + \delta\rho\, g(z_0 - z) \tag{2.2}$$

where subscript $_0$ indicates reference level conditions and z is the coordinate in the direction and sense of $-g$.

The interface mean curvature is constant along equipotential curves (z = constant) and throughout regions in which the variations of δp can be neglected.

Several surfaces of constant mean curvature are known: planes, circular cylinders, spheres, nodoids and unduloids. The only axisymmetric surface with zero mean curvature is the catenoid, generated by a catenary curve rotating around an axis normal to the axis of symmetry of the catenary. Other surfaces of constant mean curvature can be found in [2.13].

The (static) Bond number measures the relative importance of gravitational and surface tension forces in hydrostatics. The order of magnitude of gravitational forces is $\delta\rho\, gL$, where L is the extent of the interface in the direction of g or its distance from the equipotential surface on which the two fluids have the same pressure (Fig. 2.10). That of the surface tension forces is σ/R, where R is the smallest radius of curvature of the interface. Hence the Bond number can alternatively be written as:

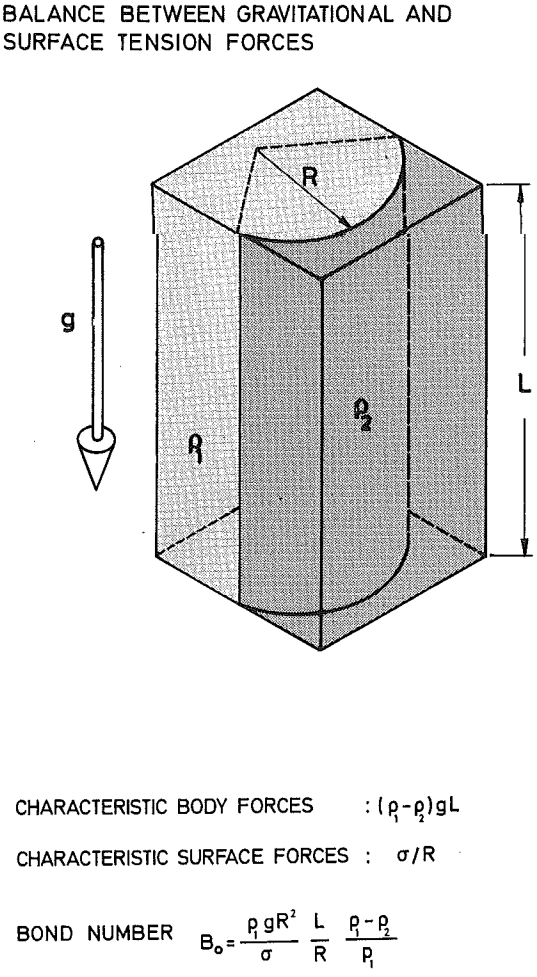

Figure 2.10 The two characteristic lengths which appear in the definition of the static Bond number.

$$Bo = \frac{\delta\rho\, gL}{\sigma/R} = RL\,\frac{\delta\rho}{\rho_1}\,\frac{\rho_1 g}{\sigma} = \frac{RL}{L_b^{\,2}}\,\frac{\delta\rho}{\rho_1} \tag{2.3}$$

where ρ_1 is here the density of the denser fluid and $L_b = \sqrt{\sigma/\rho_1 g}$ is the so-called Bond characteristic length, which is scaled as the inverse square root of the gravity level. For liquid/gas systems ρ_1 is the density of the liquid, and $\delta\rho/\rho_1 \simeq 1$. For most liquids of interest, L_b is of the order of 10^{-1} cm on earth and of the order of 10 cm in a typical Spacelab environment ($g/g_0 \simeq 10^{-4}$).

Gravitational effects are negligible (and hence the interface mean curvature is constant) when $Bo \ll 1$. This will be discussed further in § 2.3.4 which deals with the conceivable alternative ways to get $Bo \ll 1$.

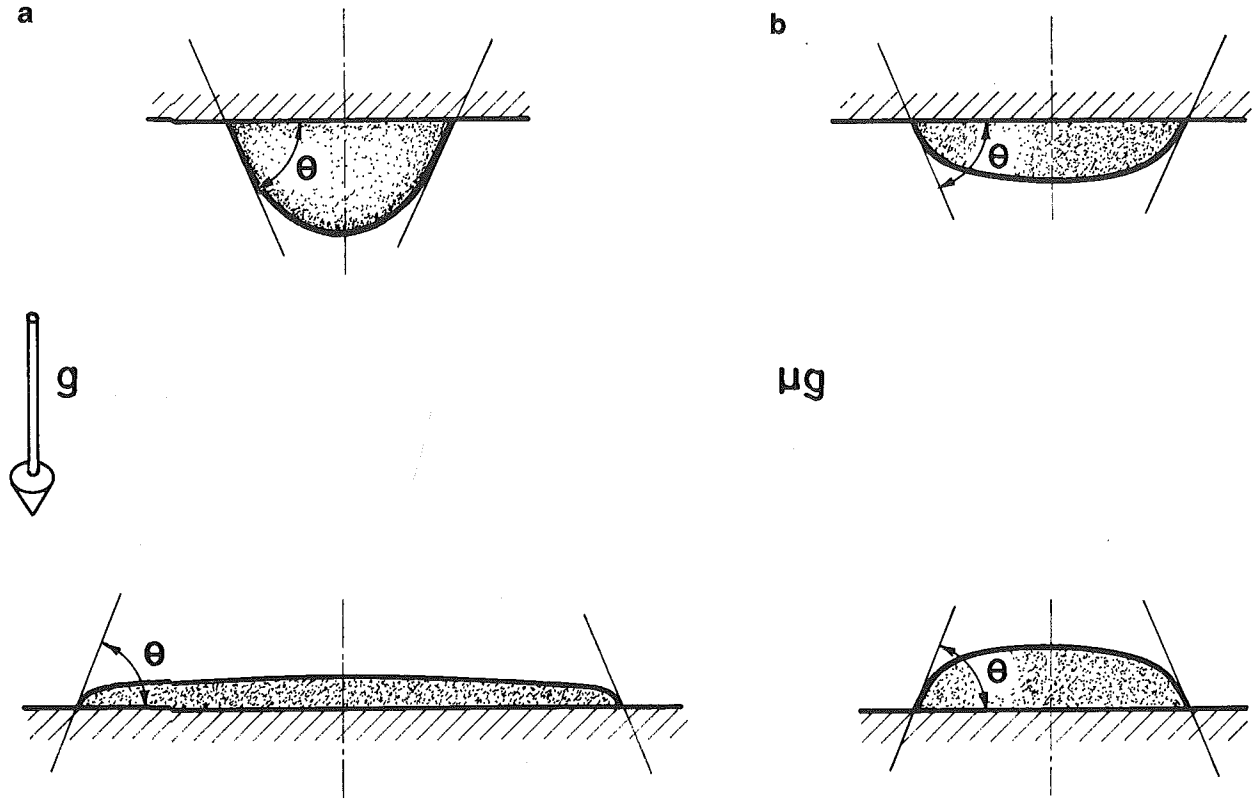

Figure 2.11 Hanging and leaning drops in a normal gravity field (a) and under microgravity conditions (b). The liquid volume is the same in all cases.

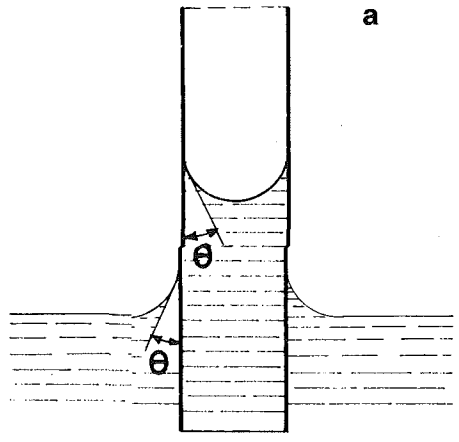

The determination of the equilibrium shapes attained by confined or partially confined fluid masses requires the solution of the Laplace equation subject to appropriate boundary conditions along the curves defined by the intersection between interface and solid boundaries (Figs. 2.11, 2.12).

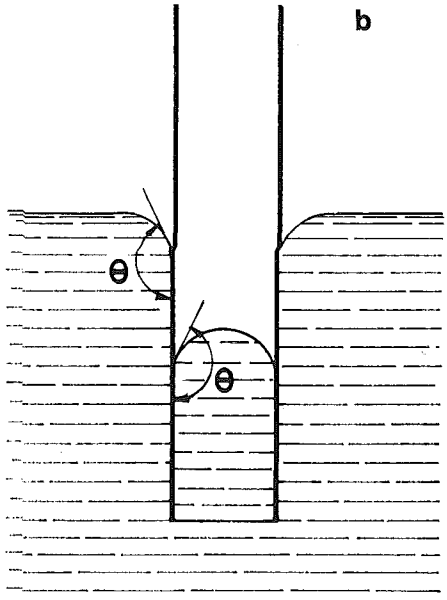

Figure 2.12 A wetting fluid (a) rises in a capillary tube, whereas a non-wetting fluid (b) drops. The figure illustrates how contact angle conditions strongly influence the equilibrium configuration of partially confined fluid masses.

Very useful information can, however, be obtained from the above expressions of the Bond number (Eq. 2.3). As *Bo* can at most be of the order of one, it follows that the product LR can at most be of the order of $L_b^2 \rho_1/\delta\rho$. Thus for liquid/gas systems, LR is at most of the order of $L^2{}_b$ and, when $L \simeq R$ each of them is of the order of L_b. This simple and straightforward estimate provides immediate evidence of some of the implications of a MGE once one recalls that for most liquids $L_b \sim 10^{-1}$ cm. Figure 2.13 shows schematically how a reduced gravity level, $g/g_0 = 10^{-4}$, influences the rise of a liquid in a capillary tube. The figure also shows that there are often constraints which prevent the arbitrary prescription of the volume of the contained fluid.

Figure 2.14 shows in histogram form the Bond number of the liquids mentioned in Table 2.3.

From the geometrical point of view, the gas/liquid interfacial systems of the greatest interest are drops, bubbles, thin liquid films or lamellae, and liquid bridges.

2.3.3 *Examples*

Several configurations of liquid volumes totally or partially bound by interphases are discussed in this paragraph. Obviously the number of examples is large, but emphasis has been placed here on situations where operating under microgravity could either represent an advantage or introduce new problems.

Drops and bubbles: The hydrostatics of a drop is very similar to that of a bubble, the only difference coming from the fact that liquids are practically incompressible while gases are readily compressed.

Drops and bubbles at rest are spherical, provided that gravitational forces are negligible and that the liquid consists of only one chemical compound at uniform temperature. The effects of gravity forces on the shape of drops and bubbles are readily deduced from Eqs. (2.1) and (2.2) where $\delta\rho = (\rho_1 - \rho_2)$ with ρ_1 the density of the confined fluid (Fig. 2.15).

For a bubble, $\delta\rho = \rho(\text{gas}) - \rho(\text{liquid})$ and thus static equilibrium will require a larger radius of curvature (more precisely a smaller mean curvature) at its bottom.

Conversely, for a drop, $\delta\rho = \rho(\text{liquid}) - \rho(\text{gas})$, so the radius of curvature will be smaller at the bottom.

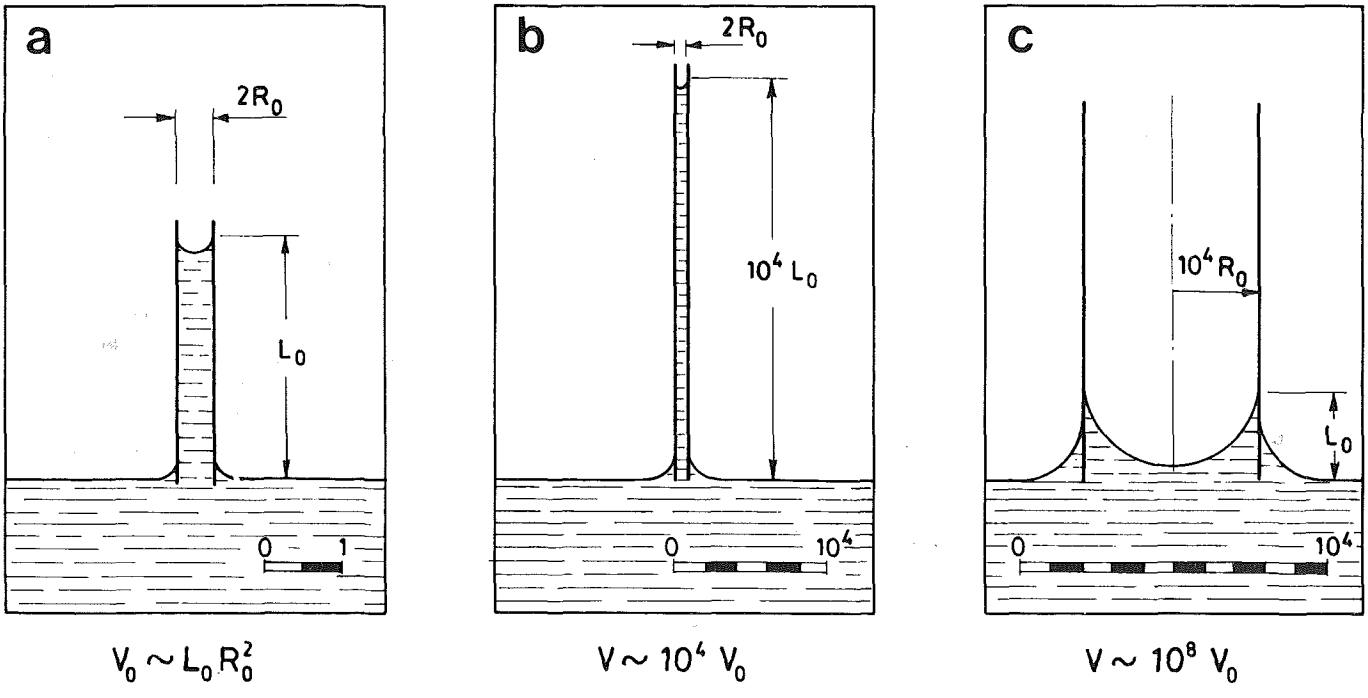

Figure 2.13 The product of the two characteristic lengths, L and R, which appear in the definition of the Bond number, is of the order of the Bond length squared, L_b^2. When the gravity level decreases by a factor of say 10^{-4}, this product increases 10^4 times. In (b), geometric constraints limit the value of R, thence L increases by 10^4. In (c), R is increased in the ratio g_0/g and therefore L remains as in (a). (The figures are not to scale.)

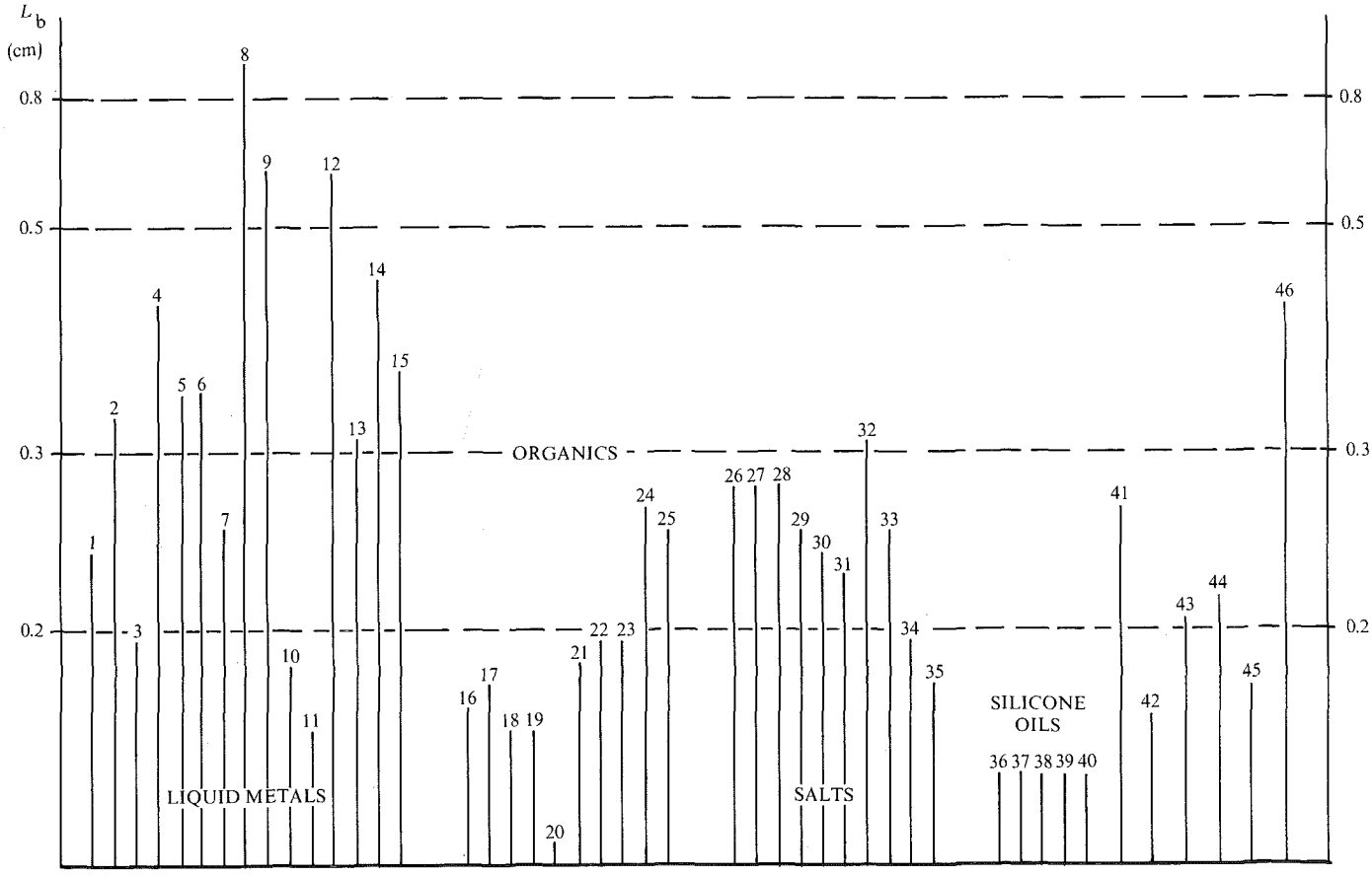

Figure 2.14 Histogram of the unit Bond length for several liquids.

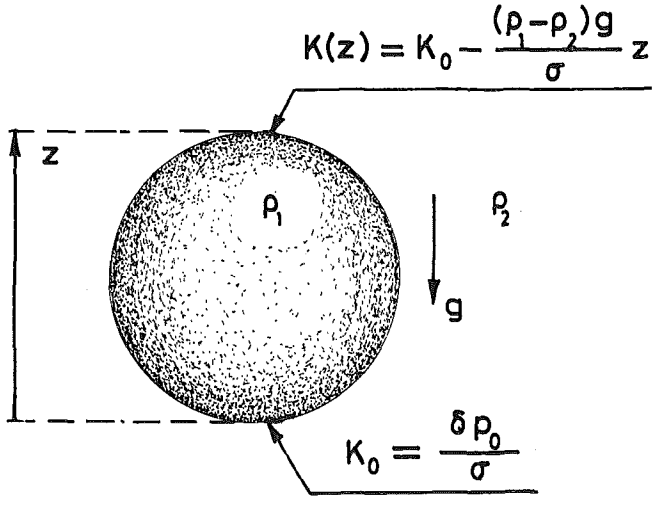

Figure 2.15 A drop in hydrostatic equilibrium. The resulting configuration is spherical when $(\rho_1 - \rho_2)\, g\, z$ is small enough.

The theory of dynamics of isolated drops and bubbles is reasonably well developed; particularly when only small deviations from the static equilibrium configuration are allowed, this normally requires that the drop or bubble is small. Experiments on rotating drops have been performed under microgravity conditions onboard Skylab [2.14].

Bubble migration is a problem of concern because of the difficulties which are anticipated under microgravity in degassing of melts. Simulation of these problems on earth, can be performed by using the 'tilted Hele-Shaw cell' techniques [2.15].

The properties of aggregates of moving drops or bubbles are discussed in § 4.3.

Thin liquid films or lamellae: Thin liquid films held by surface-tension forces appear in many technical applications, and are also present in foams, which can be either viewed as agglomerations of bubbles or as structures composed of liquid films.

For sufficiently thin films, gravitational forces may be

neglected, their shapes being determined by surface tensions alone. Nevertheless, instances where gravitational forces are important have been mentioned [2.16]. The first example corresponds to tall vertical films whose characteristic length in the direction of gravity is very large. A thin film of a pure liquid having constant width, w, and constant thickness, δ, cannot be stabilised in a gravitational field since, in the absence of inertia forces, surface tension forces, $2\sigma(w+\delta)$, must balance at each level the weight (minus the Archimedean force) of the film beneath that level, and the surface tension is constant whenever the temperature is constant. Liquid films as tall as 6 m are quoted in the literature.

Horizontal liquid films cannot persist in a gravitational field. Let us consider a foam lamella in a cylindrical tube (Fig. 2.16). Far from the tube walls the lamella is horizontal, but the free surface is strongly curved near the walls because of the contact-angle requirement in the line where solid, liquid and gas meet. These curved parts of the lamellae are called Plateau borders.

Let p_B be the pressure in the lamella and p_A that of the surrounding fluid. According to Eq. (2.1), $p_B = p_A$ in the central region ($K=0$) whereas $p_B < p_A$ in the Plateau borders (where $K>0$). Thus hydrostatic conditions cannot be maintained and liquid streams from the centre to the periphery of the lamella producing its drainage and bursting.

In spite of the mentioned destabilising effects, liquid films can persist for minutes, hours or even years. The explanation for this surprising persistence is attributed to three not fully understood effects [2.16], namely:

- surface viscosity;
- increased surface tension of locally stretched areas because of a transient defect of the foaming agent, which needs some time to reach these areas by diffusion; and
- mutual repulsion of electric double layers.

Liquid bridges: Liquids can bridge the gap between two solid bodies provided the gap is not too great. The equilibrium of the resulting configuration is controlled by the balance between hydrostatic pressure and surface tension.

There is an extensive literature on the shape of axisymmetric liquid bridges under the action of gravity and surface tension forces since Young, Laplace and Gauss first formulated the problem (see [2.17] or [2.18]). The early attempts to solve the problem were restricted

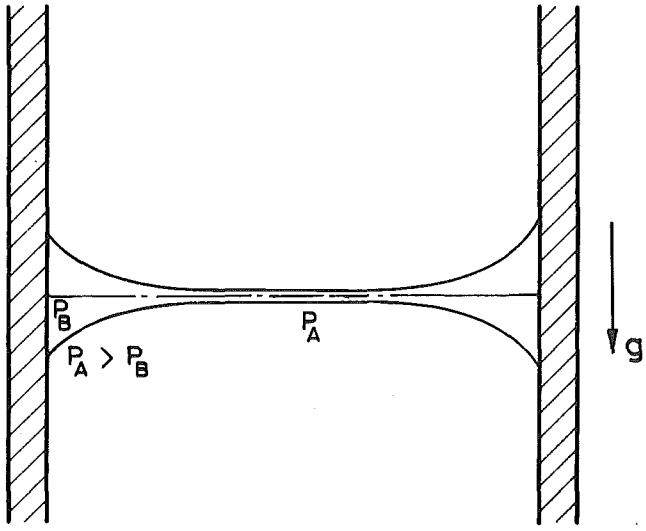

Figure 2.16 A foam lamella in a cylindrical tube.

by the need to obtain solutions by analytical calculations. With the advent of modern computing aids it has become a relatively simple matter to obtain such solutions and attention is tending to turn more towards the stability of the equilibrium configurations. Particularly relevant in connection with microgravity is the cylindrical cross section with axis parallel to the gravitational vector. Here L is the height of the bridge and D the diameter of the disk (Fig. 2.17).

As discussed in § 2.3.2, equilibrium considerations lead to the conclusions that the ratio (LR/L_b^2) can be at most of the order of one. In this expression R is the smallest radius of curvature of the interface, which is not necessarily equal to the radius, $D/2$, of the end disks.

Stability requires that the ratio (L/L_b) be of the order of one. Heywang [2.19] has shown that, in a gravitational field, the maximum stable length, L_M, of the cylindrical bridge is given by:

$$L_M = 2.84\, L_b = 2.84\sqrt{\sigma/\rho g}, \quad \text{for } D/L_b > 4,$$

where (§ 2.3.2) ρ is the density of the liquid. From $LR/L_b^2 \simeq 0(1)$ it then follows that also $R/L_b \simeq 0(1)$ and consequently $L_M/R \simeq 0(1)$.

Microgravity conditions increase the value of the maximum stable length, but have no influence on the ratio L_M/R that remains of the order of one, a limitation that is implied, as just seen, by stability. Thus too slender bridges are *also* unstable in a microgravitational

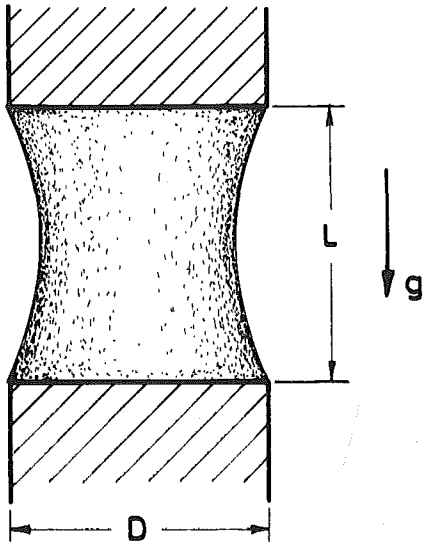

Figure 2.17 A liquid bridge between two parallel solid pieces.

environment (necking-type of instability) and there is a maximum stable length to characteristic radius ratio. In the particular case of cylindrical bridges ($R = D/2$) we have $L_M/D = \pi$, as first noted by Rayleigh [2.20].

According to what was discussed in § 2.3.2, in microgravitational environment $Bo \ll 1$ and thus the shape of the free surface bounding a liquid bridge at rest is that yielding uniform mean curvature under the constraints imposed by bridge length, disk diameter and liquid volume.

From given bridge length and disk diameter the liquid volume cannot be fixed at will. It is bounded from above and from below by several stability constraints.

The lower bound of the dimensionless volume in the bridge is defined by either of the following criteria [2.21]:

- In the case of very short bridges ($L/D \leqslant .4$), liquid can be sucked out the bridge up to detachment from the disk edges. Figure 2.18a has been sketched under the assumption of zero minimum contact angle.
- For slenderness in the range 0.4 to 2, a relative minimum for the volume, in the mathematical sense, exists. Further liquid suction will result in the bridge breaking down through necking of its mean section, yielding two practically equal liquid volumes attached to each disk (Fig. 2.18b).
- The above criterion becomes invalid for more slender bridges; it will predict, for example, a maximum value $L/D = 4.5$ for cylindrical bridges, much larger than that, $L_M/D = \pi$, predicted by Rayleigh. It can be shown that beyond $L/D = 2$, the liquid bridge first evolves towards a non-symmetrical configuration which splits itself into two different spherical zones attached to each disk (Fig. 2.18c).

The upper bound of the volume is often defined by an attachment condition at the disk edge. Figure 2.18d corresponds to the assumption that the maximum achievable contact angle is equal to 180°. Liquid bridges of maximum stable volume have been deduced from stability considerations by Gillette & Dyson [2.22]. The contact angle of the resulting bridges is larger than 180°, so they are difficult to observe since detachment from the end disks could appear first.

2.3.4. *Simulation of microgravitational hydrostatics*
Under hydrostatic conditions, the only relevant non-dimensional number is the (static) Bond number, which measures the relative importance of gravitational and surface tension forces (§ 2.3.2). Hydrostatic simulation of microgravitational environments can therefore be accomplished on earth (Eq. 2.3) if one can attain low values of the Bond number. Three obvious opportunities

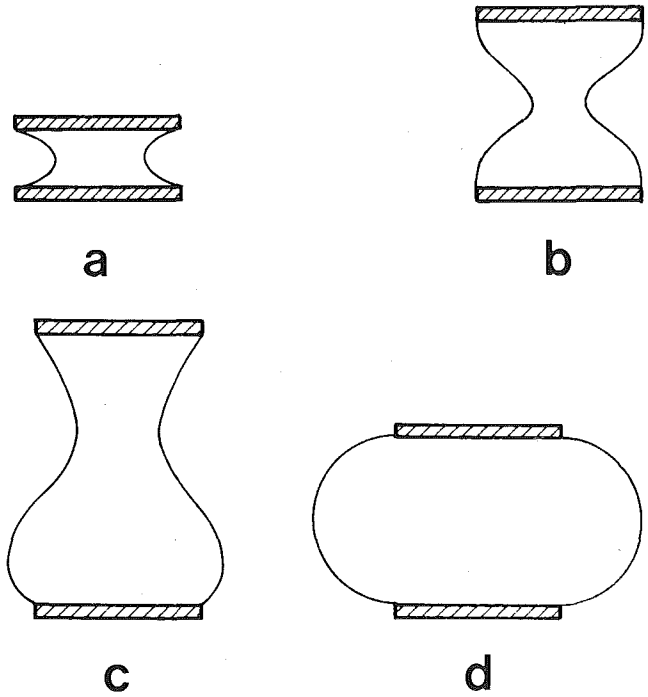

Figure 2.18 Effects bounding from below (a, b and c) or from above (d) the liquid volume in the bridge. (a) detachment from the disk edge, (b) symmetrical breakdown, (c) non-symmetrical breakdown, (d) spillover.

for such low Bond number operations arise that may give identical results:
- microgravity, which is the object of this brochure;
- thin layers, such as those studied in § 2.3.4;
- neutral buoyancy.

Neutral buoyancy was originally used by Plateau [2.23]. He showed, by means of this technique, that the maximum stable length L_M of a uniform cylinder of liquid, contained at its ends by non-wetting solid surfaces, was roughly equal to three diameters. More recently, Mason [2.24] performed a more refined, but basically similar experiment, arriving at the conclusion that the value of L_M/D at which a cylindrical floating zone becomes unstable is between 3.14 and 3.1417: Compare these values with that ($L_M/D = \pi$) found by Rayleigh.

The same technique has been used by Carruthers & Grasso [2.25] to study the maximum stable L/D ratio for initially cylindrical, spinning, liquid bridges.

However, simulation of dynamical problems by use of the neutral buoyancy technique should be looked at carefully, since both inertia and viscous forces have to be taken into account. It is well known, for example, that Skylab experiments involving rotating drops and rotating liquid bridges yielded deformation modes not previously observed by using the Plateau technique.

The discrepancy between Plateau-simulated and real microgravity experiments can be attributed in most cases to inertia forces whose effect is to severely modify the pressure field at the interface. For example, rotation of the outer liquid cancels the centrifugal forces at the interface.

Viscous effects are sometimes important. A typical example is the spin-up of an axisymmetric two-fluid configuration held between two parallel coaxial disks of infinitely large radius. When the spinning velocity of the disks is suddenly increased, the highly viscous liquid follows the spin-up more rapidly than the less viscous one. This results in changes in the balance of forces near the interface between the liquids. Severe distortions of the interface ensue which again demonstrate the limitations of the Plateau simulation technique (Fig. 2.19).

Plateau techniques have been used for the amplification of non-Newtonian effects. It is well known, for example, that certain viscoelastic fluids will climb rotating rods of small diameter (Weissenberg effect). See, for example, Truesdell [2.26] for an account of several non-Newtonian effects. On the other hand, an accurate determination of the form of the free surface will permit the characterisation of important properties of these fluids.

Although climbing can be amplified by increasing the rod rotation rate, the flow pattern is steady and axisymmetric when the angular velocity of the rod is not too large, which is why Plateau simulation (and μg operation) can be used to amplify this climbing effect.

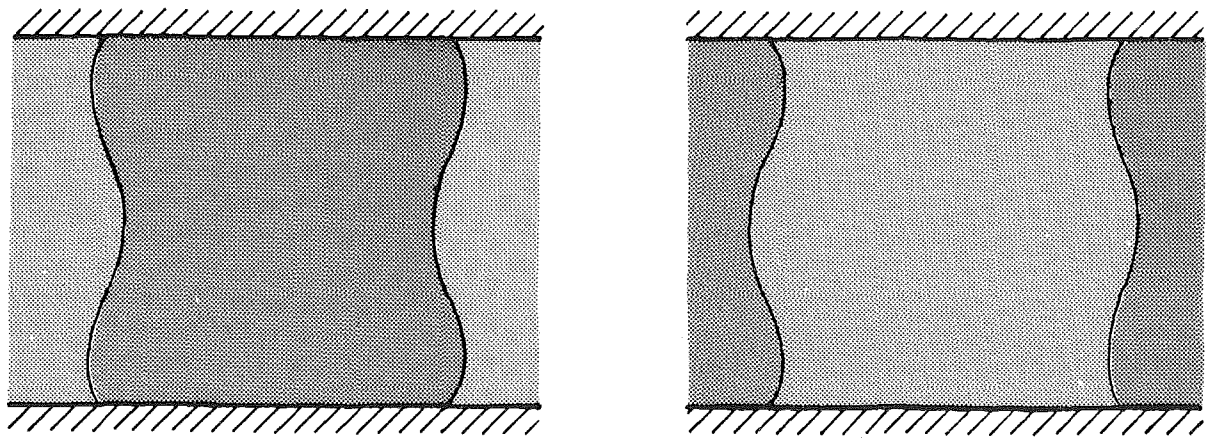

Figure 2.19 Plateau simulation of the spin-up of a cylindrical liquid bridge using the less viscous liquid either outside or inside.

Joseph & Beavers [2.27] considered, both theoretically and experimentally, the rod climbing of a layer of a viscoelastic liquid floating on another immiscible liquid (Fig. 2.20). The top liquid climbs up the rotating rod into the air and down the rod into the bottom liquid. The down climb h_B is much larger than the up climb h_A. According to Joseph & Beavers,

$$\frac{h_B}{h_A} \sim \frac{\sqrt{\sigma_A(\rho-\rho_A)}}{\sqrt{\sigma_B(\rho_B-\rho)}} \quad \frac{4+a\sqrt{(\rho-\rho_A)g/\sigma_A}}{4+a\sqrt{(\rho_B-\rho)g/\sigma_B}}$$

This equation shows that the down climb can be arbitrarily amplified by making the density difference $\rho_B-\rho$ small.

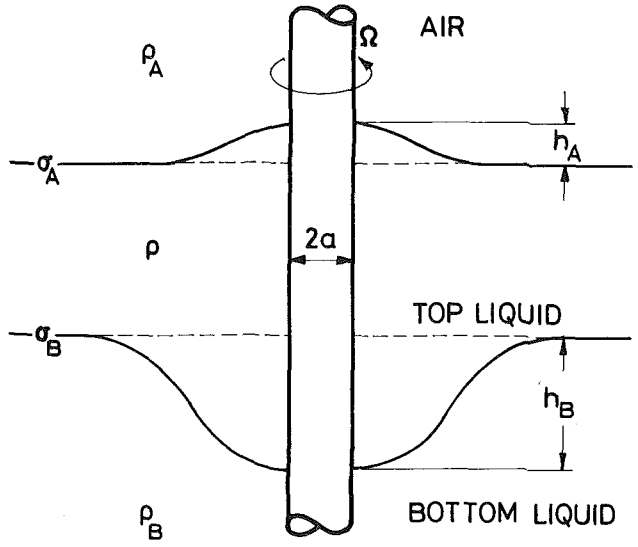

Figure 2.20 Rod climbing of a layer of visco-elastic liquid floating on a second liquid with which it is immiscible.

2.4 Transport phenomena

For any experimental configuration where size or other parameters cannot be changed, the microgravitational environment offers an opportunity to reduce free convection. Even though the naive assumption of a convection-free state will usually not be valid, this may have drastic consequences for total heat and mass transport, i.e. the entire system of transport phenomena is altered and must be analysed.

The evolution of any fluid system is governed by a set of balance equations which represent the mathematical formulation of the relationship existing between the time rate of change, the 'transport', and the 'production' (creation or destruction) of any extensive fluid property (neutral or charged masses; mechanical and electromagnetic momentum and moment of momentum, all forms of energy, entropies).

The amount of an extensive property contained in any given system (Σ) can vary with time if and only if there is an exchange of the property between the system and its environment (Σ') and/or a production of the property within the system (Fig. 2.21). The exchange is a consequence of the transport of the property across the surfaces S' bounding the system and, in the continuum range, can be expressed in terms of its flux.

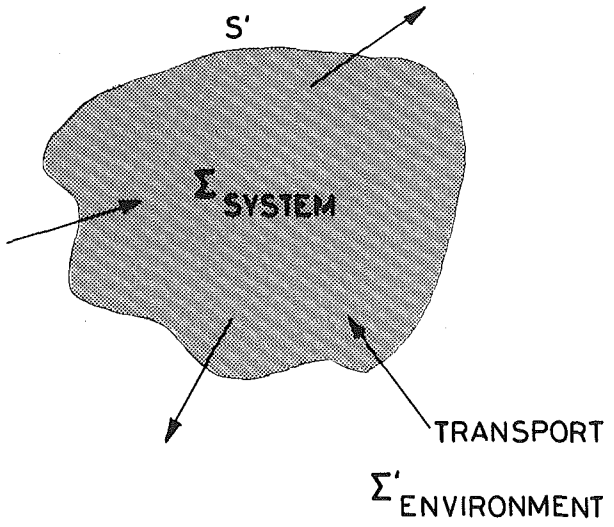

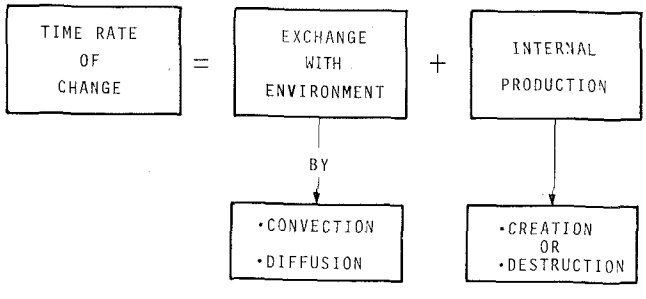

Figure 2.21 Schematic representation of a balance equation.

The balance equations express 'physical principles': balance of momentum expresses the equilibrium of all forces acting on the system; balance of total mass and of total energy expresses the principles of conservation of total mass and total energy; balance of entropy expresses the second principle of thermodynamics. The analysis of the role played by transport phenomena in any fluid system must always be made in the framework of the entire set of balance equations.

Two basic transport mechanisms are usually distinguished: convection, associated with the transport of the total mass, and diffusion, characterising, at macroscopic (phenomenological) level, the observable consequences of the phenomena taking place at microscopic (molecular) level.

Transport of total mass is related to the mass flux ($\rho\mathbf{V}$) where ρ is the density of the medium and $\mathbf{V}$ its mass or baricentric velocity. Transport of any other property is related to its total flux, sum of convective flux (property per unit mass times the mass flux) and a diffusive flux (Fig. 2.22). Total and convective fluxes, as the mass velocity $\mathbf{V}$, depend on the motion of the reference frame; the diffusive flux, independent of the motion of the reference frame, is an intrinsic property of the medium.

If there is a reference frame (inertial or not) in which a fluid system is at rest (hydrostatic equilibrium, § 2.3) transport may occur only by diffusion. Diffusion of momentum manifests itself, at macroscopic level, as a stress tensor and that of internal energy as the 'heat'. By definition, there is no diffusion of total mass but only that of different species.

2.4.1 *Genesis and types of convection*

The genesis and types of convection are best analysed in terms of the momentum balance equation. In the simpler case of a neutral, non-polarisable, non-elastic fluid, this equation can be written, for a fluid particle and in terms of forces per unit mass, as:

$\mathbf{a} = -\frac{1}{\rho}\nabla\pi$ pressure force (resultant of pressure referred to the hydrostatic pressure p_h; $\pi = p - p_h$)

$+ \mathbf{f}_v$ viscous force (resultant of viscous stresses)

$+ \frac{\rho - \rho_h}{\rho}\mathbf{g}$ buoyancy force (ρ_h = hydrostatic density)

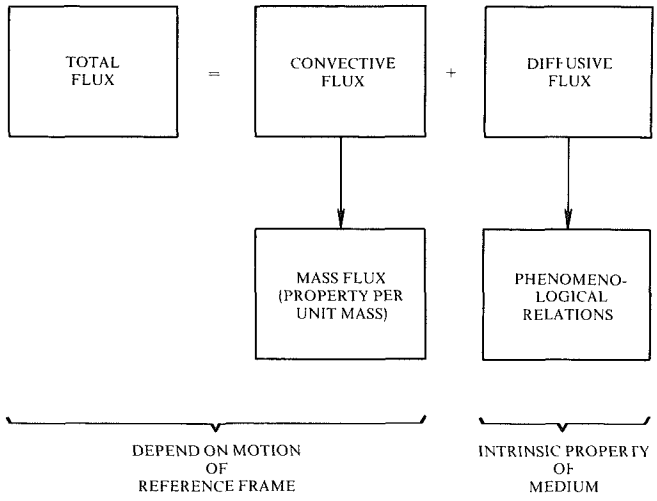

Figure 2.22 Convective and diffusive fluxes.

The first two forces are surface forces, the last one is a body force. In stable hydrostatic equilibrium each one of these forces is and remains null. The boundary conditions determine which force 'drives' the motion and, obviously, there can be more than one driving force. The situation is summarised in Table 2.4 where, for the sake of simplicity, only the more common boundary conditions are considered. In the more general case, body forces of electromagnetic origin should also be included (§ 2.1). They become driving forces in the presence of imposed electric and/or magnetic fields.

Imposed velocities and differences of pressure or interfacial tension always induce motions. The same is not necessarily true for imposed density difference. For example, in the absence of F-F interfaces, density gradients can be compatible with stable hydrostatic equilibrium (see § 2.3 for more details) and thus do not induce motion.

Convection in the absence of imposed pressure differences and imposed velocities is usually referred to as *free convection.* In the other cases it is called *forced convection.*

Free convection may be due to buoyancy forces (body forces) or to viscous forces (surface forces). The latter case arises only when there are F-F interfaces: motion on interface caused by gradients of interfacial tension σ (§ 2.2.2) induces equilibrating viscous stresses which drive the motion in adjacent bulk phases (Fig. 2.23). Whenever there is an imposed difference of a property affecting both σ and ρ, both types of driving forces are

Table 2.4

Boundary conditions	Driving force		Term	Typical examples	Classification
Imposed pressure difference	Surface forces	Pressure force	$-\frac{1}{\rho}\cdot\nabla p$	Pipe flows	Forced convection
Imposed velocity at S-F interface		Viscous force	$\mathbf{f}_v$	Sustained motion through fluid	
Imposed velocity at discharge section				Jets	
Imposed interfacial tension difference*				Marangoni flows	Free convection
Imposed density difference**	Body forces	Buoyancy force	$\left(\frac{\rho-\rho_h}{\rho}\right)\mathbf{g}$	Buoyant flows Sedimentation	

* Equivalently: imposed difference of any property upon which the equilibrium interfacial tension depends (§ 2.2)
** Equivalently: imposed difference of any property upon which the density depends.

present. The terminology adopted here is given in Table 2.5.

Further subdivisions can be envisaged in terms of the agent causing the variations of density and interfacial tensions, as exemplified in Table 2.6 for the case in which ρ and σ depend on temperature and composition.

Table 2.5

Name	Main Driving Force
Natural convection	Body force
Marangoni convection	Surface force
Combined convection	Both

Table 2.6

	Imposed difference / Free convection	Temperature	Concentration
Combined	Natural	Thermal	Solutal
		Thermosolutal	
	Marangoni	Thermal	Solutal
		Thermosolutal	

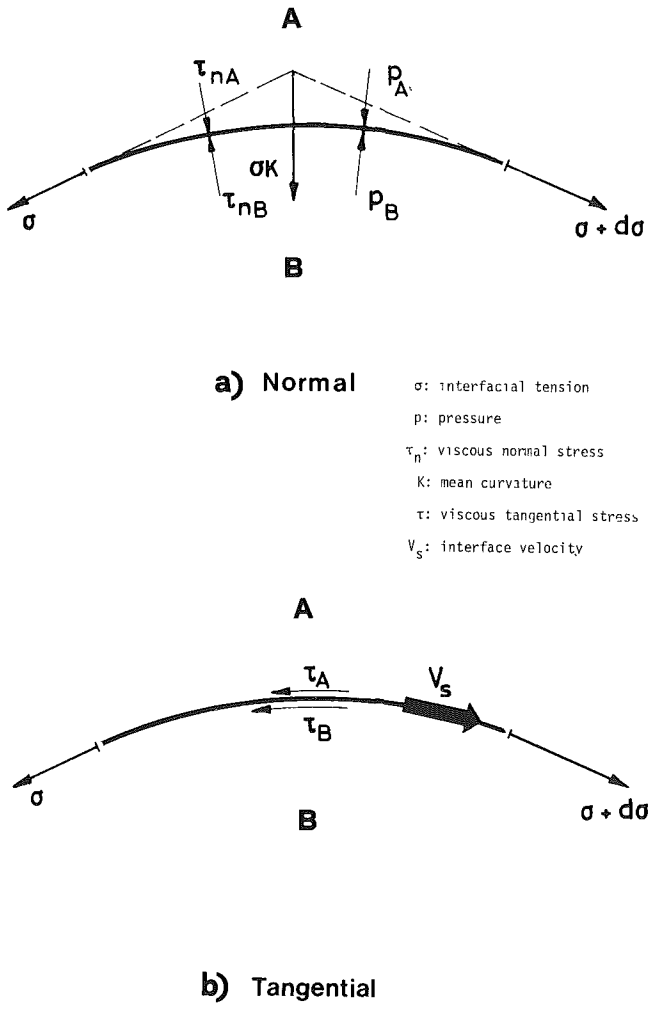

Figure 2.23 Main forces acting on interface in dynamic conditions (surface irreversibility negligible).

2.4.2 *Influence of gravity*
The consequences of a reduced gravity level vary according to whether fluid/fluid interfaces are present or not, and to whether or not there are imposed pressure differences and/or velocities.

Case in which there are no fluid/fluid interfaces: when pressure differences and/or velocities are imposed (forced convection) buoyancy forces may be of the same order of magnitude as pressure and/or viscous forces only in certain regions of the flow field whose nature and extension are well assessed (see § 4.5). The availability of a reduced-gravity level is not scientifically relevant in forced convection since its consequences and the corresponding scaling laws are, in general, fairly simple and well known.

When neither pressure differences nor velocities are imposed, convection is driven by the buoyancy force. Since its intensity depends also on the density difference, the velocity field is coupled with the temperature field or the concentration field, or both, depending on the agent of density variation.

The local intensity of the driving force is influenced by all phenomena contributing to the momentum, energy and mass balance equations (unsteadiness; transport of momentum, energy and masses; chemical reactions; phase changes; radiation). A number of relevant features of this type of coupling are fairly well known and theoretical and experimental investigations pertaining to more complex problems are being actively pursued, especially for fluid in enclosures and related stability problems (§ 3.1). Possible relevance of microgravity can be assessed from the consideration of two factors:
- the reduction of the buoyancy force and
- the manner in which this is achieved.

In principle, when the buoyancy force is very small, other driving forces may take over. The implications of this situation for particles and/or suspensions of particles, clusters, and so on, are discussed in § 2.5. For uncharged and non-polarisable fluid systems the only additional force capable of driving the motion is the pressure force which can be different from zero only if the boundary conditions (perhaps time dependent) induce productions (chemical reactions, phase changes) within the system.

A perhaps more important aspect of microgravity is the fact that buoyancy may be kept small or altogether negligible with much higher density differences than on earth. The possibility of imposing large temperature and/or concentration differences without inducing motion should make it possible, in principle, to investigate and quantify experimentally the range of validity of linear phenomenologies for the diffusion of heat and mass (§ 2.4.3). Reduced gravity experiments in enclosures without fluid/fluid interfaces should be considered in the above perspective. For a given geometry, spaceborne and on-earth experiments should give the same qualitative and quantitative results for the same values of the relevant characteristic numbers (e.g. the Rayleigh and Prandtl numbers) unless the much higher density differences in the spaceborne experiment induce, *within* the fluid in the enclosure, new phenomena (excitations of internal degrees of freedom, chemical reactions, non-linear transport phenomenologies).

Case in which there are fluid/fluid interfaces: the scientific relevance of reduced-gravity levels is much greater and becomes paramount when there are no imposed pressure gradients or velocities. This is ascribable to a number of factors: the increased relevance of a different type of surface driving force, the very limited actual knowledge of the consequences of the coupling induced by this force, and the greater extensions of interfaces (§ 2.3). In the absence of imposed pressure gradients and velocities, ultimate causes of motion in the bulk fluids, when buoyancy forces are negligible, are the shear stresses acting on interface tension through the momentum balance equation of the interface itself (Fig. 2.2 ↑). Thus, once again, the intensity of the force driving the convection is influenced by unsteadiness, transport and productions of momentum, energy and masses in the bulk phases and, in addition, by the analogous processes in the surface phase. Matters may be further complicated by non-equilibrium (thermal or others) between bulk and surface phases. Velocity, temperature and/or concentration fields are coupled. Whereas coupling due to buoyancy forces is 'distributed' throughout the volume, coupling due to surface forces is 'concentrated' on the interface and involves its dynamics and thermodynamics. The features and consequences of this different type of coupling are very little known. Modelling of surface phenomena and evaluation of flow fields are in strong need of experimental results that can only be provided, reliably, in a reduced gravity environment.

Besides the practical difficulties of the on-earth simulation of reduced gravity environments in dynamical situations, spaceborne experiments are indispensable for another fundamental reason.

As pointed out, velocity, temperature and concentration fields are influenced, among other things, by all fluxes,

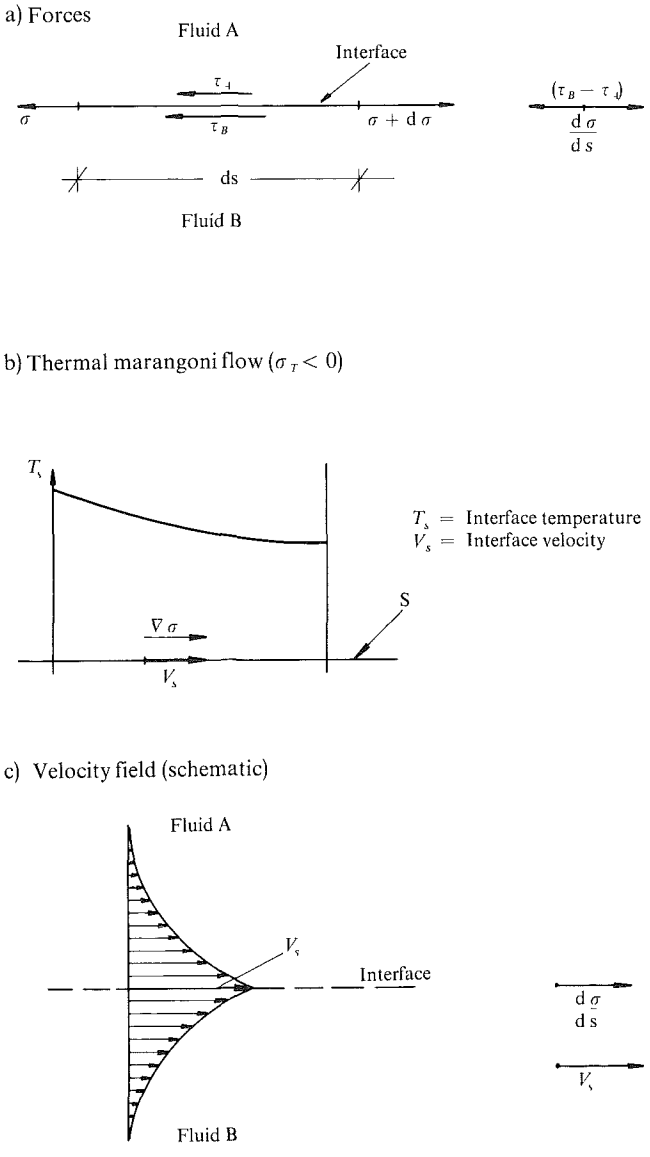

Figure 2.24 Schematic representation of the genesis of Marangoni thermal convection.

convective and diffusive, of momentum, energy and mass. Their relative order of magnitude is measured by appropriate characteristic numbers which depend also on the imposed boundary conditions and on the extension of the interface. On account of the greater extensions of the interfaces, 'controlling' processes in spaceborne environments may be substantially different from those prevailing on earth (§ 2.4.4). Any earth-bound simulation is thus a fortiori defeated and only in-situ experiments can shed the much needed light on these flow fields.

2.4.3 *Diffusion*

All diffusion fluxes, with the exclusion of the equilibrium part of (volume or surface) stress tensors, contribute to the production of entropy and thus their study falls within the realm of irreversible thermodynamics. At the macroscopic level, dissipative diffusive fluxes are considered to be due to the action of generalised forces and the relations between fluxes and generalised forces are called phenomenological relations. They were originally derived on an empirical base (e.g. Newton, Fourier, Fick laws) for special cases and now rest on a firm theoretical base, at least for volume phases and within the limits of a linear phenomenology.

The subject matter being very vast, a number of topics of comparatively less frequent occurrence (superfluids; elastic, micropolar, nematic liquids; charged and/or polarisable systems, presence of imposed electromagnetic fields) will have to be omitted or, at most, just mentioned. In particular, attention will be mostly restricted to volume phases and to linear phenomenologies, for which Curie's principle holds (fluxes depend upon all and only the generalised forces of the same tensorial order) [2.28, 2.29]. Although diffusion of internal energy and mass are in general coupled, they will first be treated separately for clarity's sake.

Diffusion of momentum

According to linear irreversible thermodynamics, the (symmetric) viscous stress tensor in fluids depends, linearly, only on the velocity gradient. For isotropic systems, this linear dependence is completely characterised by two viscosity coefficients, *functions of the thermodynamic state variables*. The first coefficient (μ) is the one entering the classical Newton law and the second (ζ, also called coefficient of bulk or volume viscosity) relates the excess of the mean normal stress over the thermodynamic pressure to the velocity divergence (time rate of change of volume per unit volume). Bulk viscosity is usually negligible in gases and plays no essential role in incompressible liquids.

The ratio $\nu = (\mu/\rho)$ is called the kinematic viscosity or momentum diffusion coefficient. As all diffusion coefficients, it has the dimensions of area per unit time. Indicative values of ν for the liquids listed in Table 2.3 and for air, as typically representative of gases, are plotted in Figure 2.25. ν is of the order of 10^{-1} cm^2/s for gases whereas, for liquids, it ranges from 10 to 10^{-3} cm^2/s ($\nu = 10^{-2}$ cm^2/s for water). Fluids obeying the above linear phenomenological relation are called Newtonian. All gases can be considered Newtonian, whereas many liquids are non-Newtonian.

Heat conduction
In systems in which only diffusion of internal energy takes place, the linear phenomenological relation for the heat conduction is the classical Fourier law which, in the isotropic case, reads:

$$\mathbf{J}_q = \lambda \nabla T$$

where $\mathbf{J}_q$ is the heat flux and λ is the heat conduction coefficient, both functions of thermodynamic state variables. The corresponding diffusion coefficient is $\alpha = \lambda/\rho c_p$ where c_p is the coefficient of specific heat at constant pressure. Indicative values of α for air and for the previously mentioned liquids are also shown in Figure 2.25. For gases, α is of the order of 10^{-1} cm^2/s, for liquids its order of magnitude covers a rather wide range going from 10^4 (glycerin) to 10^{-2} or 10^{-3} for liquid metals.

The ratio between momentum and heat diffusion coefficients is the Prandtl number ($Pr = \nu/\alpha$) whose order of magnitude measures the relative importance of the two diffusion processes. For gases, Pr is of the order of one (diffusions of momentum and heat have the same importance). The Prandtl numbers for liquids considered in Figure 2.25 range over about seven orders of magnitude. There is a very large difference between the high-viscosity, low-thermal-conductivity materials (silicone oils, glycerin, glasses) for which $Pr \sim 10^4$ and the electric conductor liquid metals for which $Pr \sim 10^{-2}$.

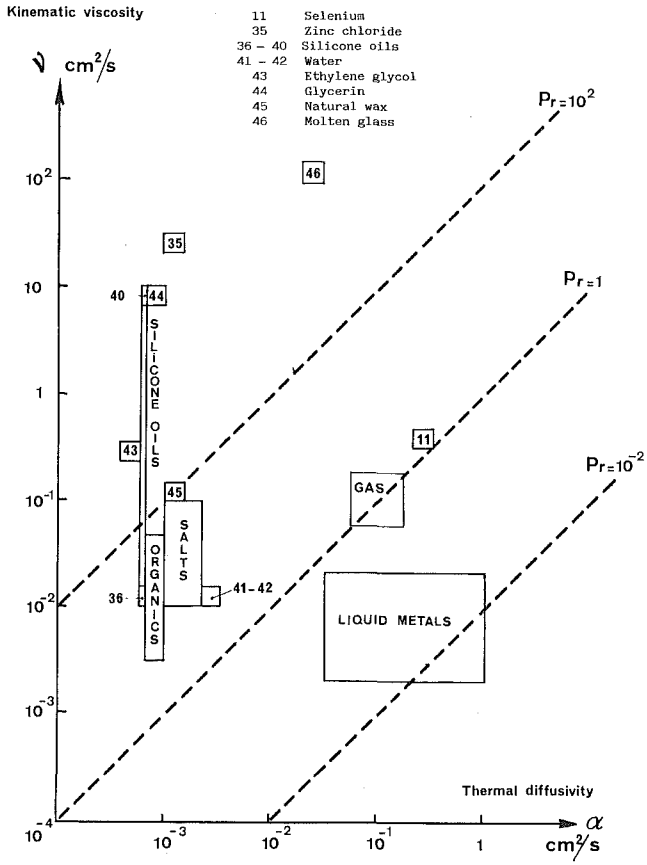

Figure 2.25 Schematic representation of the variation of kinematic viscosity ν and heat diffusion coefficient α for various kinds of materials: $\nu/\alpha = Pr$.

Isothermal mass diffusion
In a n-component mixture, the diffusion of mass of the i-th component is described by its mass flux $\mathbf{j}_i$ referred to the barycentric velocity:

$$\mathbf{J}_i = \rho_i(\mathbf{V}_i - \mathbf{V})$$

(where the subscript (i) refers to the i-th component) and only (n − 1) fluxes are independent:

$$\left(\sum_{i=1}^{n} \mathbf{J}_i = 0\right).$$

In the absence of electric charges the (n − 1) generalised forces $\mathbf{F}_i$ causing the fluxes $\mathbf{J}_i$ can be expressed as a linear combination of the forces per unit mass $\mathbf{X}_i$ [2.28]:

$$\mathbf{X}_i = (\nabla \mu_i)_{T,p} - (v - v_i)\nabla p$$

where v is the specific volume of the mixture, v_i the partial specific volume of the i-th component and $(\nabla \mu_i)_{T,p}$ the isothermal and isobaric gradient of its chemical potential μ_i. The second contribution to $\mathbf{X}_i$ has clear physical meanings. Whenever the pressure is not uniform, the force per unit volume ($-\nabla p$) induces a force per unit mass driving the relative motion of the i-th component on account of the difference between its partial specific volume and the specific volume of the mixture.

Each flux $\mathbf{J}_i$ depends on all generalised forces $\mathbf{F}_i$ (Curie principle) and the phenomenological coefficients of the corresponding linear relations are function of the thermodynamic state parameters. For a binary system there is only one generalised force. The diffusion flux is proportional to $\mathbf{X}_1$ and hence depends, in general, also on the pressure gradient. The classical Fick's law:

$$\mathbf{J}_1 = -\rho D \nabla C_1$$

(where D is the diffusion coefficient and C_1 the mass

concentration) is recovered under isobaric conditions (e.g. hydrostatic equilibrium in the absence of rotation and of external forces). For n-component mixtures under isobaric conditions each of the independent concentration gradients $\nabla C_j (j = 1,2,..,n-1)$ contributes to the diffusion of the i-th species with a term $(-\rho D_{ij} \nabla C_j)$. The diffusion coefficients D_{ij} satisfy a number of equalities following from Onsager's principle and a number of inequalities following from the principle of positive entropy production [2.28]. Other equivalent formulations of linear diffusion laws can be given, on the basis of Prigogine's theorem, in terms of fluxes referred to velocities other than the barycentric velocity (e.g. mean molar velocity, mean volume velocity, the velocity of any component). In particular physical situations (e.g. isotropic or isomeric mixtures, mass or molar diluted systems, perfect gases, liquid systems) these formulations lead to simpler forms of the mass balance equations [2.28].

Diffusion coefficients D are of the order of 10^{-1} cm^2/s in gases and of the order 10^{-5} cm^2/s in liquids. The relative importance of mass diffusion compared with momentum and heat diffusion is measured by the ratios of the corresponding diffusion coefficients which are known as Schmidt (Sc) and Lewis (Le) numbers:

$$Sc = \frac{\nu}{D} \qquad Le = \frac{D}{\alpha}$$

These numbers, like the Prandtl number, are of the order of one for gases and cover a rather wide range for liquids.

Simultaneous diffusion of heat and mass
In a non-isothermal mixture, temperature gradients and each generalised force $\mathbf{F}_i$ contribute to the diffusive fluxes of both mass and heat. Flux of matter caused by a temperature gradient and, reciprocally, flux of heat caused by concentration gradients (or, more generally, by the forces $\mathbf{F}_i$) are known as cross-coupling effects. The first one is usually called the Soret effect in liquids, the second one, when caused by concentration gradients, is called the Dufour effect.

For a binary mixture under isobaric conditions, the phenomenological relations for the mass diffusion flux $\mathbf{J}_1$ and the reduced heat flux $\mathbf{J}'_q = \mathbf{J}_q - (h_1 - h_2)\mathbf{J}_1$, where the h_i are the partial specific enthalpies, can be written as (for non-isobaric conditions replace ∇C_1 by $\mathbf{X}_1$) [2.28]:

$$\mathbf{J}'_q = \lambda \nabla T - \rho C_1 \mu_{11} T D'' \nabla C_1$$

$$\mathbf{J}_1 = -\rho C_1 C_2 D' \nabla T - \rho D \nabla C_1$$

where $\mu_{11} = (\partial \mu_1 / \partial C_1)_{T,p} > 0$ (upon thermodynamic stability), D' is the thermal diffusion or thermal migration coefficient, D'' is the Dufour coefficient ($D'' = D'$ upon Onsager's relation) and $\lambda \geqslant 0$; $D \geqslant 0$

$$k^2 = \frac{(D')^2 \rho T C_2 C_1^2 \mu_{11}}{\lambda D} \leqslant 1$$

upon the positivity of entropy production.

D' is of the order of 10^{-4} to 10^{-6} (cm^2/s K) in gases and 10^{-8} to 10^{-10} (cm^2/s K) in liquids. The Soret coefficient $St = (D'/D)$ has the same range, 10^{-3} to 10^{-5} (1/K), in gas and liquid mixtures. The number k^2 is of the order of 10^{-2} to 10^{-3} for gases and 10^{-4} to 10^{-5} for dilute solutions.

The cross-coupling between heat and mass diffusion has many implications (in systems with electric charges it gives rise to thermoelectric effects such as Seebeck and Peltier effects and, with the added presence of external magnetic fields, to galvanomagnetic and thermomagnetic effects) but is often negligible. Typically, the ratio $(\Delta T / \Delta C_1)$ between imposed temperature and concentration differences must be of the order of $(1/St\, C_1\, C_2) \simeq 10^3$ to 10^5 K for thermal diffusion to be of the same order as concentration diffusion.

Likewise, in stable stationary states ($\mathbf{J}_1 = 0$) attained upon imposition of a fixed temperature difference ΔT between two walls of a closed vessel, there is a concentration difference at the walls of the order of $C_1 C_2 S_t \Delta T \simeq 10^{-3}$ to $10^{-5}\ \Delta T$ and a reduction of the heat flux (cross-coupling opposes heat conduction) compared with pure conduction in the ratio $1/(1-k^2)$ (thus, at most, of some percent).

Cross-coupling effects, in spite of their relative smallness, may substantially influence the stability of systems (§ 3.2.2, 3.3.2).

Influence of gravity level on phenomenological relations
According to the Curie principle, generalised forces driving tensorial fluxes (viscous stress tensor, diffusion of electric and magnetic polarisation) and scalar fluxes (chemical reactions, excitation of internal degrees of freedom, diffusion of mean normal momentum) do not depend on the gravitational force and hence the gravity level has no influence on the corresponding phenomenological relations. When the Curie principle does not apply (non-linear irreversible thermodynamics) the above statement may no longer hold. From this point onwards, remarks will be limited to linear phenomenologies.

Generalised forces directly driving mass diffusion (and, through cross-coupling, heat diffusion) contain contributions due to pressure gradients and, in charged systems, contributions due to the Lorentz force, per unit mass, acting on the charged components.

The gravity level affects these driving forces, since it helps to determine the magnitude of the pressure gradient via the momentum equation, which can be written as:

$$\frac{\mathbf{V}p}{\rho} = \mathbf{g} + \mathbf{f}_b + \mathbf{f}_e + \mathbf{f}_v - \mathbf{a}_r$$

where $\mathbf{f}_b$ and $\mathbf{f}_e$ denote the d'Alembertian and electromagnetic body forces, $\mathbf{f}_v$ the viscous forces and $\mathbf{a}_r$ the relative acceleration. The assessment of the influence of gravity levels on phenomenological relations hinges on two subsequent evaluation criteria. First, one must ascertain whether or not pressure-gradient contributions to the forces are relevant. Only when this contribution is not negligible (e.g. in studies of electrophoresis, of stratification process and so on) must one ascertain (second evaluation criterion) the effects of reduced gravity levels on the pressure gradient. A reduced-gravity level may be relevant insofar as the action of gravity is reduced with respect to that of other forces and/or insofar as it produces effects of action that are usually overshadowed by earth-level gravity.

As an indicative simple example consider the hydrostatic equilibrium of an isothermal non-reacting gas mixture in a vessel rotating with a steady angular speed $\boldsymbol{\omega}$ and suppose that the boundary conditions are compatible with a stable equilibrium characterised by the vanishing of all fluxes. Then all forces $\mathbf{X}_i$ must vanish and, clearly, the contribution of the pressure gradient cannot be neglected. As in this case $\mathbf{f}_v = \mathbf{a}_t = \mathbf{f}_c = 0$ and $\mathbf{f}_b = \boldsymbol{\omega}^2\mathbf{r}$ the role of gravity is then readily assessed. Concentration gradients have components parallel to $\mathbf{g}$ and normal to $\boldsymbol{\omega}$, proportional respectively to

$$(1 - \rho v_i)\frac{g}{h_i T} \quad (R_i \text{ gas constant of i-th component}),$$

and to

$$\frac{(1 - \rho v_i)\omega^2 r}{R_i T}$$

Their intensities are in the same ratio $(g/\omega^2 r)$ as that of the corresponding forces ($\rho\,\mathbf{g}$ and $\rho\,\omega^2\mathbf{r}$) contributing to the pressure gradient. The implications of all this are self-evident. The application of the two evaluation criteria may in other cases (e.g. stability problems) require detailed and extensive theoretical investigations.

Important as it is, the assessment of the relevance of gravity to the generalised force is not per se sufficient since diffusion is only one of the phenomena contributing to the evolution of fluid systems. Detailed descriptions of the influence of gravity cannot be given without the contextual analysis of the relative importance of the other phenomena. This is particularly true when one tries to assess the influence of gravity levels on temperature and/or concentration distributions. Without a detailed investigation of the specific problem, it may be difficult to separate the effects induced by gravity from those associated with concomitant phenomena since they may be qualitatively the same.

Consider, for instance, the steady-state temperature and concentration distributions for a quiescent, binary, single-reaction mixture in an enclosure. Temperature, concentration profiles and transport processes are strongly influenced by the coupling between chemical reaction and diffusion of heat and mass, measured by the ratios between the rate of the reaction compared with those of the transport phenomena (involving the diffusion coefficients α, D, D' and the dimensions of the enclosure). In particular, temperature and concentration profiles are linear only in the limiting cases in which the above ratios are either very small or very large (chemical reaction 'frozen' or in 'equilibrium'); chemical reactions enhance heat conduction, and so on [2.28]. The same qualitative features are caused by gravity-driven convection. Hence, even in this comparatively simple case, there is an evident need for detailed investigations aimed at discriminating between similar consequences of different causes.

Diffusion in surface phases

For surface phases one can develop, in principle and formally, the same treatment of irreversible phenomena as for volume phases. One could thus introduce the notions of surface coefficients of viscosity, heat conduction, diffusion, cross-coupling coefficients and so forth [2.30, 2.31].

As surface phases are not necessarily in thermodynamic equilibrium with the adjoining volume phases, irreversible exchanges of momentum, mass and energy may take place among them. In principle they may be phenomenologically cross-coupled with a number of diffusive transport within the bulk phases. Recent developments of linear theories for surface

irreversibilities have contributed to put these subjects on rather firm and internally consistent grounds. Non-linear theories and stability theories for far from equilibrium systems have also been achieving stimulating progress [2.32].

There is, however, a great need of experimental data to support these theories and/or to suggest their further developments. The availability of much larger interface extensions afforded by a microgravity environment makes this research area one of the most promising and rewarding for its high potentiality of increasing the understanding and mastery of surface irreversibility phenomena.

2.4.4 *Simultaneous convective and diffusive transport*
When both convective and diffusive transport may occur, it is important to be able to determine, a priori, whether, and in which region, the effects of one can be neglected with respect to those of the other. The order of magnitude of the convective flux of any extensive property (.) is given by $\rho_r V_r(.)$ (where the subscript r denotes reference quantities) and that of the diffusive flux in the direction of main motion can be expressed, to within a linear phenomenology, as $\rho\mathscr{D}(.)/L$ where L is a geometrical length in the direction of the main flow, characteristic of the problem, and $\mathscr{D}$ denotes the diffusion coefficient of the transported property. The ratio $V_r L/\mathscr{D}$ of these two quantities defines, for momentum ($\mathscr{D}=\nu$), internal energy ($\mathscr{D}=\alpha$) and masses ($\mathscr{D}=D$), the (non-dimensional) Reynolds (Re), Peclet (Pe) and Reynolds × Schmidt ($Re\,Sc$) numbers:

$$Re = \frac{V_r L}{\nu}$$

$$Pe = \frac{V_r L}{\alpha} = Pr\,Re \qquad (*)$$

$$Re\,Sc = \frac{V_r L}{D}$$

Their values depend on V_r and L and, as will be seen presently, this has important implications. The ratios of any two of them, on the contrary, depend only on the local thermodynamic state of the medium, as they are given by the already mentioned Prandtl, Schmidt and Lewis numbers (§ 2.4.3).

The numbers (*) are related to the measures of the relative importance of convective and diffusive fluxes and of their corresponding effects. Diffusive fluxes in the direction normal to the main flow may be larger than those in the direction parallel to the motion. The order of magnitude of the former ones is given by $\rho\mathscr{D}(.)/\ell L$, where ($\ell$) is a scale length factor of the order $\leqslant 1$. Thus the relative importance between convective and largest diffusion fluxes is measured by the numbers (*) multiplied by (ℓ).

Since the effects of the transport processes depend on the gradients of fluxes, a further multiplication by the scale factor (ℓ) is needed, for the reason mentioned above, to obtain the measure of the relative importance of convection and greatest diffusion effects. Thus, representing these measures by a ratio, we have:

$$\frac{\text{Inertia forces}}{\text{Viscous forces}} = Re\,\ell^2$$

$$\frac{\text{Heat convection}}{\text{Heat conduction}} = Pe\,\ell^2$$

$$\frac{\text{Mass convection}}{\text{Mass diffusion}} = Re\,Le\,\ell^2$$

The a priori evaluation of the order of magnitude of (ℓ) poses no problem when there is an imposed velocity V_i, for then one takes $V_r = V_i$ and the orders of magnitude of the numbers (*) are known a priori. For instance, when Re is of the order of one, $\ell = 1$ and viscous forces are of the same order as inertia forces throughout the fluid. When $Re \gg 1$, there are regions near solid boundaries (dynamic boundary layers, Fig. 2.26) or near discontinuity surfaces (mixing layers), whose extent normal to the streamlines is of the order $L\,Re^{-1/2}$. Within these regions, leading viscous forces are of the same order as inertia forces; outside them, all viscous forces are negligible. Similarly when Pe or $Re\,Sc$ are much larger than one there are thermal or concentration boundary layers, whose thicknesses are of the order $L\,Pe^{-1/2}$ and $L\,(Re\,Sc)^{-1/2}$, respectively, in which the effects of normal diffusion are of the same order as convection effects and outside which diffusion is negligible. Thicknesses of dynamic, thermal (Fig. 2.27) and concentration boundary layers are in the square root ratios of the corresponding diffusion coefficients. These thicknesses are all of the same order for gases (since the Prandtl and Schmidt numbers are all of the order of one for gases). The same is not true for liquids. Thus, for instance, for most liquid metals, the thermal boundary layer is thicker than the dynamic boundary layer ($Pr \sim 10^{-1} \div 10^{-3}$) whereas the opposite happens with most organic liquids and molten salts ($Pr \sim 1 - 10^2$) (Fig. 2.28).

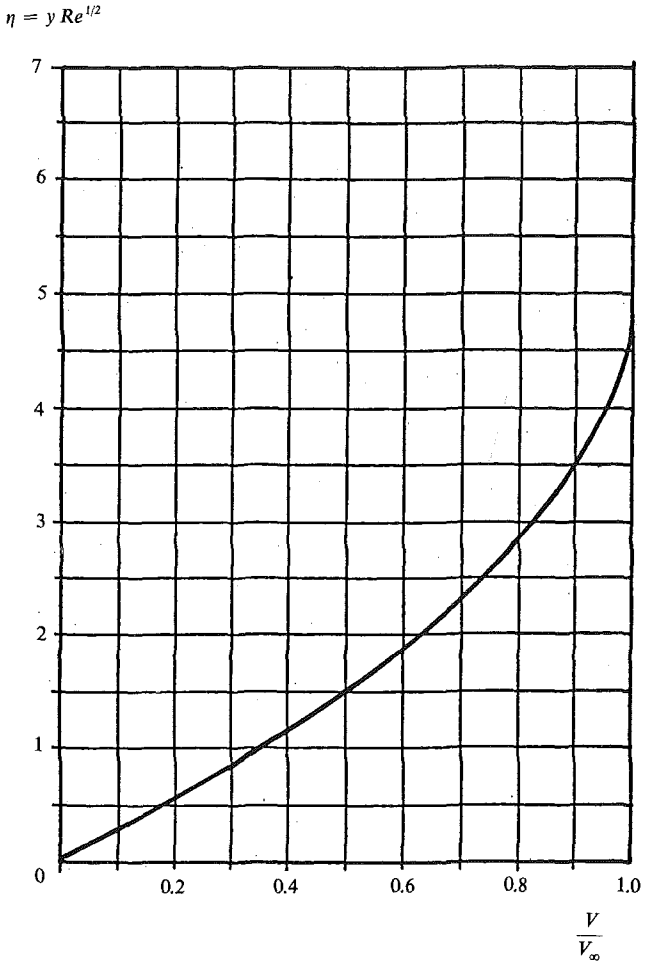

Figure 2.26 Extensions of dynamic boundary layers or of mixing layers.

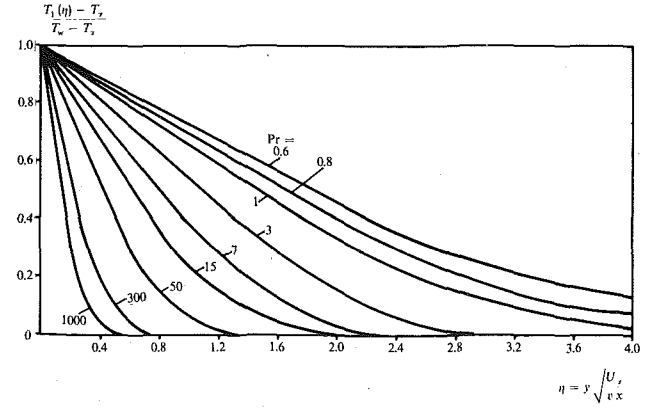

Figure 2.27 Temperature distribution on a heated flat plate at zero incidence, with small velocity plotted for various Prandtl numbers (frictional heat neglected).

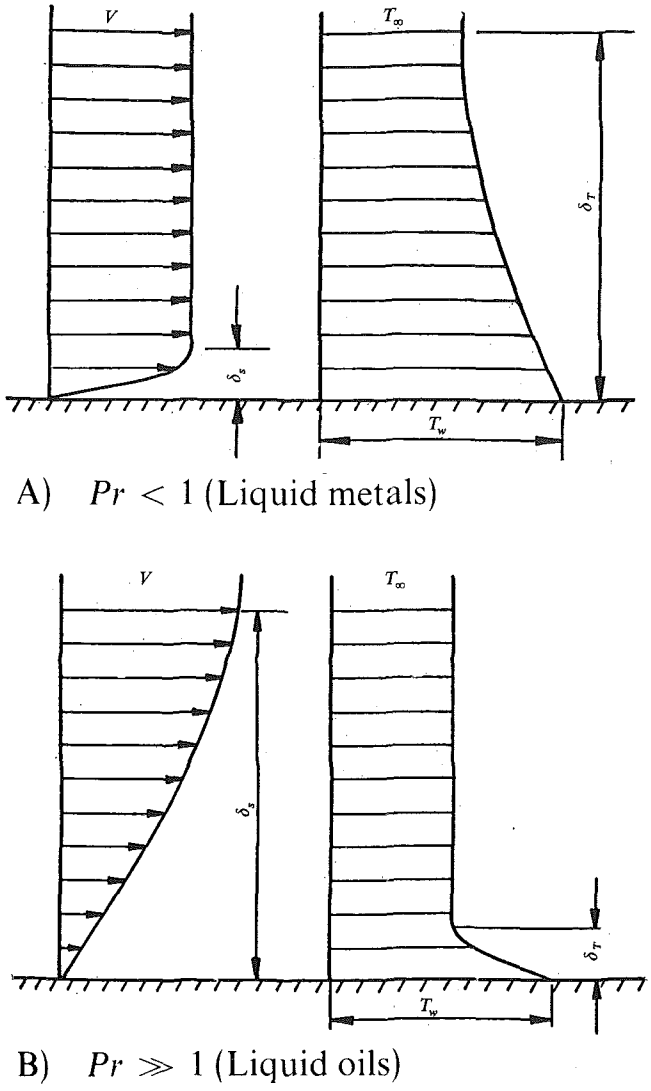

Figure 2.28 Temperature and velocity distributions in the laminar boundary layers on a hot vertical flat plate in natural convection.

When there are no imposed velocities, the choice of V_r is not so evident. It must be determined from an order of magnitude analysis of all balance equations relevant to the specific problem considered [2.33]. V_r can be expressed as the product of a known characteristic speed V_f and a power ℓ^p of (ℓ), with V_f and p depending on the particular problem considered. The values of the transport numbers defined in terms of V_f are again known a priori and the scale factors are determined as before. Thus, for instance, if Re turns out to be of the order one, ℓ is one and inertia and viscous forces are of the same order throughout the fluid. If Re is much

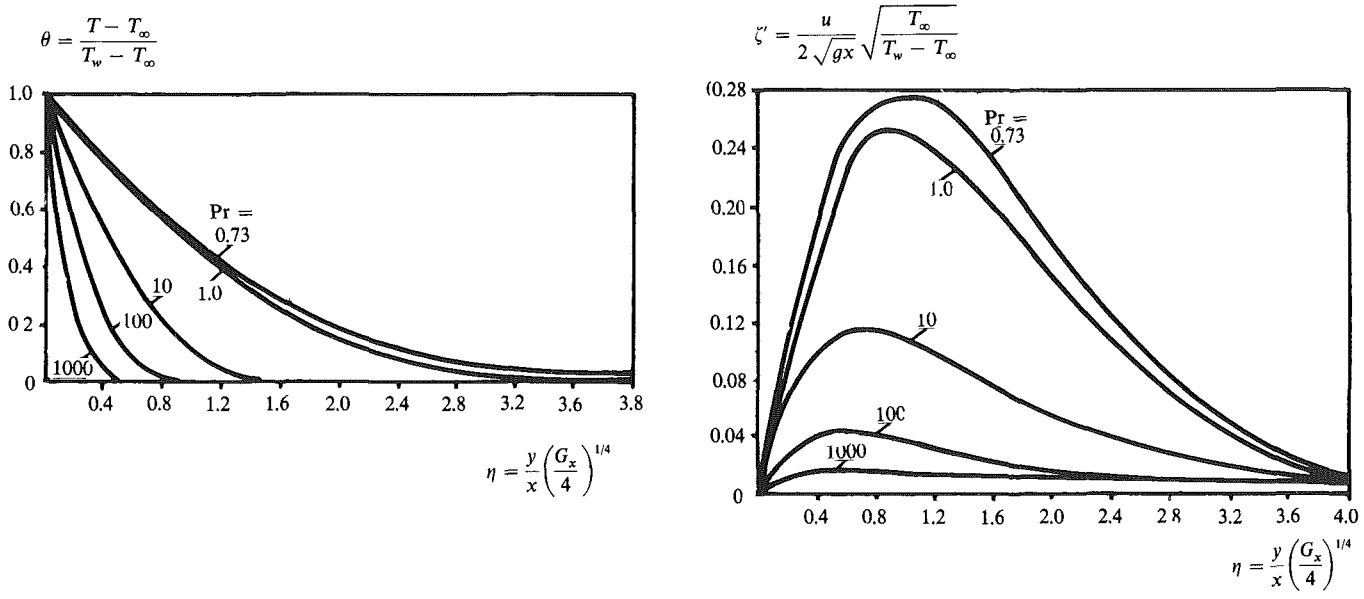

Figure 2.29 Thermal and dynamic boundary layers for various Prandtl numbers.

greater than one, the thickness of the dynamic boundary layer is of the order of $L/Re^{1/(2+p)}$. For natural convection in the absence of interfaces (§ 2.4.1) it is $V_f = (\alpha/L)$ for $Pr \simeq 1$ or $\gg 1$, $V_f = (\nu/L)$ otherwise and $p = 2$ in both cases (Fig. 2.29). Although perhaps formulated differently, these are, so far, well-known classical results [2.34].

More recent developments fostered by the prospects of microgravity, pertain to flow fields in the presence of interfaces.

For thermal Marangoni flows (Table 2.6) in gas/liquid systems V_f is equal to the Marangoni speed $V_m = (|\Delta\sigma|/\mu)$ of the more viscous fluid and $p = 1$. Marangoni boundary layers occur when Reynolds (Re_m) or Peclet (Pe_m) numbers referred to V_m are much greater than one. The thickness of these layers is of the order of $(L/Re_m^{1/3})$ or $(L/Pe_m^{1/3})$ [2.33, 2.35], (Fig. 2.30).

Many different regimes of temperature and velocity fields in the two adjacent bulk fluids may occur, depending on the order of magnitude of the Reynolds and Peclet numbers of the two fluids.

Figure 2.31 [2.35] gives values of unit Marangoni speed $\overline{V}_m(\Delta T = 1\ \mathrm{K})$ for the liquids listed in Table 2.3. $\overline{V}_m$ ranges between 1 and 20 cm/s but attains much lower values for zinc-chloride (10^{-3} cm/s) and for very viscous liquids (1000 Cs silicone oil, glycerin) and is the smallest (10^{-4} cm/s) for molten glass.

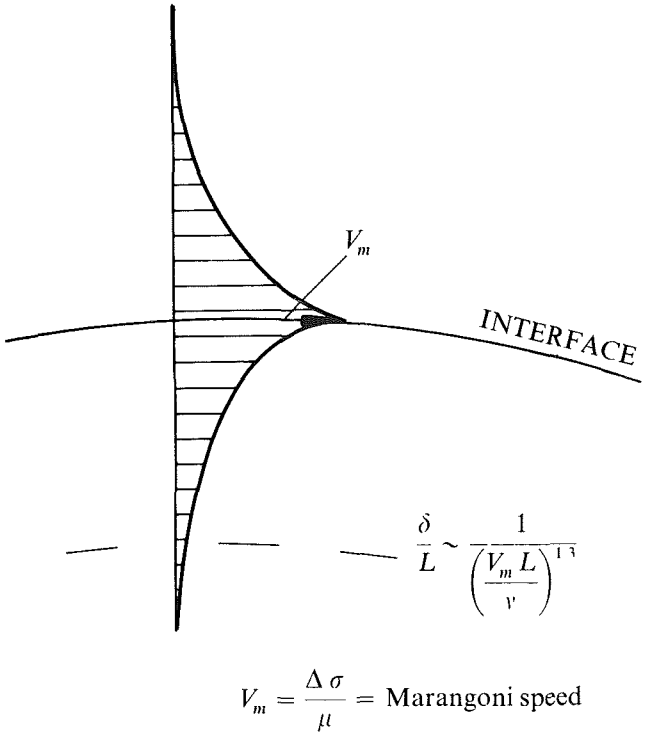

Figure 2.30 Dynamic Marangoni boundary layer.

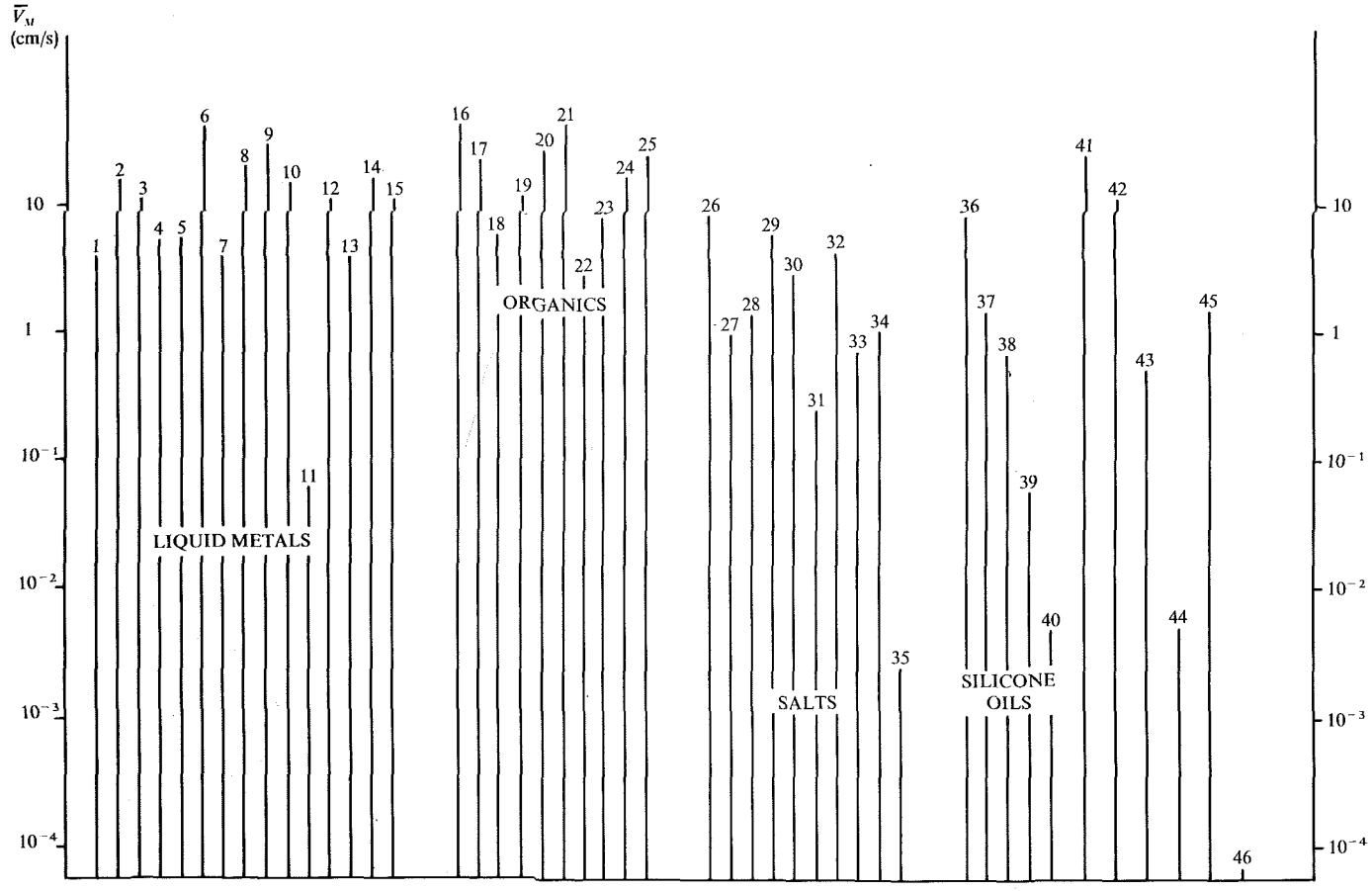

Figure 2.31 Histogram of the unit Marangoni speed for the liquids considered.

Unit Reynolds ($\overline{Re}_m$) and Peclet ($\overline{Pe}_m$) numbers ($\Delta T = 1$ K; $L = 1$ cm) are shown in Figure 2.32. Reynolds numbers span over about 10 orders of magnitude, but, in each class, the scatter is rather limited, with the obvious exception of the silicone oils. The range of Peclet numbers is less wide (about seven orders of magnitude). Organic liquids exhibit the largest values, liquid metals have the largest scatter (about 3 orders of magnitude). The smallest value pertains to molten glass.

For given interfacing fluids, Re_m and Pe_m increase with the extent (L) of the interface parallel to the imposed temperature gradient. Hence, under microgravity conditions, Marangoni flows may have much larger values of Re_m and Pe_m and, consequently, the flow patterns and features may be substantially different from those on earth. Similar remarks apply to solutal Marangoni flows.

Theoretical and numerical studies are obviously required, but the appropriate experimental verification can only be carried out in a microgravity environment.

Velocity estimates in Marangoni flows

The reference velocity V_r also gives the order of magnitude of the velocity in thermal Marangoni flows. On the basis of what has just been said, it can be estimated a priori and this estimate provides an additional example of how flow features depend on the relative importance of transport phenomena. In a typical floating-zone configuration, V_r is given by [2.33]:

$$V_r = \text{smallest}\left\{V_m; \frac{V_m}{Re_m^{1/3}}; \frac{V_m}{Pe_m^{1/3}}\right\}$$

$$= \text{smallest}\left\{\overline{V}_m \Delta T, \frac{\overline{V}_m}{\overline{Re}_m}\left(\frac{\Delta T^2}{L}\right)^{1/3}; \frac{\overline{V}_m}{\overline{Pe}_m}\left(\frac{\Delta T^2}{L}\right)^{1/3}\right\}$$

The barred unit quantities depend only on the properties of the liquid and of the interface. The other quantities evidence the scaling laws for the dependence of V_r on (ΔT) and L. When there are no Marangoni dissipative

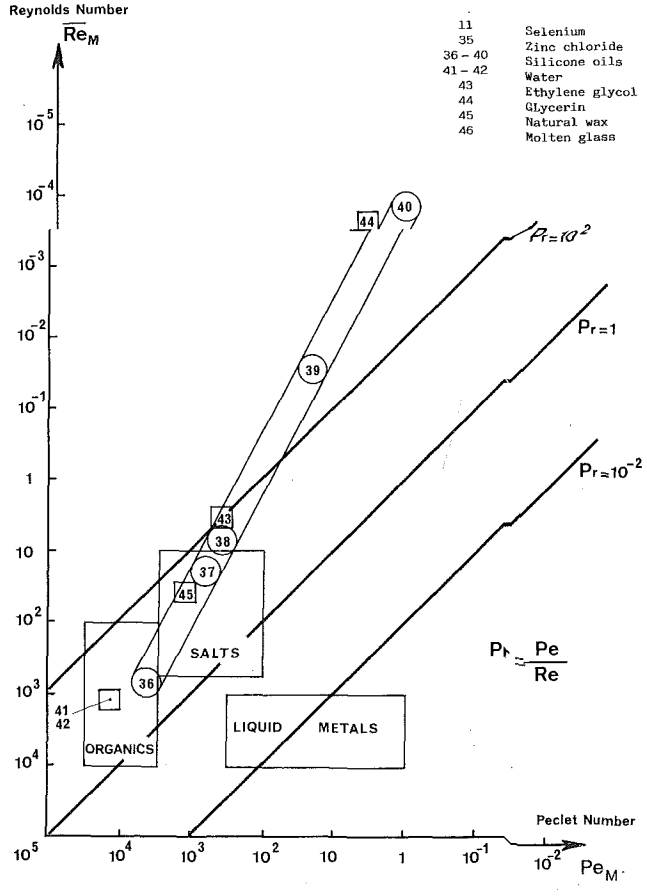

Figure 2.32 Schematic representation of the variations of Reynolds number and Peclet number for various kinds of materials: $\overline{Pe}_m/\overline{Re}_m = Pr$.

layers (Re_m and Pe_m at most of the order of one), V_r coincides with the Marangoni speed V_m, is independent of the interface extent L in the direction of the imposed temperature gradient, and increases linearly with T. When Marangoni dissipative layers are present, V_r is smaller than V_m, depends on L, and increases with the (2/3) power of ΔT. These a priori theoretical estimates of the order of magnitude of velocity in thermal Marangoni flows have been confirmed by experiments and detailed numerical calculations [2.4].

In §2.4.3 and 2.4.4 it has been systematically assumed that the dissipative regimes are laminar. Turbulent transport processes will not be considered in any detail. Areas of main concern under microgravity conditions are expected to be:

- decay of turbulence in forced or mixed convection, and
- transition to turbulence in free convection.

2.5 Motion of macroscopic particles in a fluid

Bubbles, drops, or solid particles floating in a fluid can be moved by a large number of 'weak' mechanisms or forces. In many situations the influence of such mechanisms on the evolution of particle distributions is *changed qualitatively when they do not have to compete* with gravity.

Many microgravity experiments are motivated by the desire to avoid buoyancy or sedimentation in heterogeneous systems consisting of a fluid phase and solid, liquid, or gaseous particles (§4.3). The suppression of these effects in space, of course, could allow a large degree of freedom in choosing a particle distribution, instead of being restricted to a unique spatial distribution dictated by gravity. This explains the intense interest that scientists working on composite materials have taken in microgravity experiments. However, it turns out that, under microgravity conditions too, it is not necessarily easy to stabilise a particle distribution and to avoid motions. An amazingly large number of transporting effects can appear that have hitherto been safely neglected, because they are small in comparison with sedimentation under normal gravity. An example is given in Figure 2.33. Under microgravity, when g sedimentation and g-driven convection are largely eliminated, one or more of these effects can become dominant and determine the evolution of a particle distribution and may thus thwart the aim of an experiment.

Only the steady linear motion of particles is to be considered here. Migration can be caused by an externally applied force field other than gravity. In other more involved situations, when particle/matrix interaction and gradients of temperature or concentration are the cause of particle migration, one may speak of transport mechanisms. All of these 'weak' effects are well known – at least in principle – but some have received little attention. They are arousing new interest now and in fact have become a subject of research in their own right, for three different reasons, as follows.

- If a microgravity experiment is to be prepared effectively, all causes of motion must be known and their respective roles must be analysed, since they may otherwise frustrate the aim of the experiment. This has happened in early space experiments with immiscible alloys, where an initially fine dispersion of droplets separated completely [2.36, 2.37].
- The controlled application of such weak effects is another prospect that holds much promise. For

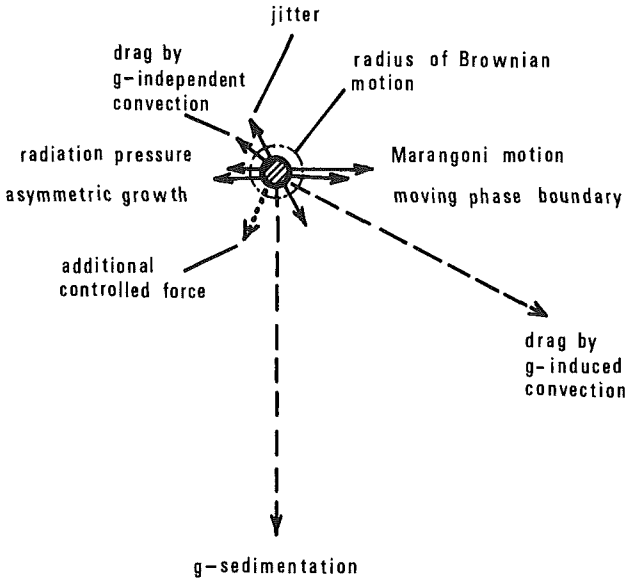

Figure 2.33 Migration of a drop in a liquid can have very different origins. The arrows represent components of the total displacement per time interval that are attributable to the indicated causes. (In case of jitter the amplitude of a periodic motion is shown). Under normal gravity the dashed arrows dominate. They are greatly reduced under μg – and the resultant of the individual components will normally have a different direction. For the purpose of an experiment the application of an additional controlled force may be sometimes useful.

example they could be used for the separation of heterogeneous particle populations (as in electrophoresis), or for the controlled generation of particle arrays. Here, too, composite materials are of considerable interest.

– Finally, it appears useful to aim for full knowledge of the entire system of transporting mechanisms, to study combinations etc., also in order to achieve a deeper understanding of their role in such natural processes as phase growth, incorporation of particles into a solid phase, phase separation and coalescence. Even under normal gravity, such effects can be relevant to the motion of sufficiently small particles, but observations may then be difficult. This holds particularly for metals where optical observations are ruled out and the evolution of a dispersion must be inferred from data characterising the final state after solidification.

Table 2.7 gives a list of 19 mechanisms or forces that have been found able to move a particle that is suspended in a fluid matrix [2.38]. No claim is made that this list is complete, and some mechanisms can actually apply to very different situations and could be subdivided. Some have side-effects that are also g-relevant and can complicate particle behaviour under normal gravity: for example, photophoresis, radiation pressure and the Lorentz force can be accompanied by

Table 2.7

Acting Mechanism or Force	Cause	Occurence System (medium/particle) G/L	G/S	L/G	L/L	L/S	radius-dependence of velocity
Residual gravity	time-independent acceleration; $\Delta\rho$	+	+	+	+	+	R^2
g-jitter	fluctuating acceleration; $\Delta\rho$	+	+	+	+	+	R^2
Brownian motion	temperature	+	+	+	+	+	$R^{-1/2}$
Drag	convection in matrix	+	+	+	+	+	R^0
Marangoni motion	gradient of interfacial tension	+	–	+	+	–	R
Electrolyte diffusiophoresis	concentration gradient of electrolyte	–	–	+	+	+	R^0
Thermophoresis	temperature gradient	+	+	?	–	–	R
Photophoresis	radiation	+	+	?	–	–	R^2
Diffusiophoresis	concentration gradient	+	+	–	–	–	R^0
Jet effect	asymmetric condensation/evaporation	+	+	?	?	?	R^0
Electrophoresis	electric field; charge on particle	+	+	+	+	+	R^0
Electrocapillary motion	electric field; $\Delta\sigma'$	–	–	–	+	–	R
Moving phase boundary	interfacial forces	?	?	+	+	+	R^0
Lorentz force	crossed electric and magnetic fields; $\Delta\sigma'$	–	–	+	+	+	R
Electromagnetic force	inhomogeneous AC field; $\Delta\mu$	+	+	–	+	+	R^2
Dielectrophoresis	gradient of electric field intensity; $\Delta\varepsilon$	+	+	+	+	+	R^2
Magnetophoresis	gradient of magnetic field intensity; $\Delta\mu$	+	+	+	+	+	R^2
Radiation pressure	radiation; absorption or reflection	+	+	–	+	+	R
Acoustic pressure	acoustic field; $\Delta(\rho \cdot c)$	+	+	+	+	+	R^2

enhanced energy dissipation in the particles and consequently by inhomogeneous heating of the fluid surrounding the particles, which under gravity generates local convection.

The list starts with four disturbing effects that set limits to microgravity experiments with dispersion, namely residual gravity, g-jitter, Brownian motion, and flow in matrix:

Residual gravity is the part of accelerations to be felt in a spacecraft that is constant over the duration of an experiment. It is mostly due to deceleration by the upper atmosphere and is expected to be about $10^{-5} - 10^{-7}\, g_0$. In some situations its effects could be reduced by rotating the entire experiment about the orbital axis of the spacecraft (§ 2.1).

g-jitter comprises time-varying accelerations of various origins with expected amplitudes up to $10^{-3}\, g_0$. Two important cases are:

- A constant acceleration acts only over a short time interval τ. A particle in a viscous fluid that is initially at rest will first be accelerated, and after g is turned off, will be decelerated by friction until it is at rest again. The total displacement of a solid spherical particle is then $d = (2/\mu) \cdot \Delta\rho r^2 g\tau$.
- A periodic acceleration $g \,.\, \sin \omega t$ causes a periodic displacement with an amplitude that depends in a rather complicated way on the densities of particle and matrix, on radius, viscosity, and frequency [2.39]. For frequencies exceeding a few cycles/s amplitudes in liquids remain small ($< 1\ \mu$m), i.e. faster vibrations can be safely neglected insofar as their effects on suspended particles are concerned. There is one exception to this rule, however: when physical conditions vary over a distance of the order of the amplitude, as in the vicinity of a phase boundary, then even a weak vibration can have important consequences (e.g. incorporation into a solidifying matrix).

Brownian motion causes a non-directional average displacement of particles by a distance

$$d_B = \sqrt{\frac{kT}{3\pi\,\mu R}}$$

Stabilisation of particle positions to better than d_B is of course impossible. On the other hand only transport by any mechanism or force by more than d_B is meaningful and needs to be considered.

Flows in the suspending matrix can have various origins and will of course take along any particle with the same velocity, independent of its size.

The next group (5 – 11) comprises mechanisms that may occur spontaneously in experiments with a dispersion and whose transporting power in a given situation is often revealed only after elimination of gravity. They may become effective when gradients of temperature or concentration arise in a fluid, or under the influence of irradiation. Their role in the generation and evolution of liquid mixtures is largely unknown and becomes more easily accessible for observation in experiments under microgravity. The most prominent mechanism in this group is probably what is called here Marangoni motion: due to interfacial-tension-driven convection a gaseous particle in a temperature field is expected to migrate with a velocity of the order of

$$v = -\frac{R}{2\mu} \cdot \frac{d\sigma}{dT} \cdot \text{grad}\ T \quad [2.40, 2.41]$$

(An analogous formula holds for a concentration field.)

Experimental verification is difficult since $d\sigma/dT$ is sensitive to contamination by surface-active substances. In practice therefore lower velocities will often be observed than are obtained from the formula with a $d\sigma/dT$ measured on a pure substance.

The other mechanisms will not be elaborated on here. We give only basic information by indicating in the table the main conditions for their occurrence [2.39, 2.42, 2.43].

Their transporting power can in principle be influenced by increasing or reducing the respective gradients, but this will usually not be a feasible or convenient means of controlling a particle distribution.

The last group comprises two mechanisms and a number of forces that depend on external fields. They can be controlled more easily and used actively to further the objective of an experiment. The advantage of their application under microgravity is of course that they do not have to compete with sedimentation. Also, in order to produce visible effects, i.e. displacement of particles, or to dominate the evolution of a dispersion, fields of lower intensities are required, and side effects such as heat dissipation or electrolysis are diminished.

While the forces and mechanisms listed in Table 2.7 are basic for understanding the behaviour of suspended

particles, the interpretation of observations, or their application for control of a dispersion is complicated for several reasons:

- The velocity of a particle may vary in a non-linear way with the driving force. For example, the above expression for the Marangoni motion holds only for low Peclet numbers $Pe = vR/a \ll 1$. (This reflects the fact that at higher velocities v, the temperature distribution near a particle is no longer controlled by conduction only, and that – as a consequence of its own motion – a particle then feels a lower grad T than is applied externally).
- When several mechanisms are acting simultaneously their combined effect may again comprise non-linear terms.
- When the number density of particles is not small, i.e. when their mean distance is no longer large compared with their radius, then interactions of the particles with the field of the driving force (e.g. the local temperature field or electric field can become distorted by the presence of particles) as well as with themselves have to be considered, and complicated and unexpected forms of behaviour can ensue.

2.6 Simulation of microgravity problems

Outcomes of physical problems, when described in suitably non-dimensionalised terms, depend on a set of non-dimensional characteristic numbers that, broadly speaking, characterise: the geometry of the problem, the relative importance of different intervening phenomena, and the boundary and/or initial conditions.

Such characteristic numbers combine several dimensional quantities and can, therefore, assume the same value for different sets of values of the quantities entering their definition. A given problem may be studied in a different set-up provided the values of all the non-dimensional numbers are the same. This procedure is generally termed 'simulation' but when this term is used, particular attention should be given to the specification of exactly what is being simulated.

In many problems there are more relevant characteristic numbers than quantities that may be changed, and hence complete simulations are not possible. Results of experiments performed by keeping the same value only for a subset of relevant characteristic numbers can be used meaningfully (or, as it is said, extrapolated to other conditions) if and only if their dependence upon the non-simulated numbers is known. Some aspects of microgravity simulation are worth stressing.

Under hydrostatic conditions, there is only one relevant non-dimensional number, the static Bond number. Hydrostatic simulation of microgravitational environment is thus comparatively easy to achieve on earth. The same is no longer true in dynamic situations. In particular, for instance, non-isothermal or other dynamics experiments with Plateau configurations, while having their own scientific interest, cannot be taken as representative of what happens in a true microgravity environment.

Detailed quantitative knowledge of the dependence of flow properties upon such numbers as Prandtl, Schmidt and Lewis are needed before results obtained (even in a true microgravity environment) with given fluids can be extrapolated to other fluids with different values of the above numbers.

The actual impossibility of obtaining, on Earth, the same (high) values of the transport characteristic numbers that may prevail in the microgravity environment is one of the most stringent motivations for the need of space-borne experimentation.

None but the most simple problems are amenable to complete simulation on Earth. The understanding of the complex microgravity fluid phenomena needed for materials and life-science experiments cannot be obtained from experiments on Earth since they very often reproduce entirely different physical situations.

References

[2.1] Gibbs J B, *Collected Works*, Yale University Press, New Haven 1948, Vol. 1.

[2.2] Defay R, Prigogine I & Sanfeld A, in *Colloid and Interface Science* **58**, 1977.

[2.3] Napolitano L G, in *Acta Astronautica* **6**, 1979, p. 1093.

[2.4] *Study on fluid phenomena influencing the design of zero-g experiments, User's guide*, ESA-LR(P)1386, Techno System Report TS-11-79, 1979.

[2.5] Dussan V, E B, in *Annual Review of Fluid Mechanics* **11** (M van Dyke, J V Wehausen & J L Lumley, Eds), Annual Reviews Inc, Palo Alto, Calif, 1979, p. 371.

[2.6] Neumann A W, in *Wetting, Spreading and Adhesion* (J F Padday, Ed), Academic Press, London, 1978, p. 3.

[2.7] Moldover M R & Cahn J W, in *Science* **207**, 1980, p. 1073.

[2.8] Dussan V, E B & Davis S H, in *J Fluid Mech* **65**, 1974, p. 71.
[2.9] Huh C & Scriven L E, in *J Colloid Interface Sci* **35**, 1971, p. 71.
[2.10] Hocking L M, in *J Fluid Mech* **76**, 1976, p. 801.
[2.11] Hocking L M, in *J Fluid Mech* **79**, 1977, p. 209.
[2.12] Dussan V, E B, in *J Fluid Mech* **77**, 1976, p. 665.
[2.13] Porter A W, in *Encylopaedia Britannica* (14th Ed), **22**, 1966, p 595.
[2.14] Wang T G, Saffren M M & Elleman D D, in *Material Sciences in Space*, ESA SP-115, 1976, p. 405.
[2.15] Siekmann J, in *Material Sciences in Space*, ESA SP-142, 1979, p. 341.
[2.16] Bikerman J J, *Foams*, Springer-Verlag, Berlin, 1973, Chaps 1 and 5.
[2.17] Huh C & Scriven L E, in *J Colloid Interface Sci* **30**, 1969, p. 323.
[2.18] Padday J F, in *Phil Trans Roy Soc* **269**, London, 1971, p. 265.
[2.19] Heywang W, in *Z Naturforschg* **11a**, 1956, p. 238.
[2.20] Strutt J J (Baron Rayleigh), *The Theory of Sound*, Vol 2, Dover, New York 1945, p. 351.
[2.21] Martinez Herranz I, in *Cospar: Space Research*, Vol XVIII (M J Roycroft & A C Sticklands, Eds), Pergamon Press, Oxford 1978, p. 519.
[2.22] Gillette R D & Dyson D C, in *Chem Eng J* **2**, 1971, p. 44.
[2.23] Plateau J, *Statique expérimentale et théorique des liquides soumis aux seules forces moléculaires*, Vol 2, Gauthier-Villars, Paris (1873).
[2.24] Mason G, in *J Colloid Interface Sci* **32**, 1970, p. 172.
[2.25] Carruthers J R & Grasso M, in *J Appl Phys* **43**, 1972, p. 436.
[2.26] Truesdell C, in *Annual Review of Fluid Mechanics*, **6** (M van Dyke, W G Vincenti & J V Wehausen, Eds), Annual Reviews Inc, Palo Alto, Calif, 1974, p. 111.
[2.27] Joseph D D & Beavers G S, in *Rheol Acta* **16**, 1977, p. 69.
[2.28] De Groot S R & Mazur P, *Non-equilibrium thermodynamics*, North-Holland, Amsterdam 1962.
[2.29] Callen H B, *Thermodynamics*, J Wiley, London 1960.
[2.30] Defay R, Prigogine I & Sanfeld A, *Colloid and Interface Science* **58**, 1977, p. 498.
[2.31] Napolitano L G, in *Acta Astronautica* **6**, 1979, p. 1093.
[2.32] Glansdorff P P & Prigogine I, *Thermodynamics of structure, stability and fluctuations*, Wiley, New York 1971.
[2.33] Napolitano L G, in *Second Levitch Conference*, Washington 1978; in *Material Sciences in Space*, ESA SP-142, 1979, p. 349.
[2.34] Schlichting H, *Boundary Layer Theory*, Mc Graw-Hill, New York 1968.
[2.35] Napolitano L G & Golia C, in *Acta Astronautica* **5-6**, 1981, p. 212.
[2.36] Gelles S H, *AIAA 15th Aerospace Science Meeting*, 1977.
[2.37] Ahlborn H & Löhberg K, DGLR-Bericht 79-01, p. 269.
[2.38] Bewersdorff A, Görler G P & Klein H, Transportmechanismen für makroskopische Partikel in Suspension, in *Z für Flugw und Weltr (ZFW)* **2**, 1981, p. 174.
[2.39] Fuchs N A, *The Mechanics of Aerosols*, Pergamon, Oxford 1964, p. 80.
[2.40] Young N O & al, The motion of bubbles in a vertical temperature gradient, in *J Fluid Mech* **6**, 1959, p. 350.
[2.41] Subramanian R S, *Euromech Colloquium* 138, Karlsruhe, March 1981.
[2.42] Anderson J L, *PCH-Physico Chemical Hydrodynamics* **I**, 1980, p. 51.
[2.43] Omenyi S N & Naumann A W, *J Appl Phys* **47**, 1976, p. 3956.

3 Stability

Systems undergoing transitions between qualitatively different states can become very sensitive to gravity and offer a chance for microgravity experiments of a fundamental nature.

3.1 Bulk phases

Systems or processes near points of incipient instability are promising subjects to display conspicuous g effects. On approaching such a point certain response properties (as compressibility) diverge, i.e. sensitivity to external influences increases. Gravity, or gravity-dependent effects, can then introduce increasingly larger spatial asymmetries, or in other cases, can shift the point of neutral stability. Furthermore, gravity can determine the spatial order in the system after crossing the point of instability.

In both ways the system can be affected drastically, i.e. it generates a strong response. Illustrative of g-relevant instabilities are phenomena occurring at the gas/liquid critical point, and chemical reactions far from thermodynamic equilibrium, including combustion phenomena.

3.1.1 *Critical point phenomena*

Phase transitions must be counted among the most important physical phenomena. Of particular interest are continuous phase transitions at critical points (in contrast to transitions via nucleation). They are characterised by the gradual disappearance of an 'order parameter' (for example the density difference of two phases). In the vicinity of a critical point the thermodynamic properties show a singular, often diverging behaviour. Mathematically this can be described by simple power laws. For example, the critical part of the heat capacity varies as:

$$c_v \sim \left| \frac{T - T_c}{T_c} \right|^{-\alpha}$$

where α is a constant.

It is well known today that very different kinds of physical systems show remarkable similarities near their respective critical points. This is explained by the so-called 'principle of universality' that unites systems like ferromagnets near the Curie point, binary liquids near the consolute point, fluids near the gas/liquid critical point, and many others. Universality is now well established, and very elaborate theoretical concepts (briefly characterised here by diverging correlation

length, scaling laws, renormalisation) have been developed over the last decade. This theory has led to a deeper understanding not only of equilibrium phase transitions but also to new ways of looking at other order/disorder phenomena in physics, chemistry and biology. With further progress the need for good, quantitative experiments increases. The principle of universality provides the experimenter with the opportunity to choose the best suited system for studying critical phenomena, and in many respects this is a one-component gas, the simplest system to display critical behaviour. However, under gravity such experiments are limited by the divergence of compressibility. On approaching the critical point, a fluid becomes compressed under its own weight and density inhomogeneities appear (Fig. 3.1). The sample is therefore not really in its critical state, except in a two-dimensional layer [3.1]. Consequently, experimental data do deviate from theoretical predictions and a rigorous test of theory in the most interesting immediate vicinity of the critical point is not possible. For example, measurements of the critical behaviour of heat capacity were done on samples with heights of only 1 mm in order to limit the influence of gravity. Figure 3.1 shows that even over this small distance gravity generates deviations of density of several percent and averaging errors cannot be avoided. Also for measuring other parameters as density, dielectric constant, correlation length, material samples of a minimum size are required and accordingly, under gravity conditions, correct data cannot be obtained near the critical point. A rough estimation shows that a reduction of gravity by a factor 10^{-3} would allow to shrink the inaccesible temperature interval by about 10^{-2} [3.1].

The role of gravity in critical behaviour is further elucidated by considering the correlation length ζ in an ideal homogeneous sample and in a sample with a density distribution as in Figure 3.1. In the first case ζ grows to infinity as the critical point is approached. However, in the second case ζ becomes infinitely large only in a layer whose height simultaneously decreases to zero. This is of course a contradiction, which means that in a strict sense the *critical point cannot be reached under gravity.*

The particular influence on correlation length seems to be at the root of observations that suggest that standard nucleation theories are fundamentally wrong near the fluid critical point. It is likely that only experiments on undercooling under reduced gravity will clarify this point.

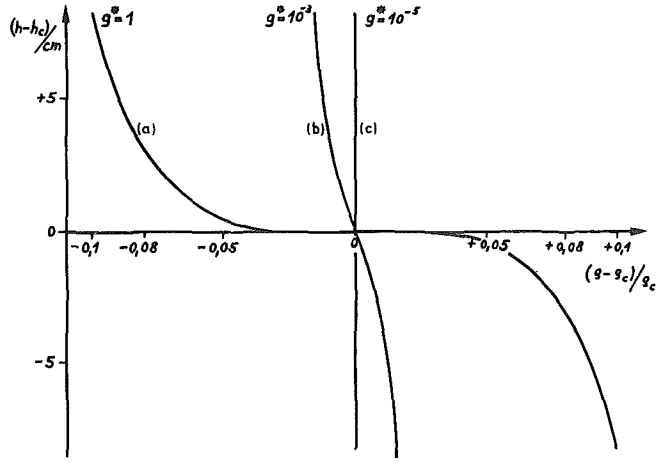

Figure 3.1 At the gas/liquid critical point a fluid is compressed under its own weight as compressibility becomes infinite. In a sample at its critical temperature density inhomogeneities appear even in a thin layer: at the edge of a 1 mm slab under normal gravity (curve *a*) the density is off its critical value by several percent. The inhomogeneities can be reduced only by lowering gravity (*b* and *c*).

3.1.2 *Chemical instabilities*

Normal gravity is far too weak to have a measurable effect on the result of a chemical reaction. It can easily be estimated that when a molecule in a liquid undergoes a reaction the change of potential gravitational energy is less than 10^{-13} to 10^{-16} of the binding energy. In other words, when states of thermodynamic equilibrium are considered gravity can be safely neglected. However, when non-equilibrium situations are considered, different conclusions must be drawn: gravity can indeed have an indirect influence on effective reaction rates in inhomogeneous systems.

Particularly reactions that are confined to surfaces or singular points are often diffusion-controlled. Gravity-induced convection will then augment rates by shortening the distance over which reactants and products are transported by diffusion only to the side of reaction. (A very good example at point is a diffusion flame whose overall reaction rate does indeed decrease to zero under zero-gravity; see § 4.4.1). If different competing reaction paths are available to a system even the relative abundance of products can depend on g, with *gravity generally favouring the path with heterogeneous reactions.*

Various possibilities for chemical-gravitational coupling appear when states far from equilibrium are studied:

Over the last decade physico-chemical systems that are far from local thermodynamic equilibrium have aroused increasing interest. It is well known today that systems in which reaction and diffusion are the only acting processes can become unstable and show new and complicated forms of behaviour, as sustained temporal oscillations, multistability (under identical constraints a system can then assume differing stable states), or chemical waves (Fig. 3.2). They may also evolve to spatially structured states, in other words a chemically reacting liquid under far from equilibrium conditions can loose its initial homogeneity and build up spatial structures. (The analogy to the Bénard instability should be pointed out here. In both cases mass transport suddenly begins to play a role beyond an instability, and spatial relationships become important. Transport is by convection in the Bénard situation and by diffusion in chemical systems.) Spatial structures can then actually be generated and maintained by diffusion. Possible applications of these phenomena range from biological pattern formation to chemical reactors in industry [3.2, 3.3].

Figure 3.2 Chemically reacting systems can show unexpected phenomena (chemical instabilities) when far from thermodynamic equilibrium. This figure gives an example of a spatio-temporal structure in the reaction of Zhabotinski. The light lines are states of chemical activity that propagate slowly through the reacting liquid under the sole action of reaction and diffusion.

The exciting new field of chemical pattern formation will undoubtedly benefit from microgravity environment, as it allows to eliminate disturbances by natural convection. However, a fundamentally different, direct influence of gravity on the spontaneous formation of spatial structures has been proposed by Prigogine. It has recently been studied by Kondepudi [3.4], who showed that in the vicinity of certain critical conditions a vastly enhanced sensitivity to gravity appears possible. A schematic illustration of the presumed mechanism is given in Figure 3.3, where λ is a parameter characterising the distance from thermodynamic equilibrium (for example the ratio of the concentrations of a reactant and a product of a reaction), and X is the response of the system (for example the concentration of an intermediate species).

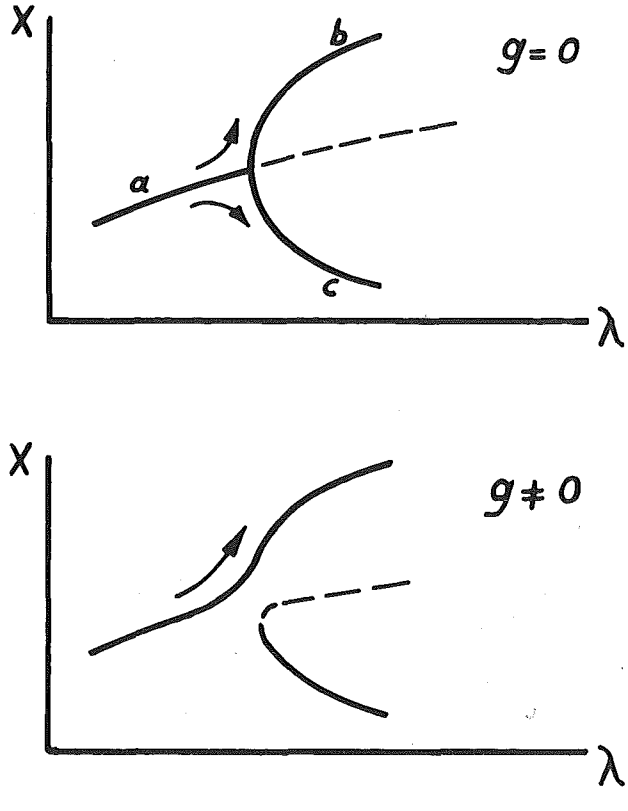

Figure 3.3 Schematic representation of predicted influence of gravity on evolution in a chemically reacting system by bifurcation diagrams. The concentration X of an intermediate species that is in balance with λ (a parameter characterising the constraints of the system, such as the concentration of a reactant) develops along the branch a when λ is increased. At critical threshold λ_{cr} the continuation of a becomes unstable and X enters b or c with equal probability (left). Gravity modifies the bifurcation diagram and b is preferred (right).

While for low λ only a single value can be assumed by X, two new branches of solutions appear beyond the critical value λ_{cr}. X_1 and X_2 can now be realized simultaneously at different locations of a reaction system. When a system is driven farther from equilibrium both branches are entered with equal a priori probability. This means that as λ approaches λ_{cr}, a weak asymmetry, as introduced by gravity, may actually decide which branch is entered and thus determines the further evolution of the system. In increasing λ the system follows the branch it has entered, and at the end the weak initial asymmetry has produced a macroscopic, unproportionally large effect. For example, g might decide whether X assumes a high or low concentration in the upper/lower part of a reaction volume [3.5]. Such a g sensing or 'g magnifying' mechanism would be of interest to biological systems. It should be stressed again that g-driven convection is not involved here.

A particular case of chemical instabilities may occur in combustion processes. Under appropriate conditions a planar flame front traversing a mixture of combustible gases can assume a cellular structure (Fig. 3.4). The structures can be stationary in the front, or in other cases may be moving perpendicular to the direction of front propagation [3.6]. Mixtures near extinction limits are most favourable for their occurrence. The cells may result from reaction/diffusion instabilities, as discussed by Sivashinski [3.7]. A formal analogy to the morphological instabilities of the solidification front (§ 3.3) is to be pointed out here. In both cases diffusion of at least two quantities (energy; chemical species) with

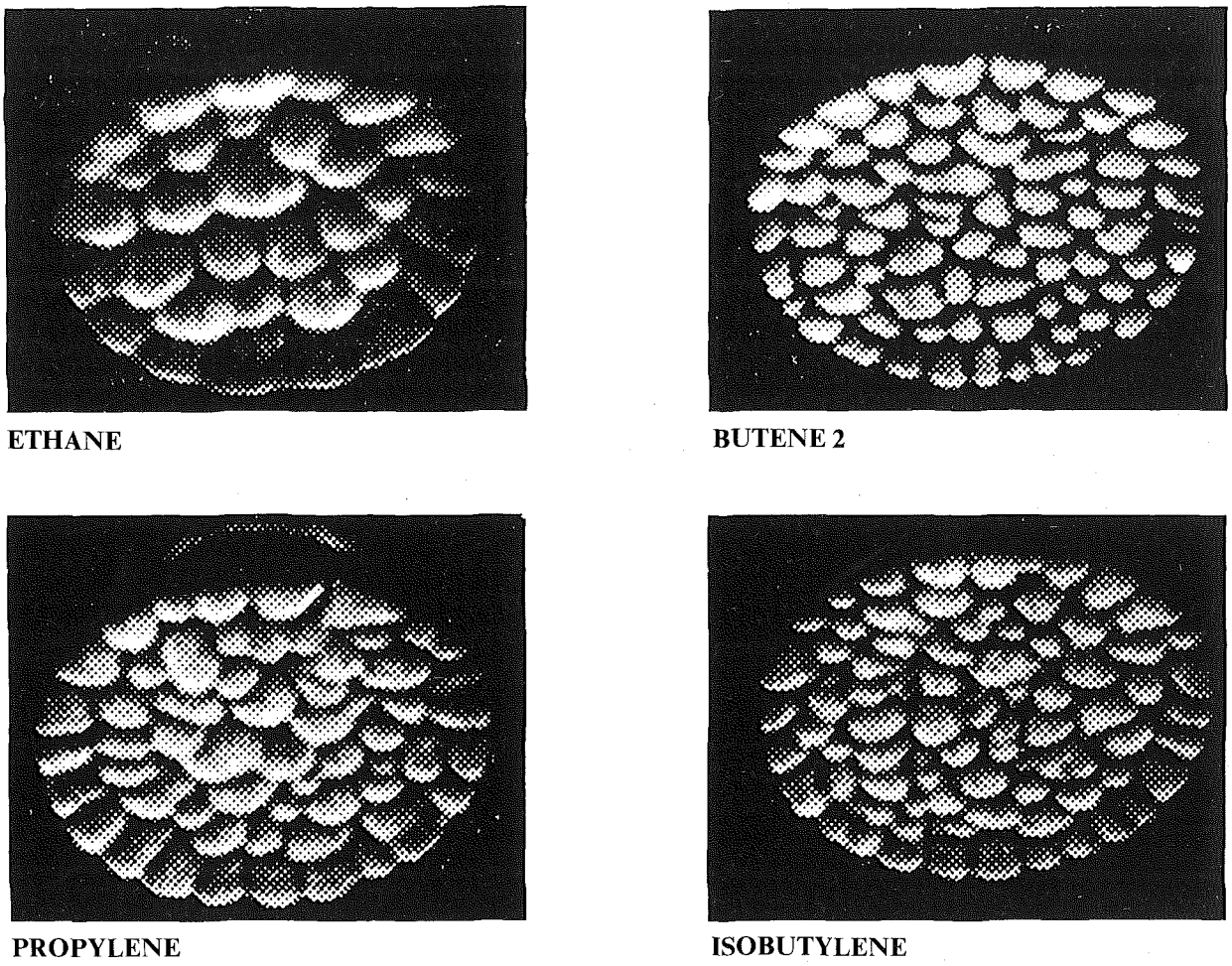

Figure 3.4 Cellular flames observed in fuel-rich hydrocarbon-air mixtures. The phenomenon could be generated by gravity-dependent fluid dynamic processes as well as by selective diffusion of chemical species.

different diffusion coefficients is at the origin of the instability and leads to the deformation on an interface. On earth the formation of cells will also be affected, or may be caused entirely, by buoyancy effects, which complicates considerably the interpretation of observations. No comprehensive treatment of this very complex situation seems presently available (§ 4.4.2).

3.2 Fluid/fluid interfaces

For various reasons, interface stability problems have attracted the interest of investigators for many years.

Sometimes, as happens to be the case with Bénard convection, a surprising and fascinating pattern of very regular cells can be easily seen once a sufficiently long time from the onset of the disturbance has elapsed. Sometimes, as in Rayleigh-type instabilities, the phenomenon is very common in the atmosphere and the ocean.

From the point of view of practical applications, the avoidance of the instabilities sets an upper limit in the range of values of the controlling parameters (there is a maximum slenderness of a liquid bridge, a critical Rayleigh number or a critical Marangoni number, and so on), although in many cases the threshold values are purposefully exceeded, for example for enhancing transport processes.

Microgravity experimentation will greatly increase the interest of these problems, either because microgravity yields configurations which cannot be observed on earth, or because other effects, hidden by gravity, could have a primary importance in driving the instability.

3.2.1 *Cylindrical bridge under solid rotation*

The stability of a cylindrical liquid bridge under solid rotation has been subject of some interest in the past years. The existence of a symmetric mode of deformation was predicted by Gillis [3.8]. A symmetric mode has been also experimentally observed by use of the neutral buoyancy simulation technique [3.9]. The connection between these experiments and Gillis' analysis is by no means clear. Later on, a 'C-mode of deformation' was detected in the Skylab's TV 101 demonstration [3.10]. It was then shown analytically [3.11, 3.12] that a cylindrical zone could evolve either toward axisymmetric non-cylindrical 'amphora shapes' or toward the C-mode. The resulting deformation mode will depend on the slenderness ($L/2R$) of the bridge, where R is the radius of the undisturbed cylinder, and on a dimensionless number, C, which measures the ratio of the pressure forces induced by rotation to surface tension forces. These results have been checked in experiments performed on earth, by use of the 'short bridge' simulation technique [3.12, 3.13].

The idea behind the analysis in [3.11] consists in relating the energy, F, of the liquid bridge (supposed to be an isothermal single-component system) with the area of the interface.

Mechanical equilibrium requires $\delta F = 0$, where δF is an arbitrary and infinitesimal variation on the system. The stability will depend on the sign of $\delta^2 F$. Change of stability will correspond to $\delta^2 F = 0$.

It is, thus, shown that the maximum stable slenderness will be given by

$$\frac{L}{2R} = \frac{\pi}{\sqrt{1 + C}} \tag{3.1}$$

for the axisymmetric mode of deformation, or by

$$\frac{L}{2R} = \frac{\pi}{2\sqrt{C}} \tag{3.2}$$

for the non-axisymmetric mode. In these equations

$C = \dfrac{\rho \Omega^2 R^3}{\sigma}$, Eq. (3.1) was first obtained in [3.7].

Which of these deformation modes will appear in practice? This can be answered by consideration of Figure 3.5, where the functions $L/2\pi R$ vs. C, as given by Eqs. (3.1) and (3.2), are shown. Both curves intersect at $L/2\pi R = \sqrt{3}/2$, $C = 1/3$. Thus we can predict that slender bridges ($L/2\pi R > \sqrt{3}/2$) will exhibit the axisymmetric mode of deformation, and not-so-slender bridges ($L/2\pi R < \sqrt{3}/2$) the non-axisymmetric one.

The issue now arises in connection with the deformation modes detected in the Skylab demonstration. Are these modes identical to that of Eq. (3.2)? Two features of the C-mode were, according to Carruthers et al. [3.10]:

(i) it was observed both in the disk iso-rotation and in counter-rotation sequences; (ii) its oscillating frequency did not depend on the disk rotation rate. In some cases both were the same, in other they were not. The result in Eq. (3.2), on the other hand, corresponds to a non-axisymmetric mode of equilibrium in solid rotation. Clearly no connection exists between the theoretical

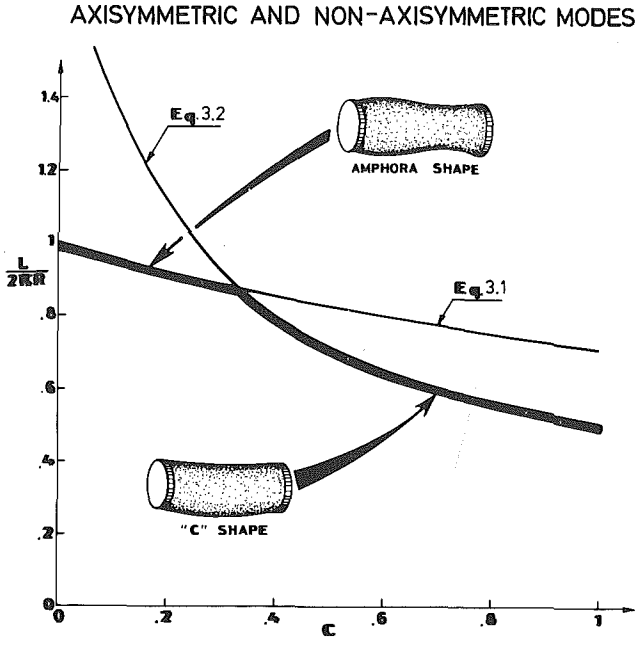

Figure 3.5 Critical length to disk perimeter ratio as a function of rotating speed for both axisymmetric and non-axisymmetric deformation modes. From [3.11].

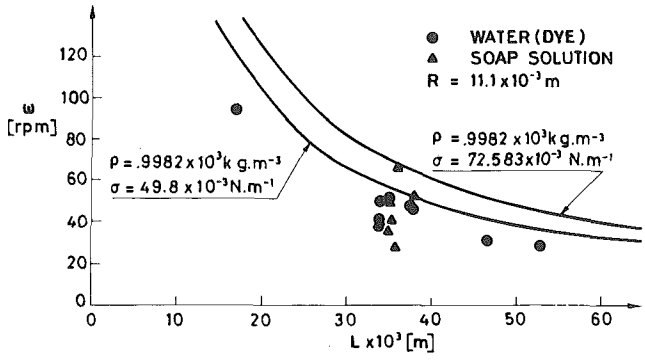

Figure 3.6 Rotating frequencies of C-modes as functions of bridge length. Experimental points have been replotted after Figure 8 in [3.10]. The curves are deduced from Eq. (3.2) with the quoted values of the fluid physical properties.

analysis and the C-mode observed in counter-rotation. Even in iso-rotation the analytical solution would only correspond to the case in which the oscillating frequency of the zone is equal to the disk rotation rate.

Even if we try to check the theoretical analysis against the quantitative results reported in [3.10] the issue remains unsolved. This is so because neither the fluid characteristics nor the ambient temperature were measured before and (or) after performing the demonstration, and the surface tension of water, the liquid used, is very prone to large variations upon contamination or temperature changes.

Experimental data from [3.10] are shown in Figure 3.6. These data correspond only to iso-rotation sequences. ● are for water and ▲ for a soap solution, which was quoted to exhibit roughly the same σ/ρ as that for water. The theoretical curves are deduced from Eq. (3.2) with the values given in Figure 3.6. The upper curve is for pure water at 293 K, the lower corresponds to *contaminated water at the same temperature. Clearly* more precise results are still required.

3.2.2 *Convective instabilities (Bénard and Rayleigh-type)*
Convective instability is a general term referred to the instabilities associated with the hydrostatic equilibrium of density-stratified fluid layers. The gravity-dependent buoyancy force may either be the only force 'driving' the instabilities (fluid layers entirely confined by solid boundaries) or may 'compete' with Marangoni forces due to gradients of interfacial tension (fluid layers with an interface).

The cells observed by Bénard [3.14], when a horizontal layer of a simple fluid is heated from below, were originally interpreted by Rayleigh [3.15] in terms of buoyancy forces alone, and, much later, by Pearson [3.16] in terms of Marangoni forces alone in an attempt to resolve a number of discrepancies between the Rayleigh theory (and its subsequent developments) and the experimental findings by Bénard and by others that had repeated and extended Bénard's experiments (see Figure 3.7). Persisting 'anomalies' led to subsequent developments of stability analysis which accounts for the combined effects of both driving forces (buoyancy and Marangoni) and a number of interface phenomena such as deformation and surface viscosity [3.17]. No equivalent treatment is available for the case of multi-component layers.

Rayleigh-type instabilities
When the only driving force is the buoyancy force the physical mechanism is, at least in principle, rather clear. The motion of an elementary particle accidentally *displaced from its hydrostatic equilibrium position is* favoured by the buoyancy force (equal, per unit volume, to the product of the gravity g times the local density difference $\Delta\rho$) and countered by the ensuing diffusion processes. Diffusion of momentum (drag) directly opposes the motion whereas diffusion of heat (internal

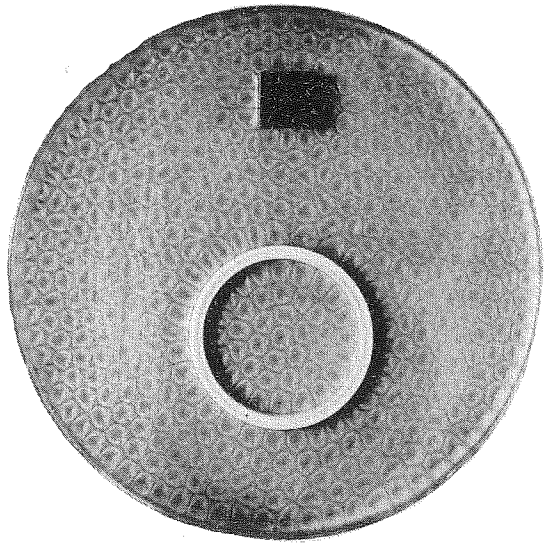

Figure 3.7 Convection cells with a characteristic polygonal geometry arise spontaneously when a thin layer of fluid is heated from below. In each cell the fluid rises in the center and sinks at the periphery. The circulation is driven largely by forces associated with surface tension, and in most fluids it assumes this form only when the upper surface is free. (After M G Velarde & C Normand, in *Scientific American*, July 1980, p. 79.)

energy) and mass tends to reduce the driving force by diminishing the density difference $\Delta\rho$.

The onset of motion, its evolution toward steady or unsteady dynamic configurations, its eventual transition from laminar to turbulent depends, at times in a rather complex and not exhaustively investigated manner, on the interplay between the above 'local' driving and opposing mechanism which is decisively affected by the nature and type of boundary conditions.
on point).

When the density depends on other parameters (say the concentrations) and the characteristic times for diffusion of internal energy and masses differ by orders of magnitude this may be no longer true. The presence of chemical reactions may induce, similarly, instabilities in a stratified layer whose overall density gradient should favour stability (i.e. denser layers at the bottom).

Analysis of these convective instabilities should take into account the thermodynamic equilibrium and non-equilibrium (e.g. direct and cross-coupling transport coefficients such as, for instance, Soret and Dufour coefficients) (§ 2.4.4).

Theoretical investigations of these topics experience a renewal of interest as well as on-earth exploratory and/or probatory experiments. Carefully designed space-borne experiments should help in throwing further light on these phenomena and will certainly promote more sophisticated theoretical models (for instance, in Rayleigh instabilities, the Boussinesq approximation may no longer be tenable because, in microgravitational environment, attainment of the critical Rayleigh number requires much larger temperature differences).

Bénard-type instabilities
This is perhaps the area where the microgravitational environment offers the greatest interest. Crucial experiments could indeed be designed to help resolving many of the still debated questions as to the relative importance and roles of Marangoni forces in convective instabilities. Only recently, it has been clarified that in the classical Bénard experiment, Marangoni forces do play a role and some noteworthy theoretical developments of instability analysis which take due account of surface phenomena have been published [3.17].

In a microgravitational environment, as repeatedly stated, surface phenomena acquire a bigger relevance Space-borne experiments should thus provide the data needed for a better understanding of the role that they play in convective instabilities.

Almost everything needs to be done in the case of multicomponent systems. The already complex bulk-fluid phenomena, previously briefly described, will be further complicated by interface phenomena (equilibrium and non-equilibrium) and by the strong coupling between the two. Some new configurations, verifiable only in microgravitational environment have already been predicted theoretically [3.18]. Others will undoubtedly be found.

3.3 Solid/liquid interfaces

Within the previous sections (3.1 and 3.2), the general problem of stability was concerned only with interfaces that were boundaries between two fluid bulk phases. This is a new problem because one of the boundary phases is now a solid phase, but this solid phase is not any type of solid since it was born by freezing the adjoining liquid. As a consequence, the inertness of such interfaces is not as high as one could imagine since the instability can show itself in the form of a complete degeneracy of the initial shape. Furthermore interface instability is not only a problem in itself, but it is also the

basic condition to be avoided before performing any crystal growth or solidification experiment, in order to achieve the highest degree of perfection of the solidified structures. It is the reason for which we emphasized the importance of this presentation within the brochure. We are however aware of the gap existing between the most advanced theories and current experience. Gravity-induced convection is the main reason of such a gap and more accurate space experimenting will improve our understanding of morphological behaviour.

3.3.1 *General remarks*

In order to limit this general problem to its specific sensitivity to g level, the following restrictions will have to be taken into account:

- The problem is limited to boundaries between at least one fluid phase (either liquid or gas) and one solid phase which are in thermodynamical equilibrium. The most usual situation is the one of the solid/liquid interfaces encountered in any solidification, or crystallization process.
- The instability is linked to a dynamic behaviour of such interfaces; any motionless interface will remain stable and consequently, instabilities will occur only with moving interfaces, either solidification or melting interfaces.
- In opposition with the cases that were approached in § 3.1 and 3.2, such interfaces are sources, or sinks, of heat (the latent heat of the transformation) and of solutes that must be distributed in the adjacent bulk phases.

Such instabilities manifest themselves as interfacial protrusions that are not related to the more or less regular shapes of the isothermal surfaces. For instance, the temperature of any motionless interface between two phases in equilibrium is the thermodynamically well-defined equilibrium temperature. Consequently, such an interface coincides with the ad hoc smooth isothermal surface. When an instability – either convective or morphological – appears, the initial regularity of the interface disappears allowing protrusions to appear. The usual scale of such protrusions is typically 10 to 100 μm. Thus, such growth features have no direct connection to smoothness or roughness on an atomic scale, such as considered in the atomistic theory of crystal growth. On the other hand, if it is obvious that any hydrodynamic instability in the boundary fluid phase will influence in return the smoothness of the interface, and thus may initiate some rippling in the interface morphology, some other changes may be of purely morphological origin: the global curvature of the solid/liquid interface or the lines of emergence of grain boundaries may be responsible for such changes.

3.3.2 *Models of interfacial instability*

They are many to be more or less sophisticated, but due to parasitic gravity effects, they are all equally difficult to check experimentally, and thus the gap usually observed between a priori predictions and real measurements often exceeds 20% when operating in the classical ground conditions. In the plane-front and constant-velocity directional solidification of all alloys other than congruent melting compounds and invariant eutectics, where liquid and solid phases have the same composition, there exists in the liquid an exponential concentration gradient which extends ahead of the solid/liquid interface (Fig. 3.8): this gradient is the consequence of the ratio k_0 (distribution coefficient) existing usually between the compositions of liquid (C_L) and solid (C_S) phases whatever the absolute values of such compositions (as low as a few 10^{-6}). The behaviour of the diffusion zone that surrounds such a moving interface is controlled by both the properties of the phases participating in the transformation and the rate of this transformation.

There also exists a temperature gradient which is essentially linear in the region in which the concentration gradient is exponential, the solutal boundary layer being usually much thinner than the thermal boundary layer, as often as the Lewis number $Le = D_L/\alpha_L$ is smaller than 1 (§ 2.4.3).

Depending on the characteristics of the elements of any alloy, this thermally caused density gradient is likely to oppose as well as to reinforce the compositional segregation at the front. When it opposes it may actually destabilize an apparently stable density stratification and lead to complicated buoyancy-driven convection. But the main consequence of such gradients near the solid/liquid interface is the 'constitutional supercooling' phenomenon.

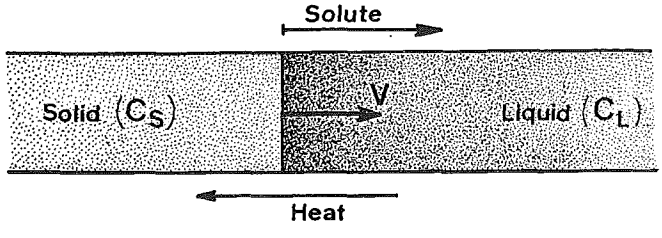

Figure 3.8 Solidification of a binary melt with $C_S/C_L = k_0 < 1$, which introduces the formation of an exponential concentration gradient ahead of the solid/liquid interface.

One generally agrees that diffusion and convection are the two dominant mass and heat transfer modes in the liquid in front of the interface. Thus the disappearance of convection phenomena will result in a decrease in the driving forces, and also, in a greater regularity of the mass and heat flows. On the other hand, it is well known that mass flows engendered by convection do affect the whole bulk of the liquid, and to a lesser extent the viscous boundary layer, that may be reduced in some degree.

In a first approximation, if the decay distance of the exponential concentration gradient is less than the viscous boundary layer, there is no effect of convection. On the contrary, in most cases the process of solute rejection will be affected by convection together with all the phenomena governed by diffusion: redistribution of the solutes, efficiency of the heat transfers, instability limits of the interfaces, or size of the solidification structures. In fact, it has been shown by Favier [3.19] that the effect of the mean velocity of the liquid phase may affect the diffusion profiles at the interface even when the convective boundary layer is five times larger than the characteristic diffusion length. This concept of a diffusion length expresses the fact that the diffusion gradient exists over a distance that is proportional to the speed of the diffusant and the time over which diffusion can occur: thus the more rapid the rate of solidification, the smaller is the diffusion length.

Furthermore thermoconvection can generate disturbances of the heat and mass fluxes that may be difficult to control, and may be responsible for pinpoint creation of structural defects in the interface, and later on, in the solid bulk. Thermoconvection can be responsible also for temperature fluctuations that may be regular, oscillatory or even turbulent depending with the value of the Rayleigh number. When these temperature fluctuations reach the solid/liquid interface,

Whatever the intrinsic difficulty that results from this coupling between mass and heat flows, such coupling involving as a rule solutions to linear field equations with non-linear, strongly coupled, boundary conditions, our basic knowledge could make great strides over the last decade, even being ahead of the experimental works mainly tainted with earthly gravity artifices.

Due to the philosophy of this approach, we could not think of exhaustively reviewing the whole field of solid/liquid interface instability. We have selected just a few of the most specific models, about which a tentative evaluation of the microgravity action could be tempted

The summarized analysis of current instability theories will begin with time-independent treatments of interfaces implying very simple shapes. In reality both the macroscopic and microscopic features of solid/liquid interfaces are controlled by such coupled heat and mass transfer mechanisms but all current models assume the initial macroscopic shape as having a specific simple geometry.

The very first approach was purely thermodynamic. Tiller [3.20] generated the first quantitative interface stability criterion for crystals growing from a binary alloy melt under a positive temperature gradient. By making use of thermodynamic arguments and restricting his attention to the liquid phase, Tiller arrived at his landmark 'constitutional supercooling' instability criterion given by $G_L < m_L G_C$ which predicts a tendency for any protuberance to grow, provided the temperature of the liquid adjacent to the interface is less than its equilibrium melting temperature (Fig. 3.9).

In the case of solutions, this criterion states in analytic form that for planar interface instability the following condition prevails:

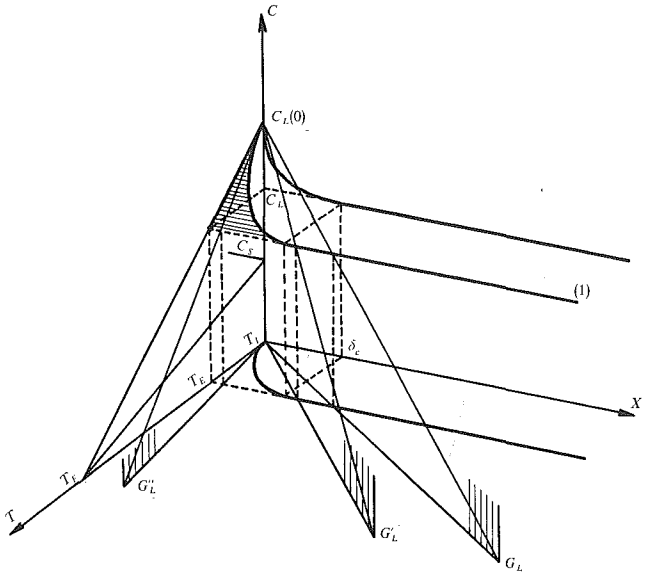

Figure 3.9 'Concentration-Temperature-Distance' diagram of a solidifying binary melt. Curve (1) presents the behaviour of the system. When the planar surfaces G_L and G'_L representing the imposed temperature gradients cut this curve, more or less extended regions of the liquid phase are supercooled. The plane G''_L being tangential to the curve corresponds to the limit of instability $G''_L = m_L G_c$. G_c is the slope of the (C, X) projection of the curve and m_L is the slope of the (C, T) projection of the curve. The composition of the liquid at the interface $C_L(0)$ is much higher than the one in the bulk C_L.

$k = 1$ in the case of no mixing of the melt, δ_c becoming very large. Conversely in the case of complete mixing, $\delta_c \to 0$ and $k = k_0$. In the case of partial mixing k ranges between k_0 and 1. As $k_0 \neq 1$, the variation range of k introduces considerable lack of precision in determining the critical ratio G_L/V.

Equation (3.3) focuses attention on the fact that a large positive G_L provides a stabilising influence which is less effective when the velocity V increases. The destabilising influence is provided by the impurity concentration C_L. Figure 3.10 gives successive steps of the destabilising process as a function of increasing constitutional supercooling amounts. As Equation (3.3) is satisfied a zone of supercooled liquid exists immediately adjacent to the interface and the planar interface has to be considered as unstable. In the case of growth from a pure melt such supercooled regions may arise from latent heat evolution if the growth rate is large enough.

But the principle of constitutional supercooling is based on the application of thermodynamic arguments to the

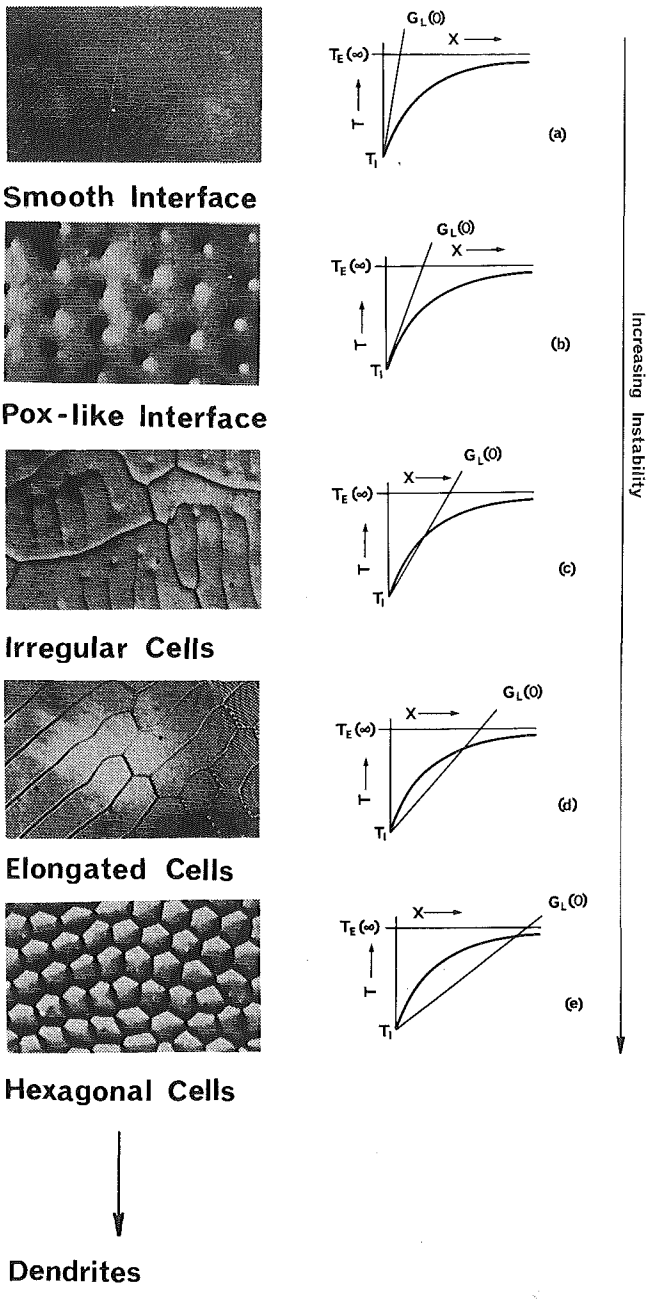

Figure 3.10 Right-hand graphs present the respective real temperatures imposed to the liquid phase adjacent to the growth interface $\{G_L(0)\}$ and the equilibrium temperature of this liquid phase. They are the projections of curve (1) of Figure 3.9 on plane (T, X). When the imposed temperature is larger than the equilibrium temperature (a) the system is stable and the interface remains smooth. When the imposed temperature is equal or less than the equilibrium temperature (b, c, d, e) the growth interface is the more destabilised as the amount of constitutional supercooling (shaded area) is more important. On the left-hand side of this figure are the successive steps of the destabilisation process.

liquid, and furthermore, this liquid is regarded as a closed thermodynamic system. In reality the situation is one in which dynamic processes play an important role, heat and solute are being transported throughout the system and their transport may even be influenced by the perturbation itself. Hence the idea of a self-consistent dynamic analysis of the instability phenomenon.

Mullins & Sekerka [3.21, 3.22] developed a first-order perturbation analysis of interface stability. Their theory is a linear theory in so far as it describes the growth or decay of an infinitesimal perturbation of arbitrary wave vector. In any real physical situation, imperfections of some type are always present that may cause small perturbations in the shape of the moving solid/liquid interface. Under stable conditions the perturbations will decay with time and the interface will return to a smooth shape. For unstable conditions, the perturbation will be enhanced in amplitude, which will cause a still greater disturbance, lateral spreading and, eventually, a somewhat corrugated interface.

Mullins & Sekerka analysed such disturbances in an equilibrium state for the governing system of heat and solute transport differential equations relevant to the plane front solidification of dilute binary alloys. They made use of a 'quasi-steady state' method, which implies critical mathematical simplifications: the time derivative in the diffusion equation for solute was neglected, and the energy equation was replaced by the Laplace equation for the temperature field. These simplifications can prove to be sufficient unless fluid convection effects are important: they result from the assumption that the heat diffusion is much larger than the heat convection, i.e. from a small value of the Peclet number (Pe = heat convection/heat diffusion = $Pr \times Re$; see §2.4.4).

In such conditions, their resulting stability criterion becomes:

$$\frac{G_L}{V} + \frac{L}{2K_L} < \frac{m_L k (1-k_0) C_L \overline{\mathbf{K}} \mathscr{S}}{D_L k_0} \qquad (3.4)$$

where $\mathscr{S}$ is a dimensionless 'stability function', that ranges typically between 0.7 and 0.9 for most systems of interest. The difference of $\mathscr{S}$ from unity represents the expected tendency of the liquid/solid surface energy to stabilise the smooth interface. When $\mathscr{S}$ is seen to differ appreciably from unity approaching zero as a lower limit, a region of 'absolute stability' can be approached: it means that the interface cannot be destabilised in any way.

Later on, Sekerka [3.23] reworked this instability problem always by using a Laplace transform method and showed, for the case in which only time derivatives in the heat diffusion equations were neglected, that the stability criterion for this time-dependent model was equivalent to that deduced by the quasi-steady state method. The other initial limitation of isotropic interface properties was got over by Coriell & Sekerka [3.24] who demonstrated the effect of the anisotropy of surface tension and interface kinetics on morphological stability, so explaining the existence of preferred directions for destabilized cellular and dendritic growth. All these dynamic approaches succeeded in strengthening the stabilizing effect of the temperature gradient and in introducing the role of the interface capillarity which tends to keep the interface plane. Unfortunately experiments have not yet been reported which could distinguish between these various criteria, mainly because of parasitic convective flows, the influence of which was not quantifiable even if they may be qualitatively perceived in terms of similarity between the anisotropy of surface kinetics and the existence of oscillatory convective flows describing specific patterns.

Previous models being limited to the case of planar interfaces, a first-order perturbation analysis was realized by Trivedi [3.25] for constant curvature interfaces with both tridimensional heat and mass transfer fields. An absolute stability criterion of a sphere of given radius could be obtained as a function of the three terms that characterise the effects of temperature, solute and surface energy.

Later on, Trivedi [3.26] undertook to generalise his previous approach to any type of interfaces including complex shapes of dendrites. The morphology of such interfaces is shown to depend once more on the three characteristic lengths of solute diffusion ($\ell_s = D_L/V$), of thermal diffusion ($\ell_t = k_0 \Delta T_0 / G_L$) and of capillarity ($\ell_c = \gamma_{SL}/\Delta S_f \Delta T_0 k$), ΔT_0 being the freezing range of the alloy.

From a qualitative point of view the evolution of the morphology can be determined by the relative magnitudes of these three lengths, and thus by the values of 2 of their dimensionless ratios. For instance, the ratio ℓ_s/ℓ_t is proportional to the Lewis number ($Le = D_L/\alpha_L$; see §2.4), but it is also inversely proportional to the growth velocity. Thus for low velocities this dimensionless parameter will increase. The second ratio ℓ_c/ℓ_s depends directly on V, thus increasing with V.

The conclusion is that for large velocities the

competition between destabilising solute diffusion and stabilising surface energy will determine the morphology, although at low velocities the interaction between solutal and thermal diffusion processes will be prevailing. It is obvious that the very nature of these dimensionless parameters makes them strongly dependent on the existing convective mixing in the liquid volume.

Apart from these limitations, both linear theories of Mullins & Sekerka, and Trivedi, allow the determination of the critical conditions for the onset of instability and of the wave number of the initially infinitesimal disturbances that are most likely to grow first. If the long time behaviour and the spatial pattern of such growing disturbances are to be predicted, or the effect of initially finite amplitude perturbations is to be ascertained, then it is necessary to take the non-linear terms into account.

This was undertaken by Wollkind [3.27] who demonstrated the existence of four situations:

- *Stable equilibrium* somewhat similar to the Rayleigh problem of cellular convection.
- *Instability*, the non-linear effects acting to reinforce the destabilising tendency shown by linear theory, and finite amplitude effects enhancing disturbance growth.
- *Subcritical instability*: whereas linear theory would predict stability to infinitesimal disturbances, non-linear theory gives instability provided the magnitude of finite amplitude disturbances is large enough; it may correspond physically to metastable dendrite growth.
- *Stability*, the non-linear effects acting to reinforce the stabilising tendency shown by linear theory: it is the region where the interface is stable to both infinitesimal and finite amplitude disturbances.

But in all preceding models, hydrodynamic effects of any origin are being neglected. It is consistent to turn the attention to the role played by convective effects on morphological stability during solidification. Such gravity-induced convections inevitably occur in the liquid phase provided the densities of the liquid and solid phases differ, and they can also be caused by horizontal or vertical temperature gradients. Many early investigators of problems in non-linear hydrodynamics were aware of the fact that their results could be adapted to a broad class of physical problems and, as soon as 1966, Kirkaldy [3.28] pointed out the similarity between patterns in Rayleigh convection and cellular patterns observed during unstable alloy solidification. Likewise, it was realistic to think that convection could also cause a non-planar solid/liquid interface since both problems are governed by the same differential equations and boundary conditions as the usual morphological instability mechanism.

3.3.3 *Coupled convective and interfacial instabilities*

Very recently, Sekerka & Coriell [3.29] undertook to generalise morphological stability theory by removing the previous assumption that the liquid density was independent of temperature and solute concentration. They restricted this approach to the case of systems displaying low Lewis numbers. In such cases the phenomenon known as 'double-diffusive convection' can arise. It is an instability phenomenon that arises whenever two diffusing species in a fluid give rise to unexpected buoyancy-driven convection because of the different rates at which the species diffuse. Such double-diffusive convection can interact strongly with constitutionally-induced morphological instability. This situation is different from the ones studied by Delves [3.30] and by Coriell & al [3.31] because the convection, there, is natural (i.e. buoyancy-driven and not restricted to the outside of the boundary layer), and no more forced (by mechanical stirring). The approach by Coriell & al [3.32] demonstrates the existence of two types of instability, a convective type that occurs for long wavelengths, and a morphological type that occurs for short wavelengths. In general these are coupled but the morphological instabilities are only slightly dependent on gravity, and thus correspond roughly to the predictions of previous morphological stability theories in which density changes and convection are neglected. On the other hand, the convective instabilities depend strongly on gravity. The main result is that for low velocities, the convective instabilities occur at much lower solute concentrations than the morphological instabilities, whereas at high velocities the reverse is true. At intermediate velocities there are oscillatory instabilities of mixed character whose periods increase rapidly when the gravity level decreases.

However imperfect this model may still be, in particular as regards some limitative hypothesis (constancy of many coefficients and elimination of cross-coupling of the heat and solute fluxes), it is the only one capable of introducing g-level as an essential parameter.

It results from all these various approaches or models that the problem of the interfacial instability is very complex to analyse in its overall dimensions. The only common points are the following:

- Instability is basically a competition between mass and heat fluxes on the liquid side of the demarcation surface.

- Real situations concern most often transient mechanisms with their own relaxation behaviours, which explains the gap existing between experimental results and academic steady-state models.
- There is a significant influence of capillarity phenomena.
- There is a significant influence of boundary layers.
- There is a significant influence of hydrodynamics instability.
- They are four imposed conditions that may influence stability or/and instability: C_L, G_L, V and g-level.
- Earth-bound experiments never succeeded in checking the respective validities of those more or less sophisticated models with the adequate accuracy.

3.3.4 *Possible influences of g level*

It results from the above analysis that space environment may modify four areas that interact at various levels with the onset of interfacial instability. They are summarised as follows:

- The reduction of gravity-induced convection flows arising from thermally or compositionally induced density gradients in fluids. Such flows on earth are important because they induce the creation of non-uniform diffusion boundary layers as well as transient segregations due to the temperature and velocity fluctuations. Thus, the reduction of convective flows makes it possible to reduce their associated secondary effects, such as alteration of heat transfer and solute redistribution, and results in more ideal transfer processes. It also leads to a better understanding of the other convection driving forces such as interfacial tensions, volume expansions, external fields, etc. (§ 2.4.2).
- The reduction or almost complete elimination of sedimentation, segregation and settling of suspended particles and associated Stokes flows. This advantage will result in more homogeneous fluid phases (§ 2.5).
- The absence of hydrostatic pressure and its influence on phase equilibria or on equilibrium shapes (§ 2.3).
- And possibly, the containerless handling of liquids that would allow to suppress interactions of mechanical, chemical and thermal natures (§ 6.3).

Given these facts, it becomes possible to examine some potential changes introduced by g level decrease in the physical mechanisms of destabilisation models, being well established that it is only the most accurate space experimentation that will be able to confirm these a priori statements.

Concentrations of fluid phases

The absence of segregation or sedimentation will result in an improved initial constitutional homogeneity after the chemical diffusion alone will have (much more slowly) suppressed all traces of the initial chemical heterogeneities. However some preferential wetting behaviour of one specific component may result in a new type of segregation in the vicinity of external boundaries, and gazeous inclusions will be more difficult to eliminate. The globally increased homogeneity will favour an increased interfacial stability because no local compositional change will be able to start the first overcritical disturbance.

Elimination of thermoconvection

It is the main point to be taken into account. The most immediate consequence will be to suppress an important component of heat transfers. As a result it would be theoretically possible to get much higher values of the stabilising thermal gradients. One order of magnitude for this increase has been announced by some specialists for specific boundary conditions, which would be a considerable improvement. Nevertheless it must be reminded that such increased values of G_L may increase parasitic phenomena such as Soret effect that can induce significant composition gradients, or Marangoni effect (when there are free interfaces) that is linearily dependent of the thermal gradients. The resulting flows can be either stabilising or destabilising depending on the relative direction of the solutal flows. Dismukes & Yim [3.33] have reviewed the possible influences Soret effect may have on interface stability, there being a stabilising tendency if thermal migration aids ordinary diffusion ($D'_L < 0$), whereas if it opposes ordinary diffusion ($D'_L > 0$) that tendency will be of a destabilising nature. Identical influences will result from Marangoni flows and thus in space such second-order phenomena will have to be carefully analysed. At last it is worth mentioning that successive destabilisation steps may occur with modified morphologies (§ 4.3): sizes, shapes, orientations may vary in possible connection with the sensitiveness to gravity of the wave numbers of the disturbances, and in direct and obvious connection with hydrodynamic flow patterns.

Elimination of natural convection may have two main effects as regards distribution of solutes: it will no more homogenize the liquid if local compositional disturbances of an origin other than buoyancy arise, and it will extend the thickness of the boundary layer. The first effect will obviously lead to reduced stability but the detrimental effect of the increased boundary-layer thickness is not so obvious, and it will be discussed now in the case of steady-state growth. According to Hurle

[3.34] who employed the boundary-layer analysis of Burton [3.35] to study morphological stability in the presence of convection, two different cases have to be taken into account: Equations (3.3) and (3.4) can demonstrate the influence of convection on stability criteria through the value taken by the effective distribution coefficient k.

As $k = k_0$ in the case of complete stirring, the instability will be less if $k_0 < 1$ and greater if $k_0 > 1$: it means that increasing convection in an alloy of fixed bulk composition C_L and of $k_0 < 1$ decreases the required G_L/V for stability, and thus enhances interface stability.

Conversely, in the case of no mixing, i.e. no convection, $k = 1$: it means that the absence of convection will enhance the instability, and thus will produce more constitutional supercooling whatever the value of k_0.

By employing the same boundary layer model along with a perturbation analysis of morphological stability, Hurle [3.34] demonstrated that the value of the 'stability function' was near to 1 for no convection, while it was decreased for strong convection. Thus, absence of convection would also enhance instability through this different approach.

Delves [3.36] also attempted to refine the theory of morphological stability when convection is important, in order to account for flow along the solid/liquid interface within the solute boundary layer. The corresponding analysis is sufficiently complicated that general results are difficult to extract. However, it seems that the interface may be stabilised by fast stirring, which is in agreement with previous approaches.

Tiller [3.37] reached the opposite conclusion, namely that stirring leads to reduced stability, and absence of convection leads to increase stability: the reason being the increase of the temperature gradient would be greater than the increase in solute gradient, in the absence of any convective mixing.

More recently, Coriell & al. [3.38] investigated the role of gravity in a linear stability analysis of the onset of coupled buoyancy-driven fluid dynamical and morphological instabilities during directional solidification.

Their conclusions are twofold:

- If the morphological instabilities are not very dependent of gravity, and thus correspond to the predictions of previous morphological stability theories with an imprecision of about 20%, on the other hand convective instabilities depend strongly on gravity by about 2 to 3 orders of magnitude.
- For low velocities of the interface, the convective instabilities occur at much lower solute concentrations than the morphological instabilities, whereas at higher velocities the morphological stabilities occur at lower solute concentrations than the convective instabilities.

Both conclusions are presented in Figure 3.11.

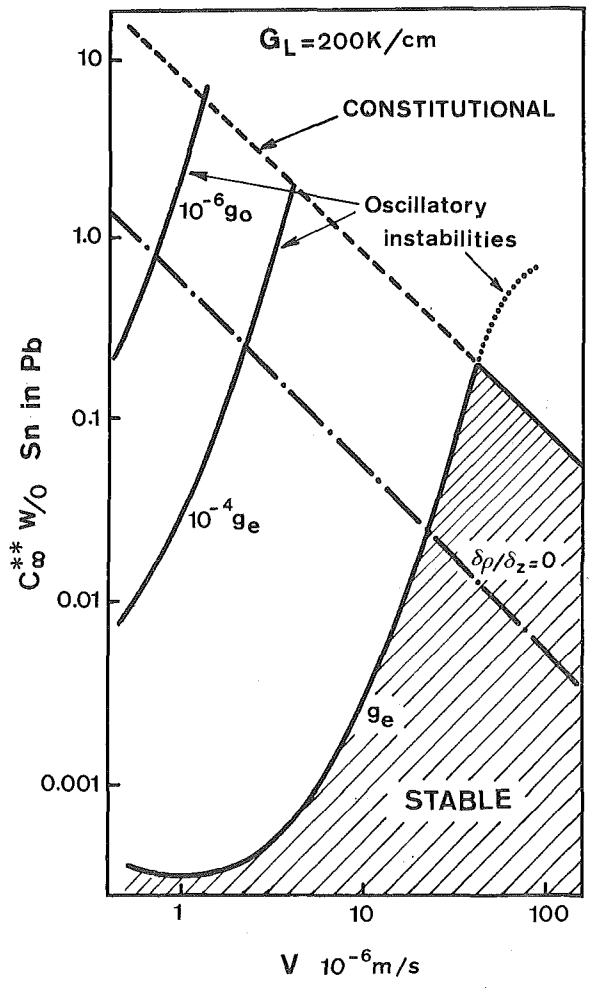

Figure 3.11 The critical concentration C_∞^{**} of tin in lead above which instability occurs as a function of growth velocity for a temperature gradient in the liquid G_L of 200 K/cm. The solid concave curves represent the onset of instabilities of fluid dynamical character for gravitational accelerations g_0, $10^{-4}\,g_0$ and $10^{-6}\,g_0$. The upper solid line that slopes downwards and to the right represents the onset of constitutionally related morphological instability; the nearly parallel dashed-dot line labelled $d\rho/dz = 0$ represents the neutral density criterion.

Another consequence of the lowering of the efficiency of thermoconvection is the increased importance of those other fluid flows such as the ones presented in § 2.4 the influence of which is most often negligible in current earth conditions. Thus, it is important to take into account all those possible resulting fluid flows before enacting a situation of no-mixing, with its relevant consequences.

Furthermore, it is necessary to be aware of the fact that all destabilisation models concern steady states that are not instantaneously obtained. When changing the g level the durations of all transient states (both chemical and thermal) are modified, and thus, the relevant stability criteria will be modified in a more or less complex manner: usually one can consider that microgravity will tend to prolong transient heat states and to shorten transient chemical states, both tendencies being able in some circumstances to act in parallel to increase the risks of interface instability.

The global conclusion is that it is not easy to determine the exact way microgravity will act on stability/instability criteria. It will be the role of careful experiments such as those proposed in § 4.3 to decide which theoretical approach is the most accurate. The closest cooperation between experimentalists and theoreticians is necessary for a successful endeavour.

References

[3.1] Moldover M R, Sengers J V & al, Gravity effects in fluids near the gas/liquid critical point, in *Rev of Modern Physics* **51**, 1979, p. 79.

[3.2] Nicolis G & Prigogine I, *Self-Organization in Non-equilibrium Systems*, Wiley, New York 1977

[3.3] Haken H, *Synergetics, an Introduction*, Springer, Berlin 1978.

[3.4] Kondepudi D K & Nicolis G, Influence of Gravitation on the Bifurcation of Steady-States in Chemical Systems, in *Z für Flugw und Weltr (ZFW)* **3**, 1979, p. 246.

[3.5] Mathowsky B J & Reiss E L, *Siam Appl Math* **33**, 1977, p. 230.

[3.6] Markstein G H, *Non-Steady Flame Propagation*, Pergamon, Oxford 1964, p. 78.

[3.7] Sivanshinsky G I, Diffusional-Thermal Theory of Cellular Flames, in *Comb Science and Techn* **15**, 1977, p. 137-146.

[3.8] Gillis J, in *Proc Camb Phil Soc* **57**, 1961, p. 152.

[3.9] Carruthers J R & Grasso M, in *J Appl Phys* **43**, 1972, p. 436.

[3.10] Carruthers J R & al, in *AIAA Paper* 75-692, 1975.

[3.11] Martínez Herranz I, in *Cospar: Space Research*, Vol XVIII (J Rycroft & A C Stikland, Eds), Pergamon Press, Oxford 1978, p. 519.

[3.12] Fowle A A, in *Material Sciences in Space*, Symp Grenoble 1979, ESA SP-142, p. 317.

[3.13] Ostrach S, Private communication, Aug 1980.

[3.14] Bénard H, in *Ann Chim Phys* **23**, 1901, p. 62.

[3.15] Rayleigh J W S, in *Phil Mag* **32**, 1916, p. 529.

[3.16] Pearson J R A, in *J Fluid Mechanics* **4**, 1958, p. 489.

[3.17] Scriven L E & Sternling C V, in *J Fluid Mechanics* **19**, 1964, p. 321.

[3.18] Castillo J L & Velarde M G, in *Physics Letters* **66A**, 1978, p. 489.

[3.19] Favier J J, in *Acta Met* **29**, 1981, p. 204-214.

[3.20] Tiller W A, Rutter J W, Jackson K A & Chalmers B, in *Acta Met* **1**, 1953, p. 428.

[3.21] Mullins W W & Sekerka R F, in *J Appl Physics* **34**, 1963, p. 323.

[3.22] Mullins W W & Sekerka R F, in *J Appl Physics* **35**, 1964, p. 444.

[3.23] Sekerka R F, in *Crystal Growth* (H S Peiser Ed), Pergamon Oxford 1967, p. 691.

[3.24] Coriell S R & Sekerka R F, in *J of Cryst Growth* **34**, 1976, p. 157.

[3.25] Trivedi R, in *Acta Met* **48**, 1980, p. 93.

[3.26] Trivedi R, in *J Cryst Growth* **49**, 1980, p. 219.

[3.27] Wollkind D J, in *Preparation and properties of solid-state materials* (W R Wilcox Ed), Chap 4, p. 111, Dekker, New York 1979.

[3.28] Kirkaldy J S, in *Non-Equilibrium Thermodynamics, Variational Techniques and Stability*, Univ of Chicago, Chicago 1966, p. 273.

[3.29] Sekerka R F & Coriell S R, in *Material Sciences in Space*, Symp Grenoble 1979, ESA SP-142, p. 55.

[3.30] Delves R T, in *J of Cryst Growth* **8**, 1971, p. 13.

[3.31] Coriell S R, Hurle D T J & Sekerka R F, in *J of Crystal Growth* **32**, 1976, p. 1.

[3.32] Coriell S R, Cordes M R, Boettinger W J & Sekerka R F, in *Cospar Proceedings*, Budapest 1980.

[3.33] Dismukes J P & Yim Y M, in *J Cryst Growth* **22**, 1974, p. 287.

[3.34] Hurle D T J, in *J of Cryst Growth* **5**, 1969, p. 162.

[3.35] Burton J A, Prim R C & Slichter W P, in *J Chem Phys* **21**, 1953, p. 1987.

[3.36] Delves R T, in *Crystal Growth* (B R Pamplin Ed), Pergamon, Oxford 1975, p. 40.

[3.37] Tiller W A, in *J of Cryst Growth* **2**, 1968, p. 69.

[3.38] Coriell S R, Cordes M R, Boettinger W J & Sekerka R F, in *J of Cryst Growth* **49**, 1980, p. 13.

4 Representative case studies

The aim of this chapter is to present examples illustrating the complexity and diversity of microgravity research in space. Its content is heterogeneous in nature. Writing of some parts has greatly profited from the experience gained from experiments performed previously. The knowledge gained from such experiments has not been completely digested yet, but it does make it possible to broaden the spectrum of new studies and emphasises the need for a cautious approach to them.

Other parts of the chapter emphasise the interest of experiments which have been suggested or even formally proposed, but have not been performed yet. Finally, the last two parts merely indicate fields where microgravity-related work should be undertaken, both because of their basic interest and their immediate application to spacecraft technology. In these parts general problems are introduced, mainly in the light of present terrestrial experience, and no attempt is made to anticipate the influence of microgravity.

It is clear from the foregoing chapters that microgravity can be looked at as a reference environment in the sense that it eliminates or greatly reduces the influence of *one* parameter that can play a multiple but not completely understood role in many experiments.

Nevertheless, microgravity in itself does not simplify the problems. In practice, an advantage obtained in space must be paid for by new and sometimes unexpected problems. The materials scientist, for example, is often confronted with situations which, for intrinsic reasons, can hardly be made complex. Complex phenomena, where many influences act and interact, are not easy to model, so theoretical predictions are often unreliable if not impossible.

The message which we try to convey in this, as in other chapters of this brochure, is that even quite familiar situations, transferred to an apparently simple space environment, require an extensive development programme on Earth, with experimental, theoretical and numerical studies, and an open mind to cope with the unpredictable.

4.1 Planar front crystallisation

Theoretical models of the instability at solid/liquid interfaces presented in § 3.3 have demonstrated the complexity of this problem and the various ways in which it can be treated. This case study will show how

more can be learnt about a very important mechanism by taking advantage of the microgravitational environment.

The simplest models reviewed involved seven parameters, some of them with wide margins of uncertainty, and the most elaborate involved more than 20 quite inaccurate parameters, which did not make comparative analysis any easier. By reducing the specific imprecision resulting, for many of them, from the fact that the measurements were made under ground-based conditions, space-borne determinations will in the first place help to increase the accuracy of some of the mandatory data and thus, by reducing the resulting error will facilitate the theoretical modelling of the phenomenon. It may also be useful to perform experiments on earth as a means of approaching the new problem of solid/liquid instability under microgravity conditions. Finally, precise comparative measurements of stability limits on earth and in space, and the accurate comparison of various morphologies obtained under identical thermal and growth conditions (Fig. 4.1) will result in a better understanding of the many possible mechanisms that have been examined in § 3.3.

It is important to recall that even if the space environment does not improve the stability of solid/liquid interfaces, it does form a reference environment in which to study the way such instability mechanisms proceed. Furthermore, some of the statements introduced under this heading would be worth taking into account in other fields of space research.

4.1.1 *Tasks to be performed on earth*

As already pointed out, any solidification process involves numerous geometrical, thermal, chemical, physical and hydrodynamic parameters which must be very accurately known if an accurate forecast of instability conditions under both terrestrial and space conditions is to be made. But the current uncertainty margins – ranging between 0.2 and 15% for each parameter – make it necessary to apply wide safety margins to the a priori definition of optimal solidification conditions in order to eliminate any risk of interfacial instability. Consequently there is the dual need to:

(i) improve the accuracy of some of the parameters by taking advantage of the microgravity environment to measure them more precisely (see § 2.4);

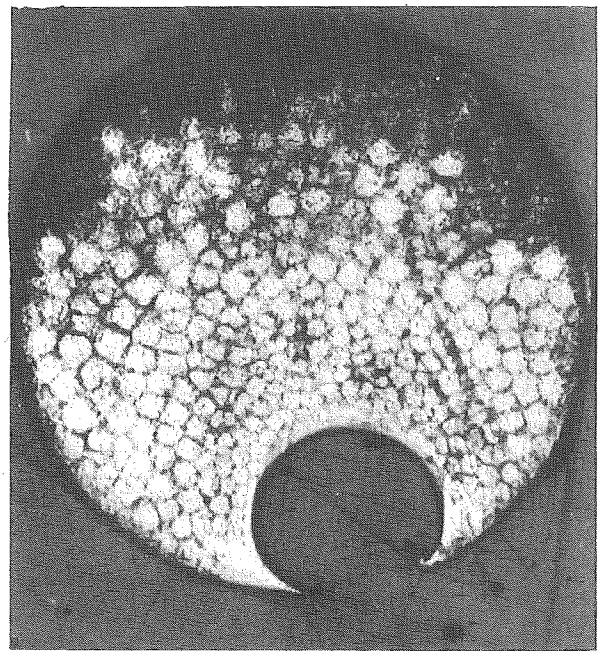

(a)

(b)

Figure 4.1 Modifications of the destabilised morphologies observed when going from earth (a) to space (b). The two morphologies correspond to various stages of destabilisation whatever the invariability of imposed thermal conditions. The space specimen is more destabilised than the earth specimen, thus demonstrating the destabilising action of the microgravity environment.

(ii) compare the experimentally observed 1-g and μ-g stability limits so that the physical behaviour under these conditions can be compared with the improved models, and the latter's merits, limitations and efficiency can be assessed. The best known and most convenient systems will be selected for such studies, so that other intrinsic uncertainties that cannot be improved in any type of environment are minimised.

The improvements derived from such academic experimental work will benefit all other situations of practical interest. Careful preliminary earth-bound experiments performed concurrently will be worth carrying out since they will make it possible to approach the critical conditions for the onset of interface instability that will prevail in space. By varying the orientation of the growth rate with respect to gravity (parallel, antiparallel or perpendicular to the g vector) one can introduce significant changes in the values of thermoconvective flows. Another way of doing this is to study systems enclosed in capillary tubes, which makes it possible to reduce the values of the Rayleigh number as does the reduction of the gravity level. Unfortunately the capillary configuration is apt to introduce detrimental wall effects at the interface.

In the case of an electrically conducting fluid a strong anticonvection action can be imposed by using magnetic fields: the effect of such a magnetic field may delay the occurrence of thermoconvection by increasing the viscosity of the liquid, which introduces a resistance to hydrodynamic instabilities. Organised solute fluxes are then reduced drastically, but the random fluctuations of chemical, and in particular of thermal fluxes, are maintained.

Finally it would be valuable to study, on earth, systems with minimum values of fractional density change and of thermal and solutal coefficients of expansion, both parameters being the driving forces for thermoconvective fluxes.

4.1.2 *Definition of optimal experimental space conditions*

The problem is twofold, depending on whether the aim is to protect the solidifying system from any instability, or to study the destabilising conditions and mechanisms. In any case, accurate calibration of the heating device in space will have to be performed in order to get realistic values of the two key parameters G_L and V and essentially of their ratio G_L/V (§ 6.1).

This constraint will make it necessary to take into account the lowest available value of G/L (Fig. 4.2), which means minimisation of the concentration of the melt and/or of the cooling rate of the furnace. If the main objective is rather to observe the onset of interfacial instability, the use of pulse demarcation techniques will help to reduce the uncertainty of the true interface velocity value. Nevertheless, some detrimental effects can be generated mainly by the distribution of the solutes, and the values of the gradient will remain rather imprecise.

As regards the concentrations, the absence of convective mixing will not allow the homogenisation of the melts to be as efficient as on earth. Chemical diffusion being the only mechanism, there is a risk that any initial solutal heterogeneity will be preserved on melting. Consequently there is a need to melt specimens that have achieved chemical homogeneity, so as to limit the post-melting diffusion time or to make allowance for the limited soaking time available. Problems of outgassing or of residual porosities will become increasingly important, owing to the increased difficulty the gases will experience in escaping. Depending on the various values

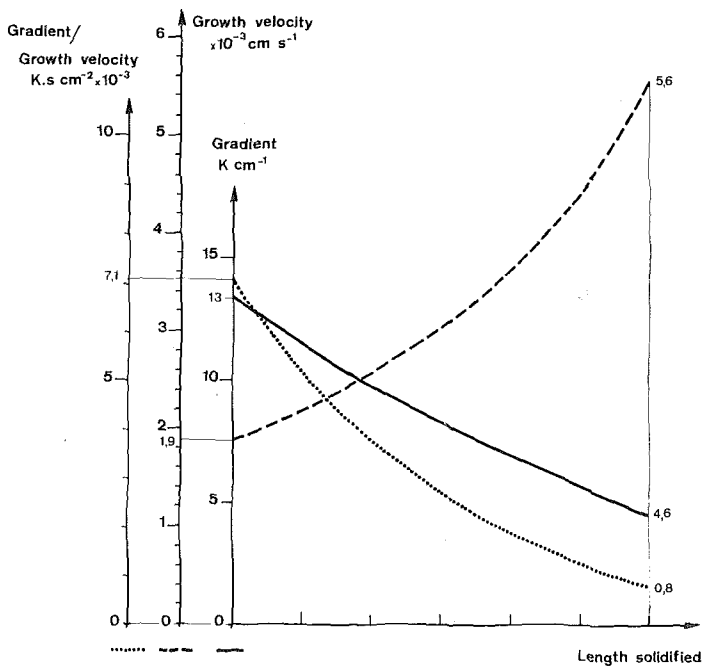

Figure 4.2 Respective variations of the thermal gradient, G, the growth velocity, V and the G_L/V critical ratio in a Bridgman furnace cooled at a constant velocity. G_L and V suffer important transients (common values of the ratios ranging from 3 to 5 for G_L and V) which can give more than one order of magnitude for the critical ratio G_L/V. This observation reduces drastically any chance of using steady state analysis of the destabilisation process.

of liquid/vapour, liquid/solid and vapour/solid surface tensions, many geometrical configurations of the melts may arise that will interfere with the mechanisms of mass and heat transfer. The only way is to find solutions permitting a permanent perfect filling of the crucibles by the melts. It means that the change of volume ΔV_m on melting/solidification will have to be accommodated without constraining the whole system. In this respect, systems with low ΔV_m values and low vapour pressures will be easier to experiment within space, mainly in the form of encapsulated materials.

Compatibility of the melt with the crucible materials will have to be checked with great care. More specifically, the wetting behaviour of pure liquids may change in an unpredictable manner in space and this point must be investigated on a wide scale (§ 4.2.1). Furthermore, in the case of solutions, preferential wetting by one of the components may introduce local segregations that will not subsequently be dissipated by thermoconvective flows: the result will be a diminished solutal homogeneity and thus a locally reduced stability.

In connection with some changes in the wetting behaviour of the melt/crucible system, the resulting nucleation processes may give rise to modified crystalline orientations. In order to avoid the consequent range of instability conditions it may be useful to initiate all space solidification processes on a single seed of predetermined crystallographic orientation, particularly when the crystallographic structures are strongly anisotropic.

The aim of this demonstration is not to propose remedies to any possible problem, but to give examples of some of the steps that need to be taken in order to prevent misinterpretation of the space results and gain the most accurate understanding of the processes.

4.2 Typical unexpected results

This heading should not be misinterpreted. The few examples that will be given do not mean that physics changes when one goes into space. It is simply that in current terrestrial approaches to certain basic technological processes some specific second-order mechanisms may have been underestimated and that consequently extrapolation from earth behaviour to space behaviour may be attended by some surprising results.

The examples that will be discussed in this section are not isolated situations. The experiments which have so far been performed in space have seldom been in complete accord with pre-flight predictions. The official reports of past manned-flight programmes are full of such puzzles. In ESA report entitled 'Materials-Science Research with Sounding Rockets' (ESA-MAT(79)5), which lists the 54 SPAR and TEXUS experiments that had been performed to date, the main unexpected results are highlighted.

Such surprises are in agreement with the general philosophy of current materials-science experimental programmes: if one could extrapolate from the behaviour on earth to behaviour in space without any risk of error, there would be no point in performing such complex flight activities. As a matter of fact, if one attempts to draw conclusions from the experiments already carried out, one finds that the results can be divided into three categories of roughly equal numerical importance:

1. Novel results, either good or less favourable, were as anticipated; assumptions have been confirmed, and at a purely scientific level, there will be little more to do other than move on to possible applications.
2. These results were neither favourable, unfavourable nor novel.
3. The results are the opposite of those anticipated, may be totally unexpected, and here the situation becomes quite engrossing with the wealth of new problems that must be resolved for a better understanding of the real nature of the mechanisms involved.

The following examples belong to this last category.

4.2.1 *Wetting anomalies*

Unexpected results obtained from experiments performed under microgravity conditions on board Skylab, Apollo/Soyuz and Saliut and during other manned and automatic missions have been attributed to the influence of anomalous wetting behaviour. The most reliable reports are the following:

Gatos & Witt [4.1] observed that under microgravity conditions quartz container walls were apparently not wetted by molten indium antimonide and germanium, whereas wetting was observed on the ground.

Barta & al. [4.2] noted that the ingots they prepared under conditions of microgravity differed in shape from what was expected (Fig. 4.3). The authors considered such deviations from the ideal shapes in many liquid salt systems as being probably connected with anomalies in the surface tensions.

The STAMPS Report [4.3] included the following comments: 'This phenomena, which was never previously observed and not predicted theoretically may have to be attributed to surface-tension effects'.

This point is not explained in the existing scientific literature and it is consequently worth taking advantage of the space environment to study the matter. Specialised scientific teams have already been in contact with a view to tackling this puzzling problem. Systematic observations of wetting angles between many substrates and many melts will be made both in 1-*g* and in microgravity environments by using short-duration microgravity facilities (drop towers, aircraft, sounding rockets) that can accommodate necessary experimental equipment and the rather short characteristic times of reshaping.

Such unexpected observations in a rather well-known scientific field must make any space investigator very careful as regards even the best known phenomena.

4.2.2 *Vapour growth anomalies*

'Chemical transport' growth is basically a very simple process: a gaseous transport agent reacts at a given temperature with a solid source of crystal material to form exclusively gaseous products. The vapour species migrate from the source to the condensation zone of the reaction ampulla where, at a different temperature, the reverse reaction occurs with formation of the crystal. In the simplest case, the process would consist of diffusion only, the reaction rates being usually much faster than the diffusion rate. A typical example is the growth of GeSe crystals in an iodine environment which has been exhaustively studied by Wiedemeier [4.4, 4.5] including growth under microgravity conditions in Skylab [4.6]. Germanium combines with iodine to form the two gaseous compounds GeI_4 and GeI_2 which react with GeSe according to the endothermic reaction:

$$GeSe_{(sol)} + GeI_{4\,(gas)} = 2\,GeI_{2\,(gas)} + \tfrac{1}{2}\,Se_{2\,(gas)}$$

The hotter source zone will have higher concentrations of GeI_2 and Se_2 and the concentration of GeI_4 will be higher at the crystal colder zone. Because, in a gravity field, the compositions at the two ends of the ampoule will be different, there will be gravity-driven convection above a critical total pressure, whereas transport will be diffusion-controlled at lower pressure. Usually the crystal quality deteriorates as the contribution of the convective component to the transport process increases.

Similar experiments performed at approximately $10^{-4}\,g_0$ showed some interesting and not easily understandable results: at pressures for which at normal gravity convection was significant, the spacegrown crystals showed the nearly perfect morphology characteristic of diffusive transport and this result was in agreement with the hypothesis that gravity causes convection (Fig. 4.4). But the surprising result was that the rate of growth was higher than expected for purely diffusive transport, whereas extrapolation from experiments at normal gravity and very low pressures had suggested that transport would be purely diffusion controlled. In fact, in some runs the growth rate at microgravity, which was presumably due to diffusion only, was higher than the growth rate at the same pressure at normal gravity, i.e. when diffusion was presumably augmented by convection. The difference between observed and predicted mass fluxes is about one order of magnitude, and these observations indicate the existence of other than gravity-driven convective transport components contributing to mass flux in a reactive solid/phase system.

New comparative experimental research in normal and near-zero gravity conditions (to consider possible flows in the vapour due to vehicular residual motions), together with further refinement of the theory mainly in

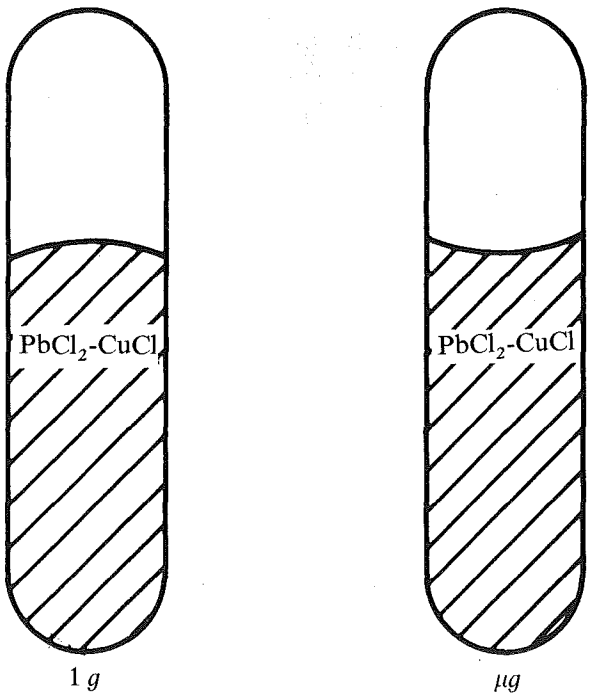

Figure 4.3 Expected and true shape of $PbCl_2 - CuCl$ system in the Czech experiment MORAVA (Saliut VI, 1978).

the fields of the thermochemistry of the gas phase reaction and of up to now secondary effects of the temperature gradient, would come under this heading. Solan & Ostrach [4.7] gave a very good review of the related problem, and of the new challenge it offers to imaginative scientists.

Figure 4.4 Laue X-ray diffraction transmission photographs of (001) oriented $GeS_{0.98}$ $Se_{0.02}$ single crystal platelets: a. ground-based (prototype), b. space-grown.

4.3 Multi-phase systems

Multi-phase systems can be arranged, according to the state of aggregation of the phases, in the following categories [4.8]:

1. Gases dispersed in liquids (foams, gas emulsions)
2. Liquids dispersed in gases (mists, fogs, liquid aerosols)
3. Gases dispersed in solids (solid foams)
4. Solids dispersed in gases (fumes, smokes, solid aerosols, dusty gases)
5. Liquids dispersed in liquids (emulsions)
6. Liquids dispersed in solids (some gels)
7. Solids dispersed in liquids (suspensions, sols)
8. Solids dispersed in solids (composite materials).

Figure 4.5 gives the same information in graphical form.

Five of the eight categories (1, 2, 4, 5 and 7) are sensitive to gravity (except for the rather particular case of vanishing difference of densities). Microgravity experiments have been proposed in each of these categories in the hope that the avoidance of buoyancy or sedimentation will help to stabilise an otherwise unstable configuration (§ 2.5).

The motion of small particles, drops and bubbles fully submerged in a viscous fluid at low Reynolds number is one of the oldest problems in fluid mechanics, and an enormous number of papers have been devoted to its study. This, together with the multidisciplinary character of its present and foreseeable applications, impedes the presentation in this document of even a very cursory review of the field. A good introductory text-book on the subject is that by Happel & Brenner [4.9]. Extensive reviews have been published recently, among them that by Leal [4.10] should be mentioned, where many additional references can be found.

The relevance to microgravitational fluid dynamics of the available analytical and experimental knowledge in this field is not clear. When sedimentation effects are to be avoided, neutrally buoyant emulsions or suspensions can be used. This solution is not completely satisfactory since data on the influence of the viscosity ratio, which is probably important, are very scanty, not to mention that additional considerations heavily restrict the choice of the couple of interfacing materials.

When the particle is placed near an interface, engulfment or rejection by one of the liquid phases can result. This situation is typical of many problems in chemical engineering, metal processing, painting, bacteriology etc.

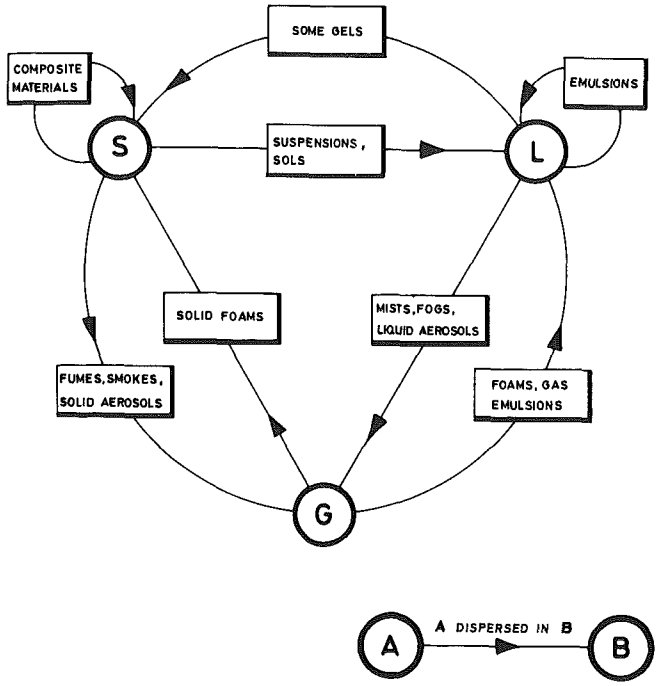

Figure 4.5 Graphical representation of various categories of multiphase systems.

From the theoretical point of view, the problem has been solved analytically only under a fairly restricted set of assumptions (the particles are cylindrical rods, since the configuration is two-dimensional, and these rods are bounded by ideal solid surfaces which do not exhibit contact-angle hysteresis), and within the classical theory of capillarity. The analysis shows [4.11] that for contact angles above some value there are two equilibrium positions of the weightless particle, but only one of them corresponds to stable equilibrium.

Gas emulsions are dispersions of a gas in a liquid when the liquid to gas volume fraction, ϕ, exceeds 0.9. Foams differ from gas emulsions in that ϕ is less than 0.1. In gas emulsions the thickness of the interstitial liquid layers is of the order of the bubble diameter, whereas in foams these layers are very thin (lamellae).

When inertia effects are negligible, gas emulsions do not differ greatly from liquid emulsions, particularly under microgravity conditions where hydrostatic pressure is absent. Gas emulsions are unstable in the gravitational field. The ascending velocity, u, of a bubble (radius r, density ρ_g, and viscosity μ_g) in a liquid (ρ_l and μ_l) is given by the following equation:

$$u = \frac{2g\,r^2}{9\mu_l}(\rho_1 - \rho_g)\frac{\mu_g + \mu_1}{\mu_g + \frac{2}{3}\mu_l} \simeq \frac{g\,r^2}{3\mu_l}\rho_1$$

since $\rho_l \gg \rho_g$ and $\mu_l \gg \mu_g$

This expression is based on the Rybczynski & Hadamard resistance law for a spherical liquid drop at low Reynolds number. It has been criticised by several authors because it does not take into account surface viscosity (Boussinesq), effect of surface-active materials (Levich), deformation of the surface etc.

The experimental values of u are usually smaller than those predicted by the theory, and in many instances satisfy the equation

$$u = \frac{2g\,r^2}{3\mu_l}(\rho_l - \rho_g)$$

valid for solid spheres in liquid. For a discussion of this problem see Levich [4.12].

The stability of a foam is controlled by that of the lamellae constituting it. The drainage of a foam has two causes. The more obvious is gravitation: gas present below liquid is unable to support it, then the liquid flows down and the gas rises up. The second cause, independent of the gravity level, is suction of liquid by the Plateau borders (§ 2.3.3).

Absence of sedimentation (or bubble rise) under microgravity conditions will permit the study and/or the use of phenomena hardly reproducible on Earth; several typical examples are given in the following.

- Study of processes like phase growth, heterogeneous chemical reactions etc., far from thermodynamic equilibrium conditions. When motions are negligible heat and mass exchange between the phases are diffusion controlled and generally proceed at lower rates. Temperature and concentration fields in the vicinity of spherical particles will have a spherical symmetry and can be modeled more easily.
- Study of the laws governing the coarsening of a dispersion of coagulating or coalescing particles through slow, finely controlled, motions.
- Study of the complicated behaviour and evolution of spatial distributions of particles under the action of an imposed field (acoustic, electric, magnetic, temperature, concentration). The transporting power of a field, and hence the particle velocities, depend on the local field intensity and gradients, which in turn are modified by the particle distribution. Particle displacements caused by a field will act back on the field. There is thus feed-back,

which means non-linear behaviour, and, consequently, instabilities are to be expected. (No such feed-back occurs when gravity acts on a particle distribution. Because of the smallness of the gravity constant, the local intensity of gravity does not depend on the spatial distribution of the particles.)
- Measurement of the so-called frozen sound speed in a dusty gas (or a bubble liquid). This measurement requires motionless particles (or bubbles), so in experiments performed on Earth, where sedimentation or rise are unavoidable, a different sound speed is actually recorded.
- Freezing of a dispersion, with the aim of obtaining a stable material combining properties of two different components. A crucial and theoretically unsolved problem here concerns the conditions for incorporation of particles into the growing solid. Experiments with immiscible alloys and metal composites are to be quoted here.
- Separation of heterogeneous particle populations. Under microgravity a weak differential transporting power could be used for this purpose (§ 2.5), provided that a sufficiently long time interval is available for the separation to take place. Electrophoresis can be mentioned here and experiments have already been conducted in space [4.13]. Electrophoresis could conceivably be employed, in a microgravitational environment, on particles whose densities deviate considerably from that of the medium (e.g. liquid drops in gas). However, so far this field has not lived up to early expectations, probably either because there are other and more subtle methods available (in the case of separation of living cells) or because no need has materialised (separation of non-living particles).
- Finally, it should be mentioned that particles will often be a nuisance in microgravity experiments, if they occur unintentionally. The quasi-automatic elimination of a bubble by buoyancy does not occur in space. The application of a controlled, artificial transport on the other hand creates new problems. Usually it also requires a longer time, since the motions that can be induced are slow.

Dusty gases and bubbly liquids with strong inertia effects have been extensively considered because of their application to rocket propulsion, and cavitation or underwater detection, respectively. (See the review papers by Marble [4.14] on dusty gases, and by van Wijngaarden [4.15] on bubbly liquids.) In all, we do not think these problems are of particular micro-gravitational relevance, although examples on the contrary are often quoted. For instance, boiling heat transfer, was considered from the very beginning a case of interest. Nevertheless, it is shown [4.16] that the gravity level does not substantially affect the evolution of the process except in some extreme cases (for example when both subcooling and fluid velocity are kept small).

The elimination or minimisation of undesired primary motions of particles is a prerequisite for experiments in these areas. As has been discussed in § 2.5, a considerable number of transport mechanisms can counteract the feeling that this is easily achieved in a microgravitational environment. In particular, the induction of motion of fluid particles by a temperature gradient will often be a new problem, since many materials sciences experiments require, or are accompanied by, temperature changes, which imply gradients.

4.4 Combustion in a microgravitational environment

The two main motivations for combustion experiments in a microgravitational environment are:
- Fire safety studies in spacecraft;
- Basic experiments for understanding the details of the combustion processes.

Experiments in space are justified if the expected results are unobtainable on earth (i.e. at the ground gravity level). To understand the reasons for space experiments in the field of combustion one must appreciate the role played by the gravity forces in the different combustion processes and in the different stages of them (ignition, steady-state, extinction). The two basically different combustion processes are: Diffusion flames and premixed flames.

4.4.1 *Diffusion flames*

A diffusion flame is a combustion process in which the reactants, initially separated, are brought together by diffusive (and convective) effects. Examples of diffusion flames are an ordinary candle or a fuel droplet burning in an oxidising atmosphere.

The propagation of a diffusion flame has been studied for years and by many researchers. Burning of a fuel droplet in an oxidising atmosphere is relevant to combustion engines (both reciprocating and gas turbines). Open fire propagation is relevant to fire safety studies. Concern over fires on board spacecraft has been particularly acute since the Apollo 13 incident in 1970.

There is no doubt that buoyancy is a dominant aspect in

ground laboratory diffusion flame combustion. The buoyancy induced convection is a very efficient mechanism by which the oxidiser (in the ambient) is brought to the flame front, thus enhancing the burning rates which could be achieved in the case of purely diffusive transport, such as could be realised under microgravity conditions.

Classical theories are available for studying the combustion of a single drop (or a single solid particle) under the assumption that the configuration is spherically symmetrical. These theories have been experimentally checked by use of short-duration free-falling techniques. See [4.17], for example, and the references therein.

The effect of natural convection can be reduced on earth by reducing the drop (or particle) size down to the order of microns, but then the performance of the experiment and the study of the internal structure of the flame become very difficult.

There are examples of practical interest where neutrally buoyant conditions have appeared by accident. This is the case with the combustion of nitric acid drops (oxidiser) in a hydrogen atmosphere (fuel). The density of the combustion products is almost the same as that of the ambient gas, and perfectly spherical configurations result.

A number of experiments performed in the past in microgravitational environments of short duration, [4.18, 4.19], were able to yield only preliminary results for the steady-state combustion, since the short run time did not permit the achievement of steady-state conditions. It is for this reason that there is so much interest in performing experiments of greater duration on board of satellites.

Typical results for the combustion of single particles in an aircraft microgravitational environment [4.20, 4.21] (see Figure 4.6) indicate that:

- there is a striking difference in flame geometry: as might be expected, in the microgravitational environment the flame appears spherical and of larger area;
- the burning rates are reduced, owing to the difficulty the oxygen has in reaching the flame front by diffusing through the combustion gases;
- this difficulty of supporting combustion by diffusion makes self-extinction highly probable;
- the ignition process is quite similar to that at 1 g.

In this area a number of possible experiments are being considered:

- Quasi-steady diffusion flame process (its very existence is still in doubt) in a microgravitational environment with spherical symmetry and no flame distortion due to convection.

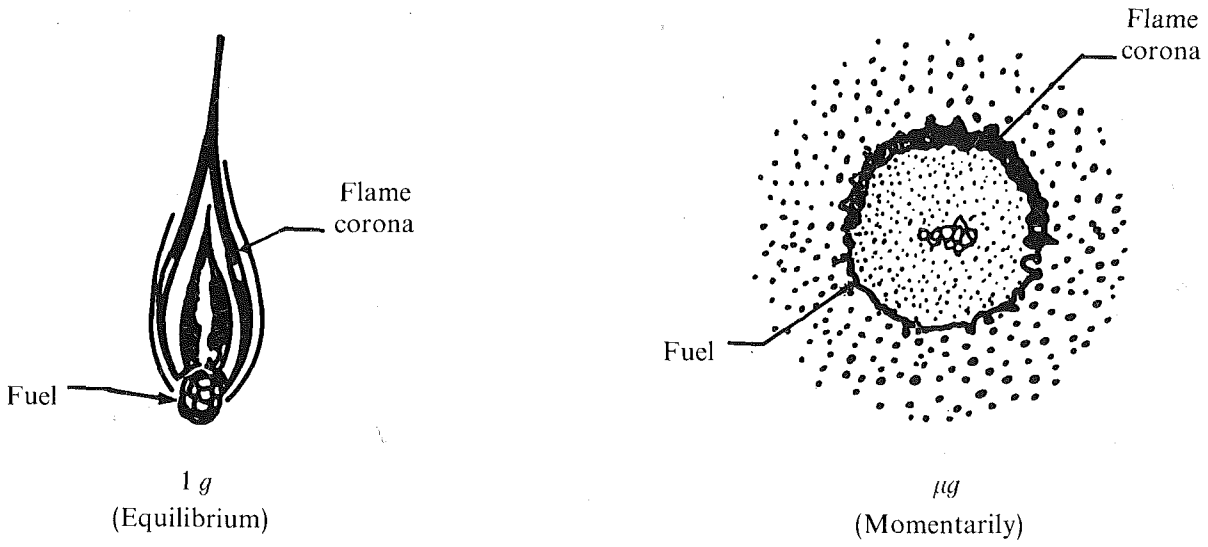

Figure 4.6 Comparison of fuel burning in an oxidiser atmosphere under 1-g and μg conditions. From [4.20].

- The effect of pressure on the combustion rate (on earth it is impossible to separate the effect of the pressure from that of buoyancy).
- The extinction process and its correlation with the radii of droplets as a function of pressure.
- Convection effects for droplets at low Reynolds number (it is difficult to set a constant low Reynolds number in the presence of a buoyancy-induced convective flow).

The role of buoyancy is also of a paramount importance in the fire spreading on large solid or liquid surfaces. The subject is of course relevant to the understanding of the occurrence of unwanted fires on board satellites, but such experiments will also provide basic knowledge on the processes occurring on earth. Typical experiments to be performed in a microgravitational environment would be the determination of steady flame-spread rate over a solid-fuel surface as a function of a steady convective flow velocity (unaffected by buoyancy-induced velocity fields) and the study of transient flame-spread rate during the variation of the convective flow velocity.

4.4.2 *Premixed flames*

In this case the combustion process takes place in a homogeneous mixture of fuel and oxidiser. Typical examples are the combustion processes in internal combustion (carburettor) engines where premixed air and gasoline burn once ignited by a spark, multidimensional flames propagating in tubes, and flames stabilised in the lips of burners (Bunsen type burners, flat porous burners...).

Quasi steady-state flame propagation is not possible beyond some extinction limits (flammability limits for the fuel/oxidiser composition, quenching limits for the size of the experimental apparatus, pressure limits). These limits can be substantially affected by buoyancy effects, and experiments have been proposed, [4.22, 4.23], for measuring them under microgravity conditions.

As mentioned above in connection with diffusion flames, the currently available theories of flame propagation and extinction ignore gravity effects, but have not been experimentally checked under 'realistic' conditions. Perhaps, in the near future, microgravity research will permit the inclusion of gravitational effects in more complete theories of flame propagation and extinction.

The stability of the flame front in a premixed flame depends on several factors. The following types of instability appear under normal gravity conditions:

- normal Rayleigh/Taylor instabilities when low-density layers are placed underneath high density layers in a gravity field;
- instabilities of hydrodynamic type (Landau) which are due to the thermal expansion of the burned gas;
- instabilities triggered by transport effects in the diffusional-thermal structure of the flame (Sivashinsky) [4.24].

The first type of instability is obviously affected by the gravity level. The diffusional-thermal mode of instability can also be sensitive to gravity. The occasional lack of agreement between Sivashinsky's theory (which again neglects gravity) and experiments performed at ground level are partially attributed to gravitational effects. Experiments performed under microgravity conditions could reveal phenomena hitherto hidden by Rayleigh/Taylor instabilities.

Although quasi-steady premixed flame propagation is less affected by gravity than diffusion flames are, some influence clearly appears when the behaviour of upward and of downward propagating flames are compared. The differences are particularly conspicuous in the neighbourhood of extinction limit conditions.

The technically interesting situation of burning two-phase homogeneous mixtures of (premixed) finely divided combustible particles (either liquid or solid) in an oxidising gaseous atmosphere combines the above presented intricacies (and reasons in favour of microgravity research) with those discussed in § 2.5 and 4.3.

Some areas which could benefit from space-borne experimentation are listed below. Needless to say, no claim for completeness is made.

- Collection of fundamental data on flame initiation, propagation and extinction under microgravity conditions and at the high oxygen concentrations normally prevailing in spacecraft environments.
- Basic research on the combustion behaviour (autoignition, propagation, extinction) of uniform clouds of quiescent particles under the perfectly characterised conditions which result from the absence of gravitational settling, buoyancy etc.
- Flame front instability studies in the absence of buoyancy-driven instabilities.

4.5 Jets

Jets are not usually associated with microgravity studies. Nevertheless, some connection exists, either because microgravity will permit the observation of phenomena which are normally hidden by gravity action or because of the present and foreseen applications of liquid jets to spacecraft fluid management or to materials processing in space.

Rarefied jets, molecular beams etc. are not dealt with here, since emphasis is placed on microgravity rather than on other characteristics of the space environment.

4.5.1 *Capillary jets*
Surface tension significantly affects the balance of forces at the interface of a capillary jet, other forces being (for Newtonian fluids) the viscous stresses and the dynamic pressure.

Gravity effects can be neglected in most terrestrial applications provided that the dynamic pressure is much larger than the hydrostatic pressure, i.e.:

$$\frac{\rho_l V^2}{(\rho_l - \rho_g) g L} \gg 1$$

where V is the characteristic liquid velocity and L the characteristic length, in the g direction, of that part of the jet which is being observed. The above dimensionless group, which is a squared Froude number, can be interpreted as the ratio of a Weber number to a Bond number.

Solidification of capillary jets for producing fibers has been suggested. This appealing idea presents some difficulties because of the tendency to expansion or contraction which jets of either Newtonian or viscoelastic liquids exhibit. That is why continuous drawing techniques are used for the above-mentioned purpose [4.25].

Expansion or contraction of a jet has been attributed in the past to non-linear properties of the liquid. Middleman & Gavis [4.26] showed that jets of Newtonian liquids expand when $Re_d < 16$ and contract when $Re_d > 16$, where Re_d is the Reynolds number based on the initial diameter of the jet. This result was later checked by Gavis & Modan [4.27]. For viscoelastic liquids the situation is similar, although a bit more complicated, see Gavis & Middleman [4.28].

4.5.2 *Disintegration of capillary jets*
This is an old classic problem, first investigated by Rayleigh around 1880 and later by Weber. The interest in these problems arose in the past from their applications to combustion processes. A revival of interest resulted from ink-jet printing techniques (see Bogy [4.29] and references therein). These techniques provide such a precise control of the resulting trains of droplets that they are being used in experiments where accurately reproduced droplets are required.

Break-up of liquid filaments is an unclear process. According to White & Ide [4.30], the filaments of low-viscosity fluids break-up through a capillary mechanism similar to that in capillary jets or in liquid bridges, whereas for very viscous liquids break-up seems to occur at a critical stress. Experiments performed with liquid bridges, by using the Plateau technique, showed, in the late stages of the bridge break-up, liquid filaments with aspect ratios well above the Rayleigh limit ($L_M = \pi D$), suggesting a fairly complex behaviour.

4.5.3 *Jet stirring and jet positioning*
Jet stirring has been experimentally studied, during short microgravity periods by Aydelott [4.31], who used the NASA Lewis Zero-Gravity Facility. Although the aim of this research was devising methods for thermal conditioning of cryogenic tanks, the same technique may be used in other situations. The requirements for the application mentioned above are extremely demanding: the jet must circulate the fluid in the liquid bulk within the partially filled container, must wet, for cooling purposes, the otherwise dry walls, avoiding entrainment of bubbles as well as excessive turbulence in the bulk liquid.

Figure 4.7 schematically shows the four observed normal flow patterns. The resulting configuration depends on the liquid inflow rate (measured by the ratio of the jet volumetric flow rate to the tank volume over testing time), the liquid volume in the tank, the position of the injection tube exit, and tank geometry. The first three parameters are probably related to the jet momentum at the interphase, as discussed below, but no attempt has been made to unify them into a single parameter.

Two undesirable patterns were also observed, namely: at tank fillings above 90% where the vapour bubble tended to become detached from the tank walls, and at very high inflow rates (above 8) which resulted in bubble entrainment into the liquid bulk.

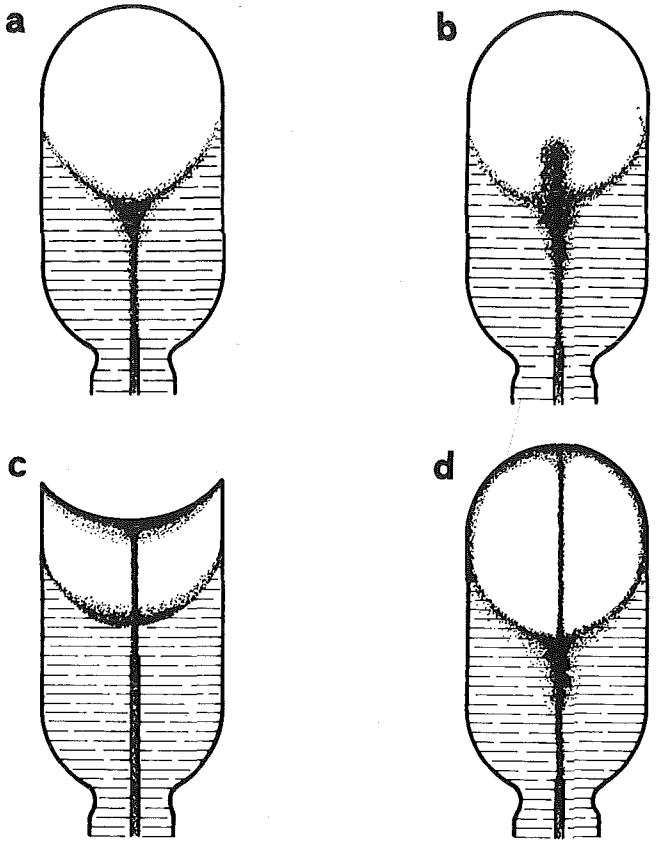

Figure 4.7 Jet mixing in a partially-filled cylindrical container under microgravity conditions. (Sketched after photographs in [4.31].)

(a) At flow rates in the range 0.6 – 1 (for 10^{-2} m long jet exit tubes) the thin laminar jet rose towards the interphase, collecting and spreading downwards with increasing time. The interphase is much more sensitive to jet impingement than under normal gravity conditions.
(b) Increasing the flow rate to about 1.5 for 10^{-2} m long tubes, or increasing the tube length, a geyser appears in the vapour-filled portion of the tank. The ultimate configuration has not been observed since longer microgravity runs are needed.
(c) The liquid jet collects on the tank end opposite the jet exit without falling back into the bulk liquid region. This configuration was only observed with the tank geometry shown. It seems that it will appear for the other geometry (a, b and d) over a very narrow range of inflow conditions.
(d) For inflow rates in the range 2 – 8 the liquid jet flows over the opposite tank end and down the tank walls toward the interphase, and then collects on the top of the bulk liquid region.

Aerodynamic positioning, which has been used on Earth, has been suggested for space (§ 6.3).

The two just-mentioned applications require understanding of the jet/interphase interaction. This is a reasonably well-known problem, for which both analytical and experimental data are available ([4.32] where the impingement at right angles of a gas jet on a liquid at rest is analysed). The two controlling parameters in Berghmans' study are the Weber number,

$$We = \frac{\rho_g V^2 r_j}{\sigma}$$

and the Bond number,

$$Bo = \frac{(\rho_l - \rho_g)\, g\, r_j^2}{\sigma}$$

both based on the radius r_j of the jet. The critical Weber number for surface instability, We_c, is related to the critical Bond number Bo_c through a very simple linear expression ($We_c = 1.04 + 3.3\, Bo_c$), which can be confidently extrapolated to zero Bond numbers.

References

[4.1] Gatos H C, Herman C J, Lichtensteiger M & Witt A F, in *Materials Sciences in Space*, Proc 2nd Symp Frascati 1976, ESA SP-114, p. 181.

[4.2] Barta C, Triska A & Okhotin A S, in *Materials Sciences in Space*, Proc 3rd Symp Grenoble 1979, ESA SP-142, p. 213.

[4.3] *Materials Processing in Space*, publ. by National Academy of Sciences, Washington DC 1978, p. 37.

[4.4] Wiedemeier H, Irene E A & Chaudhuri A K, in *J of Cryst Growth* **13/14**, 1972, p. 393.

[4.5] Wiedemeier H & Irene E A, in *Z Anorg Allg Chem* **400**, 1973, p. 59.

[4.6] Wiedemeier H, Klaessig F C, Irene E A & Wey S J, in *J of Cryst Growth* **31**, 1975, p. 36.

[4.7] Solan A & Ostrach S, in *Preparation and Properties of Solid-State Materials* **4**, (W R Wilcox, Ed), Marcel Dekker, NY 1979.

[4.8] Bikerman J J, *Foams*, Springer-Verlag, Berlin 1973, p. 1.

[4.9] Happel J & Brenner H, *Low Reynolds-Number Hydrodynamics*, Prentice-Hall, Inc, Englewood Cliffs, NJ 1965.

[4.10] Leal L G, in *Annual Review of Fluid Mechanics*, **12** (M van Dyke, J V Wehausen & J L Lumbley, Eds), Annual Reviews Inc, Palo Alto, Calif 1980, p. 435.
[4.11] Neumann A W, in *Wetting, Spreading and Adhesion* (J F Padday, Ed), Academic Press, London 1978, p. 3.
[4.12] Levich V G, *Physicochemical Hydrodynamics*, Prentice-Hall, Inc Englewood Cliffs, N J 1962, p. 395.
[4.13] Hanning K & Schindler R, in *Materials Sciences in Space*, Proc 2nd Symp Frascati 1976, ESA SP-114, p. 27.
[4.14] Marble F E, in *Annual Review of Fluid Mechanics* **2**, (M van Dyke, W G Vincenti & J V Wehausen, Eds), Annual Reviews Inc, Palo Alto, Calif 1970, p. 397.
[4.15] Van Wijngaarden L, in *Annual Review of Fluid Mechanics* **4** (M van Dyke, W G Vincenti & J V Wehausen, Eds), Annual Reviews Inc, Palo Alto, Calif 1972, p. 369.
[4.16] Cochran T H & Aydelott J C, *Effects of Subcooling and Gravity Level on Boiling in the Discrete Bubble Region*, NASA TN-D-3449, 1966.
[4.17] Kumagai S, Sakai T & Okajima S, in *Thirteenth Int Symp on Combustion*, The Combustion Institute, Pittsburgh, Penn 1971, p. 779.
[4.18] Cochran T H & Masica W J, in *Thirteenth Int Symp on Combustion*, The Combustion Institute, Pittsburgh, Penn 1971, p. 821.
[4.19] Edelman R B, Fortune O F, Weilerstein G, Cochran T H & Haggard Jr J B, in *Fourteenth Int Symp on Combustion*, The Combustion Institute, Pittsburgh, Penn 1973, p. 399.
[4.20] Kimzey J H, in *Space Processing and Manufacturing*, NASA TM-X-53993, 1970, p. 323.
[4.21] Naumann R J & Herring H W, in *Materials Processing in Space: Early Experiments*, NASA SP-443, 1980, chapter 6.
[4.22] Berlad A L & Killory J, *Combustion of Porous Solids at Reduced Gravitational Conditions*, NASA CR-3197, 1979.
[4.23] Strehlow R A & Reuss D A, *Effect of a Zero-g Environment on Flammability Limits as Determined Using a Standard Flammability Tube Apparatus*, NASA CR-3259, 1980.
[4.24] Sivashinsky G I, in *Acta Astronautica* **6**, 1979, p. 569.
[4.25] Denn M M, in *Annual Review of Fluid Mechanics* **12** (M van Dyke, J V Wehausen & J L Lumley, Eds), Annual Reviews Inc, Palo Alto, Calif 1980, p. 365.
[4.26] Middleman S & Gavis J, in *Phys Fluids* **4**, 1961, p. 355.
[4.27] Gavis J & Modan M, in *Phys Fluids* **10**, 1967, p. 487.
[4.28] Gavis J & Middleman S, in *J Appl Polymer Sci* **7**, (1963), p. 493.
[4.29] Bogy D B, in *Annual Review of Fluid Mechanics* **11** (M van Dyke, J V Wehausen & J L Lumley, Eds), Annual Reviews Inc, Palo Alto, Calif, 1979, p. 207.
[4.30] White J L & Ide Y, in *J Appl Polymer Sci* **22**, 1978, p. 3057.
[4.31] Aydelott J C, *Axial Jet Mixing of Ethanol in Cylindrical Containers during Weightlessness*, NASA TP-1487, 1979.
[4.32] Berghmans J, in *J Fluid Mech* **54**, 1972, p. 129.

5 Specific constraints of space experiments

The intention of this chapter is to focus attention on the specific constraints of microgravity, rather than on its advantages, which have been considerably emphasised in the available literature of the past few years. Furthermore, it will cover preferentially the many differences between experiments on earth and those on microgravity platforms, whatever the nature of such differences.

Thus, in contrast to the previous sections, this one will be of a much more practical nature.

In planning materials science experiments in space one must take into account the constraints associated with the type of space platform to be used, each one having its own levels of microgravity, its own limitations as regards time, power, energy, cooling, data acquisition and safety regulations, and its own equipment. This set of imposed conditions will necessarily influence all aspects of the microgravity experiments from the earliest works to the post-flight analysis philosophy, the only common point being an increase of both the global complexity and the individual difficulties, even in the case of experiments being already perfectly known in their classical terrestrial environment. It is important that any new space investigator be aware of such problems and of their possible solutions before entering this very intriguing but not so simple field. The order of this presentation cannot be chronological, because of the numerous ways in which the topics overlap. Furthermore these topics are only specific points of general interest since any exhaustive analysis would be quite unreasonable as yet.

5.1 Preparation of the experiment

Even in the case of the simplest and the best known materials science experiments, space implementation will require much extra work. In this section, we shall consider the work that an investigator will have to perform in adapting his experiment to multi-user equipment; obviously, implementation of a complete piece of equipment would require much more effort. A good example is the choice of the materials. Under both space and earth conditions, the main limitations are academic and physico-chemical, but the space choice is limited by other constraints as well. These are as follows.

- Experimental materials must be compatible with all the materials involved in the construction of the facilities in order to lower the risk of leakage.
- Energy consumption must be minimised by avoiding the use of materials with excessive thermal conductivity.

- Heat transfer between heating sources and sinks must be controlled in order to adapt systems to time limits.
- In order to comply with safety regulations (mainly with manned flights) the use of any forbidden materials must be avoided, and non-forbidden materials must be submitted to prescribed tests.
- In preparing experiments, it is necessary to take into account the possible risks of an increased stockage time due to a shift of flight dates (stability of the residual atmospheres, possible corrosion events, radio-active decay laws); the leakage levels will be the subject of special attention.
- For studies involving convective phenomena in microgravity, it will be necessary to consider phase configurations of fluids in terms of surface-tension equilibria, free-volume changes and possible fluid flows induced by various forces.
- In defining the geometry of the hardware, the requirements of the scientific objectives will have to be adapted to those of the facilities. For instance, in the event of diffusion-controlled processes, overall lengths of the specimens will be determined by the permitted durations of the processes.
- The encapsulated experiment will have to withstand specified mecanical tests as a proof that it can survive shocks and accelerations associated with the launching and landing phases of the flights (some high-temperature testing procedures may also be necessary.
- Each materials science experiment involves many physical parameters that have to be known with the highest accuracy. Identifying them will be one of the tasks to be performed by any principal investigator.
- It may be necessary to resort to simulation methods or the use of short-duration microgravity facilities in order to test or to validate mandatory data or steps.

5.2 Performing the experiment

The main difficulty is the lack of flexibility in the performance of the experiment itself. The experiment cannot incorporate last minute changes inspired by new events. Such problems are standard in classical space-science activities, but they become increasingly important in the field of materials science because such a new discipline often requires continual modification of set-ups, parameter ranges and the like. This is not rarely possible with the present structure of flight opportunities and management which, on the contrary, tends to require too detailed and too complete advance knowledge. Moreover, in the case of failure, it is frequently impossible to modify or repeat the experiment during the same mission, even in the favourable situation of manned programmes. Consequently the very accurate preparation work just described is amply justified.

Another point of great concern to the investigators is the problem of data acquisition. Many materials science experiments need very precise measurements of temperatures in many points of the system. Unfortunately, in space, the capabilities of electronic devices (rates, format, storage of the data) and the availability of thermal sensors (number, location, branching) are less than on earth and accurate mathematical modelling from only a few measurements has to compensate for their deficiency. Section 6.1 throws more light on this point.

5.3 Man's role

This point is of importance only when manned missions are planned. There are many advantages in having payload specialists in the immediate vicinity of materials science experiments, since these are likely to have some surprises in store, however well they may have been prepared. The payload specialists' ability to take decisions in the case of unexpected behaviour or for adjusting, calibrating and repairing equipment onboard are examples of such advantages. The importance of the presence of a human operator increases with the transmission time between earth and spacecraft. Unfortunately, there are also disadvantages, particularly in the existing programmes where the crew capabilities are underused. The main reason for this is that it is not always certain that a payload specialist is completely familiar with the all peculiarities of the experiments to be performed. Moreover, without sufficient previous experience some tasks that would be quite easy on earth are much harder in space. These factors limit the potential advantages of the human role because at the moment costs outweigh benefits, there being inadequate compensation for expensive safety precautions.

5.4 Post-flight analysis contingencies

The overall cost of the experiments, their long preparation time and the small number of flight opportunities make it essential to maximise the scientific return of each space experiment. This will be facilitated if efforts are made to seek cooperation in advance and if work is coordinated right from the definition phase so that the various experiments within a project can both

complement and supplement one another. In such a concerted approach, it will be necessary to make sure that the various systems are used to maximum advantage so as to ensure that as many tests as possible are performed and that the maximum amount of information is obtained. In some circumstances, different experiments on the same piece of equipment will yield complementary results, thus enhancing the overall scientific return, but such advantages will depend on the various experimenters' willingness to cooperate with one another. Experimenters will have to realise that the kind and number of parameters that can be measured are limited and that accuracy cannot always be as high as it is in their earth-bound laboratories. They will have to adopt new attitudes. Finally, it will have to be borne in mind that post-flight data analysis, which will have to be exhaustive, will require the same level of manpower, financial and management resources as the pre-flight tasks. If project teams are not aware of this, they may get into difficulties. In any case, they should realise that their planning should allow sufficient time to elapse between two launches of the same payload for observed shortcomings in the first to be remedied in the second and for the second to be adapted in the light of the results obtained with the first.

5.5 Relations between materials scientists and space agencies

Materials scientists contemplating experiments in zero gravity – and therefore potential customers of space agencies – may experience difficulties in their relationships with these agencies if they are not aware of the sort of surprises that may be in store for them. For example, the agency may not have the sort of structure that the experimenter needs or the instructions for work in space may presuppose information that the experimenter does not possess.

The first point of contact will be the 'call for experiments". This may not be directed specifically at materials scientists; it may contain a lot of space jargon that is unfamiliar to the potential experimenter; and much of the information requested may seem irrelevant. Answering the questions is often made difficult by the fact that the descriptions of equipment and facilities are incomplete because a great deal of effort still has to be expended by the experimenter and those responsible for the equipment in reaching a compromise between the experiment's requirements and the facilities' capabilities.

The next point at which the experimenter may receive a rude shock is when he discovers the length of time over which he will have to organise his planning and the detail with which he will have to describe the tasks to be performed. Such detailed, long-term planning is made necessary by the fact that the flight date has to be fixed far in advance and that appointments have to be made for testing on the ground in multi-user facilities. Materials scientists are unaccustomed to adapting their work to such bottle-necks. Moreover, since the test facilities are usually not tailored to their needs, they will have to expend a considerable amount of effort in adapting their hardware to the fixed characteristics of the ground facilities as well as to the limitations of time, energy, power, data-acquisition capacity, crew activity etc. that have already been frozen long ago. It is an unfortunate fact that many investigators are left with the nagging suspicion that their experiment has been chosen not so much for its scientific soundness as for the ease with which it could be incorporated into the existing set-up.

Both equipment and flight programmes are so rigidly determined that in the end the investigators are the only flexible element in the system. This flexibility is diminished, however, by the fact that, because the implementation times for materials science experiments are currently so long – usually more than three years – investigators are unable to employ young Ph. D. candidates (their main work force) in such activities.

The foregoing remarks are not intended to discourage materials scientists from undertaking experiments in space, but to act as warnings and to prepare the future investigator for the traps and pitfalls he is likely to encounter in the present system. It would be a pity if such a potentially fruitful field of investigation should remain barren as a result of misunderstandings between the two main parties. Pioneers must realise that easy access to opportunities for work in zero gravity will have to be bought by disciplined adherence to the rules of the game as it is now played. Then, in time, it will be possible for space agencies to recognize their special needs. In any case, future success in the field is crucially dependent on good relations between the two partners.

5.6 Development and adequacy of equipment

So far, only few pieces of equipment have been developed in such a way as to accord closely with the specific objectives of the scientists. The rather high cost of multi-user equipment will mean that it will have to be used as long as possible without major modification, which cannot in any case take place until space calibration has been completed. It must be emphasised that current

space equipment is in fact ground equipment that has been modified for space use in only the most superficial way. Some very surprising results may be produced by such equipment during the first few microgravity runs on the experience of which any urgent improvements will have to be based. It will be quite a long time before we emerge from the current situation, where we are studying two superimposed types of space behaviour – that of the equipment and that of the experimental materials – into a situation closer to the ideal where we need only consider the effect of microgravity on the materials and the processes involving them.

Each pioneer investigator must realise that he will have to draw his own conclusions about how his experiment has run. And he and his colleagues will have to share such experience, since improvement will be strongly dependent on such information feed-back.

5.7 Consistency between requirements and performance

Proposed experiments must be so structured that some difference between initial experimental requirements and measured results can be accommodated. Experimentation in microgravity is still largely an unknown field, and surprising results are to be expected. Requirements that are too specific run the risk of not being satisfied, particularly in the early stages. Obviously, things will become clearer in the future. But it is perhaps as well to bear initial limitations in mind as a means of avoiding disappointment and of being tempted to draw overly harsh conclusions about the usefulness of performing experiments in microgravity.

Reading this fifth chapter should have made the reader aware that the intellectual and psychological aspects of zero-gravity work are quite as important as the purely technical side. Such a new science must be approached with great care and with new doubts, new imagination and new methods. Our aim has been to prepare the potential investigator and help him to overcome the inevitable initial difficulties that he will find easier to solve if he perceives them in advance and if his greater preparedness strengthens his motivation.

6 Facilities: features and improvements

All equipment dedicated to current space programmes have been described in detail elsewhere [6.1, 6.2, 6.3]; therefore, only some typical examples will be briefly considered here. Such kinds of equipment fall into two categories: either common facilities (30 experiments of the FSLP use only four sets of equipment), or individual facilities. The advantages of the 'common facility' include weight saving, better definition of each experimenter's responsibility (in terms of space integration) and simplification of the mission management, but this concept generally fails to satisfy fully the researcher's requirements. One of the reasons for this relative gap between the initial investigator's requirements and the space characteristics stems from the complex procedures of space integration that make the classical materials scientist reluctant to commit himself. The only solution left so far is to introduce some flexibility in the definition of space experiments, with the inherent risk of lack of precision in the objectives. The ideal situation would be to develop two types of equipment:

- *Specific equipment* for research programmes of high interest, with ambitious, well-defined objectives and long-term utilization perspectives.
- *Common equipment* including specialised modular elements, for first-generation demonstration experiments.

In any case a large cooperation is to be encouraged between scientists and space specialists in order to maintain the initial objectives under firm control. Furthermore, the new equipment envisaged must be designed in such a way as to meet the specific conditions or constraints of space environment, and not only simply be extrapolated from traditional experience gained on earth.

This chapter will briefly review the main multiuser facilities that have been developed in Europe either for the first Spacelab mission (FSLP) or for future European ventures.

6.1 Heating facilities

Up to now all heating facilities are multipurpose facilities that need to be adapted to specific experimental conditions.

Most often materials-science experiments must be encapsulated many times for safety reasons, and this increases the number of the thermal barriers between the test specimens and the heating sources.

Due to these thermal barriers (Figs. 6.1 & 6.2) and independently of the thermal characteristics of the materials, thermal transients have durations of about one hour when operating on earth. When going to space, heat transfer is less efficient, due to the absence of thermoconvection in fluid phases. This phenomenon tends to prolong critically transient heat states. In consequence the analysis of solidification in the non-steady state is essential, resulting in constant variations of the displacement rate of the isotherms (solidification rate) and of the values of the thermal gradient. Furthermore, this overisolation increases the electrical energy consumption without any benefit for the scientific significance of the experiment.

It is worthwhile mentioning that any improvement in the general characteristics of the heating facilities (maximum temperature level and inertia of the heating and cooling sources) will not change the nature of the problem. The only way to improve the functioning conditions would be to reduce the number of the thermal barriers, a

Table 6.1 Main characteristics of the Isothermal Heating Facility

Operating temperatures	
Range	200 – 1600°C
Accuracy	±4°C(250°C) – ±10°C(1600°C)
Constancy	±5°C
Resolution	±0.5°C
Maximum power (peak)	1000 W
Dimensions of the isothermal zone	100 mm (L) × 40 mm (ϕ)
Atmosphere	
Heating	vacuum or helium
Cooling	air or helium
Heating rate	15 mn to 1200°C
Cooling rate (helium)	60 mn from 1200°C

Table 6.2 Main characteristics of the Gradient Heating Facility

Operating temperatures	
Range	150 – 1200°C
Gradient	<5°C/cm – 200°C/cm
Accuracy	±8°C
Constancy	±2°C
Resolution	±0.5°C
Maximum power (peak)	800 W
Dimensions of the hot zone	330 mm (L) × 25 mm (ϕ)
Atmosphere	
Heating	Vacuum
Cooling	vacuum or helium
Heating rate	45 mn to 1200°C
Cooling rate (helium)	105 mn from 1200°C

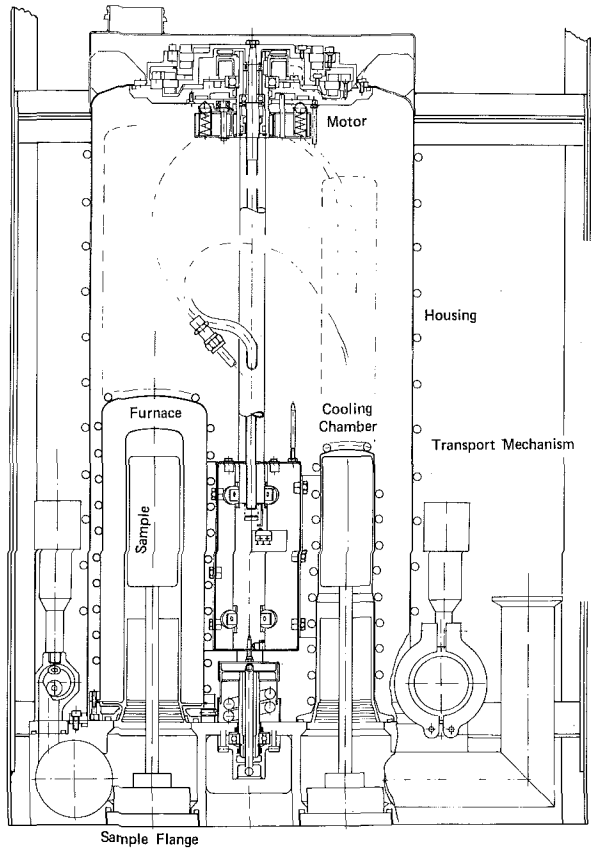

Figure 6.1 Cross-section of the Isothermal Heating Facility of MSDR/FSLP.

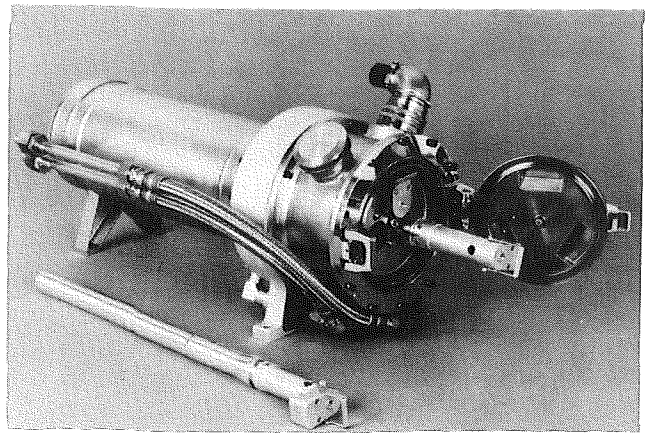

Figure 6.2 View of the Gradient Heating Facility of MSDR/FSLP and of the included cartridge.

tendency strongly opposed by the usual safety regulations. Actually the only solution is to modify the temperature-time profiles and programmes; this can be done only after an accurate calibration of the heating facilities under space conditions. The present remedies must be considered as purely qualitative, all the less adapted as the heating kinetics is more rapid.

One exception is the Mirror Furnace (Fig. 6.3), since energy focusing on the specimen is still the best way to shorten transient heat states. Nevertheless this technique introduces new limitations as regards the range of the potential materials apt to be so heated: vapour pressure, oxidability, stability of the floating zone etc, and as such it cannot be considered as a fully multipurpose facility.

Finally, in order to test the g influence on the metallurgical mechanisms the same thermal conditions must be applied to the systems both in μ-g and 1-g environments. This will require the precise measurement of the thermal conditions in space and their subsequent reproductibility on earth, since the reverse process is not possible.

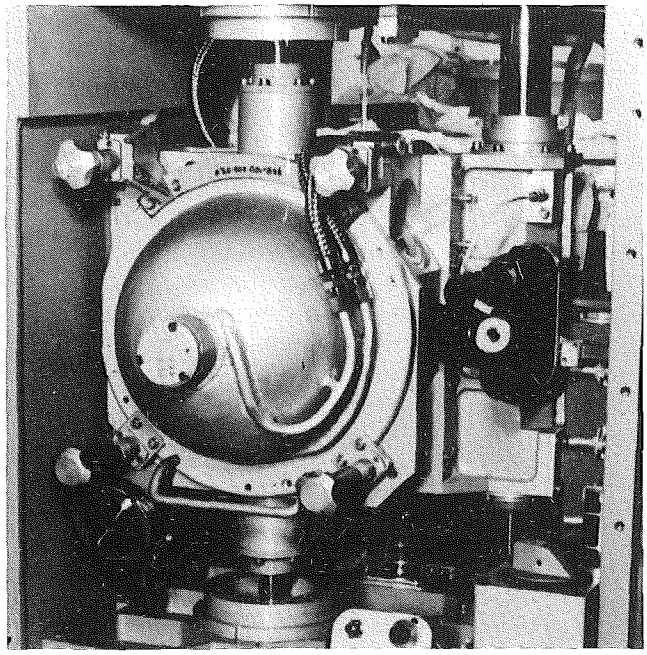

Figure 6.3 Schematic cross-section of the Mirror Heating Facility of MSDR/FSLP.

Table 6.3 Main characteristics of the Mirror Furnace

Operating temperatures	
Range	200 – 2100°C
Accuracy	
Constancy	±5°C
Resolution	
Maximum power	800 W
Dimensions of the hot zone	10 mm (L) × 20 mm (ϕ)
Atmosphere	vacuum
Heating rate	–
Cooling rate	–

6.2 Fluid Physics Module

The Fluid Physics Module (FPM) is the first European multi-user facility supporting fluid physics experiments on board the manned orbiting laboratory Spacelab.

A short brochure providing some guidance for potential users has been issued by ESA [6.4]. The following description has been borrowed mainly from that brochure.

The basic idea for the FPM is to provide a precision apparatus for establishing a liquid bridge between two parallel coaxial disks (Fig. 6.4) in a microgravitational environment, allowing for some disturbances to be applied to the liquid, whose behaviour is then studied. The liquid, contained in an interchangeable reservoir, is injected into the test section through the center of one of the end disks. Disk separation and liquid volume can be varied at will (within the bridge stability limits), and several small disturbances applied to the liquid mass through the solid disks (rotation, vibration, heating, etc.). Means are provided for photographically recording the liquid-bridge outer shape and the velocity field in its interior (using tracers), in a meridian plane and at right angles to the longitudinal axis.

Keypoints in the definition of the facility are:

- to provide for 'a liquid-bridge making apparatus', particularly cylindrical bridges up to 10 cm long;
- to allow for independent control of the liquid volume in order to attain any possible equilibrium shape;
- to accept different disks and liquids according to the user requirements on size, shape, wetting and spreading characteristics, liquid viscosity, and so forth.

With the above baseline, several fundamental fluid-physics problems can be investigated: natural and enhanced liquid-bridge stability, onset of surface-tension

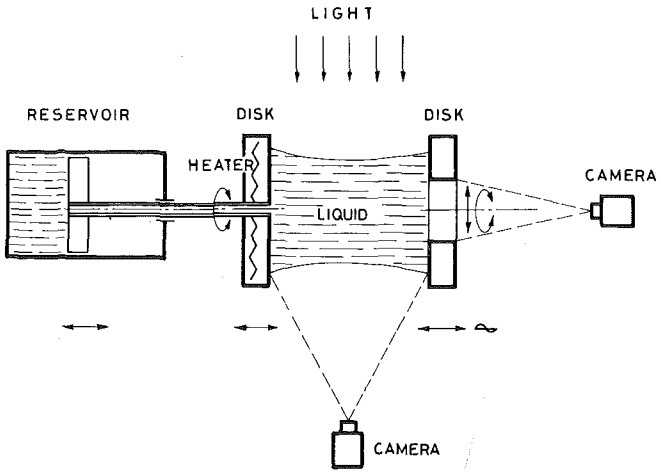

Figure 6.4 Schematic representation of the Fluid-Physics Module.

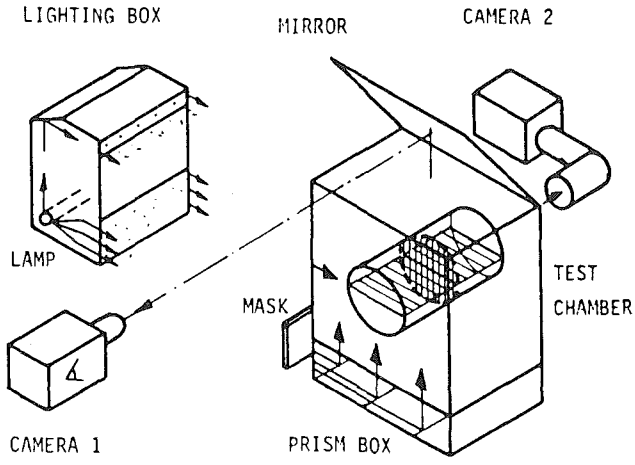

Figure 6.5 Visualisation system of the Fluid-Physics Module.

induced convection, drop coalescence, interfacial forces, etc.

In addition, a number of controlled disturbances acting upon the liquid are made available to the user. These disturbances can be mechanical (rotation, vibration and disalignment), thermal (heating) and electrical (potential difference between the end disks). Furthermore, a photographic recording system has been included as an integral part of the FPM.

The overall visualisation system is shown in Figure 6.5. Present performances of the FPM are summarised in Table 6.4.

Table 6.4 Main characteristics of the Fluid-Physics Module

Liquid volume	0 – 1300 cc (step: 0.8 cc)
End-plate diameter	up to 100 mm (different shapes, sizes and materials)
Rotation speed of the plates	±5 – 99.9 rpm (step: 0.1 rpm); separate operation possible
Oscillations	0.1 – 1 Hz (step: 0.01 Hz); 0 – 0.5 mm amplitude
Liquid injection speed	0.01 – 20 cc/s (step: 0.1 cc/s)
Thermal capability	ambient to 60°C (feeding end plate)
Electrical potential	±100 V DC at one end plate
Photographic recording	two 16-mm cine cameras
Electrical power required	360 W max

Operation of the FPM requires the intervention of the payload specialist.

Although experiments using the FPM under micro-gravity are yet to be performed, some improvements have been already proposed. It is suggested, for example, either to limit the present model, or to design new experiments. The limitations and improvements suggested are mentioned below.

- A problem which will be investigated in the first Spacelab Mission, and which could be worth a second look, is bridge setting-up. At present, the bridge grows by simultaneous liquid injection (through a small hole) and disk separation. This procedure is awkward, time consuming and unreliable.
- A two-fluid injection system would greatly enhance the usefulness of the FPM, which could be used to study mixing problems, to provide selective visualisation, and so forth.
- Local interface heating, radial heating, radial electric fields and, generally speaking, disturbing procedures not applied from the end disks, are not available at present, not to mention real phase changes which would be considered in the future.
- At present data acquisition relies mainly on the visualisation system. Non-intrusive temperature measurements in the fluid bulk and measurement of very low pressure differences cannot be achieved.
- Experiments requiring accurate redundant measurement of liquid volume and capillary pressure would face unsurmountable problems. At present liquid volume can be measured, at best, with an accuracy of 0.8 cc and capillary pressures cannot be directly measured.

6.3 Contact-free positioning

Positioning devices for use on board spacecraft are still in a less advanced state compared to the facilities described in the preceding sections. This may seem surprising since reducing gravity by 10^{-4} or 10^{-6} should make the contact-free processing of material samples so much easier. However, even under microgravity permanent countermeasures against critical displacements are necessary. As for most uses also mating to a furnace is required, the technical development even of a basic positioner has turned out to be rather difficult. (Not to speak of an ideal positioner which should be compatible with various manipulations as mixing, deforming, controlled moving of several samples, and must also leave access for observations.)

The advantage of microgravity is that positioning can be achieved with compensating forces of relatively low intensity. This reduces disturbances by side-effects as inhomogenous heating, vibrations, generation of convection, deformation and splitting of the sample. Several methods are possible, each offering different advantages or drawbacks. Presently items 1, 2 and 4 of the following list are considered the most promising ones to be used in space experiments:

1. *Acoustic.* The sample finds a stable position in potential minima of a standing acoustic wave. This method has the advantage of having only weak mechanic and thermal disturbances but requires a surrounding atmosphere. A device with one driver for positioning in a tube has been developed by Battelle. The allowed sample size is 8 mm diameter. An acoustic levitator furnace has recently been flown successfully on a SPAR rocket, and a more sophisticated 3-axial positioner is under development at JPL.
2. *Aerodynamic.* The sample is kept in desired position by intermittent gas jets. A stable position does not exist and feed-back control is required.
3. *Electromagnetic.* An inhomogenous alternating magnetic field exerts a force on currents that are induced in the sample. A minimum conductivity of about $10\,(\Omega \cdot \mathrm{cm})^{-1}$ is required under space conditions. Heat dissipation and generation of convection in liquid samples are disturbing side-effects, but contamination of the sample by a surrounding medium can be avoided entirely. An apparatus for heating up to above 1500°C and positioning of a 9 mm sample has been developed by GE and flown on a SPAR rocket.
4. *Electrostatic (or magnetostatic) positioning* in inhomogeneous fields. Feed-back control is required. A multiaxial electrostatic positioner (4 electrodes in tetrahedral configuration) with mating compatibility to the ESA Isothermal Heating Facility is presently under development. It will allow to position high-density samples (steel) of 10 mm diameter under residual acceleration of up to $10^{-3}\,g$ at operating temperatures of 1500°C (Fig. 6.6), [6.2].
5. *Positioning in a standing, electromagnetic wave* could be a further possibility but apparently offers no specific advantages. No such development is in progress.

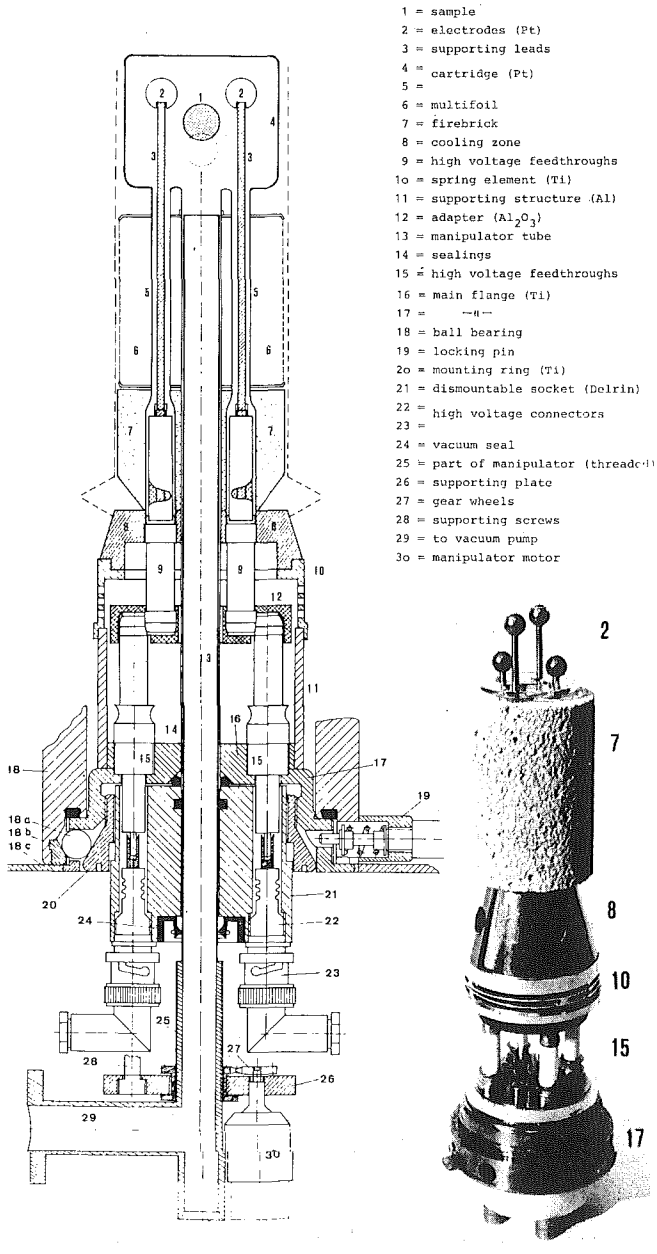

Figure 6.6 Electrostatic positioner with mating compatibility to the isothermal heating facility.

The development of positioning devices so far has been directed at keeping only one sample in a specified position, where the tolerable amplitude of displacements is limited by the diameter of an enclosure. The advantage of microgravity for this purpose has been demonstrated. The field for future development of more sophisticated devices for containerless processing seems rather large. Besides improving precision, their aim could be to position not just one sample, but several ones or even large numbers, simultaneously. Controlled variations of their relative distances down to collision should be made available. Also a means for contactless mixing of collided droplets should be provided. For these purposes the combination of different manipulation methods will be necessary.

References

[6.1] Materials Sciences in Space, *Proc 2nd European Symp*, Frascati 1976, ESA SP-114.
[6.2] Materials Sciences in Space, *Proc 3rd European Symp*, Grenoble 1979, ESA SP-142.
[6.3] *Spacelab User's Manual*, publ by the European Space Agency, 1979, ESA-DP/ST(79)3.
[6.4] Martinez I, *Fluid-Physics Module – Utilisation Brochure*, ESA-Lamf 1979.
[6.5] Ceronetti G & Rovera G, in *Materials Sciences in Space*, 1979, ESA SP-142, p. 137.

7 Conclusion

The initial goal of the authors when beginning to work on this brochure was to provide assistance to all new users of the microgravity environment, but it rapidly became apparent that it would be unrealistic to cover all the possible fields of activity. The lists of all the proposals already received by the various space agencies have merely allowed us to select a minimum range of topics of widest interest for inclusion in this short text.

Because the resulting brochure 'freezes' our knowledge and know-how, as well as our main points of perplexity, at this moment, we are aware that there will be many deficiencies in this first document. As our knowledge of the behaviour under microgravity of basic physical phenomena further develops, we will do our best to revise, up-date and hopefully upgrade this treatment. Any criticisms or suggestions for improvement from our readers and future co-workers in the microgravity environment will therefore be very welcome.

Symbols and units

$\mathbf{a}$	acceleration (cm/s^2)
$\mathbf{b}_r$	acceleration (cm/s^2)
C	concentration of a component (cm^{-3})
C_i	mass concentration of the ith component (cm^{-3})
C_L	composition of liquid phase (cm^{-3})
C_S	composition of solid phase (cm^{-3})
C_p	constant pressure specific heat (erg/K.g. mole)
C_V	heat capacity (K)
d_B	average dislocation (cm)
D	diameter (cm)
D	diffusion coefficient (cm^2/s)
D_L	diffusion coefficient in the liquid phase (cm^2/s)
D'	thermal migration coefficient (cm^2/s K)
D''	Dufour coefficient (cm^2/s K)
$\mathbf{f}$	force per unit mass (dyne/g)
$\mathbf{f}_b$	d'Alembertian force (dyne)
$\mathbf{f}_e$	electromagnetic body force (dyne)
$\mathbf{f}_v$	viscous force per unit mass (dyne/g)
F	free energy (J/mole)
g	effective gravitational acceleration (cm/s)
g_0	earth gravitational acceleration (9.81 cm/s^2)
G_C	concentration gradient in the liquid phase (cm^{-3})
G_L	temperature gradient in the liquid phase (K/cm)
h_B	height (cm)
h_T	height (cm)
h_i	partial specific enthalpie of the ith component (erg/mole)
$\mathbf{J}_i$	mass flux of the ith component (g/cm^2 s)
$\mathbf{J}_q$	heat flux (erg/cm^2 s)
k	Boltzmann's constant (1.38×10^{-16} erg/K)
k_0	distribution coefficient
$\overline{K}$	mean thermal conductivity (W/cm K)
K_L	thermal conductivity of the liquid phase (W/cm K)
K	mean curvature (cm^{-1})
L	extension of an interface (cm)
L_b	Bond characteristic length (cm)
L_M	maximum stable length (cm)
ℓ	scale length factor (cm)
ℓ_c	characteristic length of capillarity (cm)
ℓ_s	characteristic length of solute diffusion (cm)
ℓ_t	characteristic length of thermal diffusion (cm)
m_L	slope of the liquidus line (K/cm^3)
p	pressure (dyne/cm^2)
r	radius (cm)
R	principal radius of curvature (cm)
$\mathscr{S}$	stability function
T	temperature (K)
T_c	correlation length (cm)
u	velocity (cm/s)
v	specific volume (cm^3/g)
V	velocity (cm/s)
V	growth rate of the crystal (cm/s)

$\mathbf{V}$	mass or barycentric velocity (cm/s)
V_m	Marangoni speed (cm/s)
V_r	reference velocity (cm/s)
w	width (cm)
$\mathbf{X}_i$	force per unit mass of the ith component (dyne/g)
Bo	Bond number
Fr	Froude number
Le	Lewis number
Pe	Peclet number
Pr	Prandtl number
Re	Reynolds number
Sc	Schmidt number
St	Soret coefficient (K^{-1})
We	critical Weber number
α	heat diffusion coefficient (cm^2/s)
α_L	heat diffusion coefficient in the liquid phase (cm^2/s)
δ	thickness (cm)
δ_c	solute boundary layer thickness (cm)
δp	capillary pressure ($dyne/cm^2$)
ΔS_F	melting entropy (J/mole K)
ΔV_m	change of volume on melting (cm^3)
ΔT_0	freezing range of a solution (K)
γ_{SL}	surface tension of the solid/liquid interface (erg/cm^2)
θ	radiant (rad)
λ	parameter characterising the distance from thermodynamic equilibrium
λ	heat conduction coefficient (J/cm Ks = W/cm K)
μ	dynamic viscosity (g cm/s)
μ_i	chemical potential of the ith component (erg/g)
μ_g	dynamic viscosity of a gas (g cm/s)
μ_ℓ	dynamic viscosity of a liquid (g cm/s)
ν	kinematic viscosity, momentum diffusion coefficient (cm^2/s)
π	pressure ($dyne/cm^2$)
ϕ	volume fraction
ρ	density (g/cm^3)
ρ_h	hydrostatic density (g/cm^3)
ρ_L	density of the liquid phase (g/cm^3)
ρ_r	reference density (g/cm^3)
σ	surface tension (dyne/cm)
σ_C	composition coefficient of surface tension (dyne/cm)
σ_T	thermal coefficient of surface tension (dyne/cm K)
Σ	surface
ω	angular speed (rad/s)